Protein aggregation in heterogeneous system

KAZUKI IWASHITA

February 2019

Protein aggregation in heterogeneous system

KAZUKI IWASHITA

Doctoral Program in Applied Physics

Submitted to the Graduate School of
Pure and Applied Sciences
in Partial Fulfillment of the Requirements
for the Degree of Doctor of Philosophy in
Engineering

at the
University of Tsukuba

Contents

Chapter 1 General Introduction

1.1 Protein aggregation processes

Proteins undergo diverse states depending on the chemical and physical environment. Protein aggregation is an important process in pathology [1], pharmaceutics [2], bioengineering [3], and food engineering [4]. Intracellular protein aggregation is related to quality control and disease [5, 6]. For example, transient appearance of aggresomes in cytoplasm protects proteins against harsh environments [7]. Beside, aggregates of fragments of amyloid β, α-synuclein, and proteins produced by the *FUS* gene are known to cause Alzheimer's disease, Parkinson's disease, and amyotrophic lateral sclerosis, respectively [8]. Not only is protein aggregation related to disease, it is also relevant to industry. Protein aggregation is often observed during purification and processing *in vitro*. As a result, there is abundant and diverse research on the control of protein aggregation [9, 10].

Protein aggregation is a complicated phenomenon compared to small molecules and simple colloids. Since proteins are polypeptides composed of 20 kinds of amino acids, the aggregation reaction is driven by complex interactions derived from various chemical structures, such as hydrogen bonds of the molecular backbone or electrostatic and hydrophobic interactions between side chains. There are inherent problems in proteins because (i) each protein forms a unique three-dimensional structure with charge and hydrophobicity on the surface [11]; (ii) the three-dimensional structure takes various states with significantly different aggregation tendencies, such as a native, unfolded, and oligomeric states [12]; (iii) degradation occurs due to chemical modification that results in molecular species with various aggregation tendencies [13]; and (iv) various types of aggregates are formed due to complex intermolecular interactions [14, 15].

Protein aggregation is characterized by complex chain reactions and state changes. However, experimental protein aggregation behavior is similar regardless of the type of protein and physicochemical stress [16]. Protein aggregation generally involves a process in which protein unfolds to expose hydrophobic regions inside the molecules, then forms small aggregates as nuclei that grow into large aggregates and form networks [17]. Various interactions contribute to the stabilization of protein structure, including intermolecular hydrogen bonding, hydrophobic interactions, and salt bridges [18]. Protein unfolding can be explained by a

two-state equilibrium model of native and unfolded states that determines the structural stability as the Gibbs free energy difference [19]. Aggregates are formed by irreversible hydrophobic interactions and disulfide bonds between unfolded proteins [20, 21]. The size of the aggregate ranges from soluble particles with tens of nanometer to dispersed particles with hundreds of nanometers to insoluble precipitates with several millimeters [22].

The understanding of protein aggregation started at the end of the 19th century [23]. Currently, protein aggregation has developed into a crucial field in bioengineering and disease research. Our fundamental understanding of molecular mechanisms and control methods has been elucidated using a system comprising a single protein. However, in real biological environments, numerous types of protein with different molecular weights, isoelectric points, unfolding temperatures, and content coexist.

1.2 Protein aggregation in heterogeneous environments

Most proteins coexist in various microenvironments and intracellular compartments through protein–protein interactions and the formation of protein complexes [24]. Therefore, it is essential that the aggregation properties of a specific protein affect the aggregation processes of other proteins in its vicinity.

Amyloid plaques have revealed the co-localization of complex composition proteins to the amyloid structure [25, 26]. The nuclei of the amyloid structure induce cross-seeding and coaggregation with other globular proteins during its growth [27]. The onset of amyloid coaggregation is dependent on amyloid-prone intermediate species of the participating proteins [28]. Several reports have shown that the amyloid structure induces an aggregation process involving other globular proteins and amino acids [29]. Interestingly, both Alzheimer's disease and Huntington's disease have been observed in the same patient [30]. In recent clinicopathological studies, the coexistence of Huntington's disease and amyotrophic lateral sclerosis within patients has been reported [31]. Although amyloid diseases are associated with the aggregation of various proteins or peptides, the heterogeneous component entities of amyloid plaques and inclusions remain unclear.

Besides pathology, coaggregation of proteins is of interest in food engineering. Foodstuffs such as casein [32], whey [33], muscle [34], soy [35], and egg white, which are important protein sources in the modern human diet, are composed of hundreds of proteins. The coaggregation behavior of these constituent

proteins has been well studied. In soy proteins, β-conglycinin solubilizes glycinin aggregates by inhibition of hydrophobic interactions between surfaces of the aggregates [36]. In whey proteins, β-lactoglobulin facilitates the aggregation of α-lactalbumin by inducing the formation of disulfide bonds [37].

It has been found that a certain protein can involve other nonspecific proteins during aggregation. However, there are few reports on the molecular mechanisms concerning aggregation in terms of the characteristics and structural changes of each protein interacting with the heterogeneous proteins. The study of aggregation in heterogeneous protein systems has made little progress compared to that in purified protein systems. Therefore, it is indispensable to greater understand aggregation in heterogeneous protein systems beyond the single system in conventional protein science.

1.3 Hen egg white proteins as a model system

In the present work, hen egg white protein (EWP) was selected as a convenient heterogeneous model system for examining coaggregation. More than 40 kinds of proteins have been identified in hen egg white [38]. Ovalbumin is the most abundant protein, accounting for 54% of the dry weight, and is responsible for the gelling properties of egg white. Ovalbumin is a globular protein with a denaturation temperature of around 70°C, a molecular mass of 45.5 kDa, and an isoelectric point of 4.5 [39]. The inside of an ovalbumin molecule has four free sulfhydryl groups, making it the only EWP with a free sulfhydryl group [40]. Ovotransferrin is one of the most thermolabile proteins and has a denaturation temperature of 55°C. It accounts for 12% of dry EWP, has a molecular mass of 76 kDa, an isoelectric point of 6.0, and contains 15 intramolecular disulfide bonds [41]. Lysozyme has a high isoelectric point of 11.4, that is a specific basic protein among EWPs. It has been well studied as a model protein with a denaturation temperature of 71°C and a molecular mass of 14.3 kDa. Due to its high isoelectric point. Lysozyme is known to bind to acidic proteins such as ovalbumin [42] and ovotransferrin [43]. Hen egg white also contains minor proteins such as ovomucoid, G2 and G3 ovoglobulin, ovomucin, ovostatin, ovoflavoprotein, and avidin [38].

Hen egg white is a common material in the food industry due to its excellent nutritional value and distinctive functional properties [44]. Due to its high protein content, egg white offers diverse functional properties for food processing, such as foaming, emulsification, and gelation, which are based on the

physicochemical mechanism of protein aggregation. Thermal treatment is the most common physical process in food processing. Each protein in egg white can form an aggregate upon heating, the nature of which depends on the protein concentration, pH, and ionic strength [45, 46]. The aggregation properties and structural changes of EWPs resulting from these factors have been extensively studied in relation to the functional properties of egg white products. To optimize the function of the final products of egg whites, it is necessary to understand the aggregation process—particularly its heterogeneous protein composition.

1.4 Objectives

This thesis aims to shed light on protein aggregation behavior in a heterogeneous protein system using egg whites. Chapter 2 reports the thermal aggregation behavior of whole EWP at a high concentration. Chapter 3 describes cooperative thermal aggregation in a binary protein system in which two kinds of proteins coexist, i.e., coaggregation. Chapter 4 discusses the molecular mechanism of the onset of coaggregation. Lastly, Chapters 5 and 6 summarize the thermal aggregation process of heterogeneous proteins compared to an ideal protein solution system and describe future prospects.

References

[1] Aguzzi, A. & O'Connor, T. Protein aggregation diseases: pathogenicity and therapeutic perspectives. *Nat. Rev. Drug Discov.* 9, 237–248 (2010).

[2] Vazquez-Rey, M. & Lang, D. A. Aggregates in monoclonal antibody manufacturing processes. *Biotechnol. Bioeng.* 108, 1494–1508 (2011).

[3] Cromwell, M. E. M., Hilario, E. & Jacobson, F. Protein aggregation and bioprocessing. *AAPS J.* 8, E572–E579 (2006).

[4] Nicolai, T. & Durand, D. Controlled food protein aggregation for new functionality. *Curr. Opin. Colloid Interface Sci.* 18, 249–256 (2013).

[5] Tyedmers, J., Mogk, A. & Bukau, B. Cellular strategies for controlling protein aggregation. *Nat. Rev. Mol. Cell Biol.* 11, 777–788 (2010).

[6] Mogk, A., Bukau, B. & Kampinga, H. H. Cellular handling of protein aggregates by disaggregation machines. *Mol. Cell* 69, 214–226 (2018).

[7] Pu, Y., Li, Y., Jin, X., Tian, T., Ma, Q., Zhao, Z., Lin, S.-y., Chen, Z., Li, B., Yao, G., Leake, M. C., Lo, C.-J. & Bai, F. ATP-dependent dynamic protein aggregation regulates bacterial dormancy depth critical for antibiotic tolerance. *Mol. Cell* 73, 143–156.e144 (2019).

[8] Eisenberg, D. & Jucker, M. The amyloid state of proteins in human diseases. *Cell* 148, 1188–1203 (2012).

[9] Shiraki, K., Tomita, S. & Inoue, N. Small amine molecules: Solvent design toward facile improvement of protein stability against aggregation and inactivation. *Curr. Pharm. Biotechnol.* 17, 116–125 (2016).

[10] Iwashita, K., Mimura, M. & Shiraki, K. Control of aggregation, coaggregation, and liquid droplet of proteins using small additives. *Curr. Pharm. Biotechnol.* 19, 953–962 (2018).

[11] Berman, H. M. The protein data bank. *Nucleic Acids Res.* 28, 235–242 (2000).

[12] Roberts, C. J. Therapeutic protein aggregation: mechanisms, design, and control. *Trends Biotechnol.* 32, 372–380 (2014).

[13] Tomita, S. & Shiraki, K. Why do solution additives suppress the heat-induced inactivation of proteins? inhibition of chemical modifications. *Biotechnol. Prog.* 27, 855–862 (2011).

[14] Yoshimura, Y., Lin, Y., Yagi, H., Lee, Y. H., Kitayama, H., Sakurai, K., So, M., Ogi, H., Naiki, H. & Goto, Y. Distinguishing crystal-like amyloid fibrils and glass-like amorphous aggregates from their kinetics of formation. *Proc. Natl. Acad. Sci. U.S.A.* 109, 14446–14451 (2012).

[15] Kroschwald, S. & Alberti, S. Gel or die: Phase separation as a survival strategy. *Cell* 168, 947–948 (2017).

[16] Morris, A. M., Watzky, M. A. & Finke, R. G. Protein aggregation kinetics, mechanism, and curve-fitting: A review of the literature. *Biochim. Biophys. Acta* 1794, 375–397 (2009).

[17] I. Kurganov, B. Thermal denaturation and aggregation assays in analytical biochemistry. *Biochem. Anal. Biochem.* 2, e136 (2013).

[18] Pucci, F. & Rooman, M. Physical and molecular bases of protein thermal stability and cold adaptation. *Curr. Opin. Struct. Biol.* 42, 117–128 (2017).

[19] Clarkson, B. R., Schön, A. & Freire, E. Conformational stability and self-association equilibrium in biologics. *Drug Discov. Today* 21, 342–347 (2016).

[20] Tomita, S., Yoshikawa, H. & Shiraki, K. Arginine controls heat-induced cluster–cluster aggregation of lysozyme at around the isoelectric point. *Biopolymers* 95, 695–701 (2011).

[21] Gerrard, J. A. Protein–protein crosslinking in food: methods, consequences, applications. *Trends Food Sci. Technol.* 13, 391–399 (2002).

[22] Schmitt, C., Moitzi, C., Bovay, C., Rouvet, M., Bovetto, L., Donato, L., Leser, M. E., Schurtenberger, P. & Stradner, A. Internal structure and colloidal behaviour of covalent whey protein microgels obtained by heat treatment. *Soft Matter* 6, 4876–4884 (2010).

[23] Dobson, C. M. Protein folding and misfolding. *Nature* 426, 884–890 (2003).

[24] Uversky, V. N. Intrinsically disordered proteins in overcrowded milieu: Membrane-less organelles, phase separation, and intrinsic disorder. *Curr. Opin. Struct. Biol.* 44, 18–30 (2017).

[25] Atwood, C. S., Martins, R. N., Smith, M. A. & Perry, G. Senile plaque composition and posttranslational modification of amyloid-β peptide and associated proteins. *Peptides* 23, 1343–1350 (2002).

[26] Liao, L., Cheng, D., Wang, J., Duong, D. M., Losik, T. G., Gearing, M., Rees, H. D., Lah, J. J., Levey, A. I. & Peng, J. Proteomic characterization of postmortem amyloid plaques isolated by laser capture microdissection. *J. Biol. Chem.* 279, 37061–37068 (2004).

[27] Anand, B. G., Prajapati, K. P. & Kar, K. $A\beta_{1-40}$ mediated aggregation of proteins and metabolites unveils the relevance of amyloid cross-seeding in amyloidogenesis. *Biochem. Biophys. Res. Commun.* 501, 158–164 (2018).

[28] Dubey, K., Anand, B. G., Temgire, M. K. & Kar, K. Evidence of rapid coaggregation of globular proteins during amyloid formation. *Biochemistry* 53, 8001–8004 (2014).

[29] Anand, B. G., Dubey, K., Shekhawat, D. S. & Kar, K. Intrinsic property of phenylalanine to trigger protein aggregation and hemolysis has a direct relevance to phenylketonuria. *Sci. Rep.* 7, 11146 (2017).

[30] Davis, M. Y., Keene, C. D., Jayadev, S. & Bird, T. The co-occurrence of Alzheimer's disease and Huntington's disease: a neuropathological study of 15 elderly Huntington's disease subjects. *J. Huntington's Dis.* 3, 209–217 (2014).

[31] Tada, M., Coon, E. A., Osmand, A. P., Kirby, P. A., Martin, W., Wieler, M., Shiga, A., Shirasaki, H., Tada, M., Makifuchi, T., Yamada, M., Kakita, A., Nishizawa, M., Takahashi, H. & Paulson, H. L. Coexistence of Huntington's disease and amyotrophic lateral sclerosis: a clinicopathologic study. *Acta Neuropathol.* 124, 749–760 (2012).

[32] Huppertz, T., Fox, P. F. & Kelly, A. L. The caseins: Structure, stability, and functionality. in *Proteins in Food Processing: Second Edition* (ed. Yada, R. Y.) Woodhead Publishing 49–92 (2017).

[33] Kilara, A. & Vaghela, M. N. Whey proteins. in *Proteins in Food Processing: Second Edition* (ed. Yada, R. Y.) Woodhead Publishing 93–126 (2017).

[34] Xiong, Y. L. Muscle proteins. in *Proteins in Food Processing: Second Edition* (ed. Yada, R. Y.) Woodhead Publishing 127–148 (2017).

[35] Nishinari, K., Fang, Y., Nagano, T., Guo, S. & Wang, R. Soy as a food ingredient. in *Proteins in Food Processing: Second Edition* (ed. Yada, R. Y.) Woodhead Publishing 149–186 (2017).

[36] Guo, J., Yang, X.-Q., He, X.-T., Wu, N.-N., Wang, J.-M., Gu, W. & Zhang, Y.-Y. Limited aggregation behavior of β-conglycinin and its terminating effect on glycinin aggregation during heating at pH 7.0. *J. Agric. Food Chem.* 60, 3782–3791 (2012).

[37] Schokker, E. P., Singh, H. & Creamer, L. K. Heat-induced aggregation of β-lactoglobulin A and B with α-lactalbumin. *Int. Dairy J.* 10, 843–853 (2000).

[38] Guerin-Dubiard, C., Pasco, M., Molle, D., Desert, C., Croguennec, T. & Nau, F. Proteomic analysis of hen egg white. *J. Agric. Food Chem.* 54, 3901–3910 (2006).

[39] Weijers, M., Barneveld, P. A., Cohen Stuart, M. A. & Visschers, R. W. Heat-induced denaturation and aggregation of ovalbumin at neutral pH described by irreversible first-order kinetics. *Protein Sci.* 12, 2693–2703 (2003).

[40] Huntington, J. A. & Stein, P. E. Structure and properties of ovalbumin. *J. Chromatogr. B Biomed. Sci. Appl.* 756, 189–198 (2001).

[41] Wu, J. & Acero-Lopez, A. Ovotransferrin: Structure, bioactivities, and preparation. *Food Res. Int.* 46, 480–487 (2012).

[42] Santos, M. B., Costa, A. R. D. & Garcia-Rojas, E. E. Heteroprotein complex coacervates of ovalbumin and lysozyme: Formation and thermodynamic characterization. *Int. J. Biol. Macromol.* 106, 1323–1329 (2018).

[43] Matsudomi, N., Takasaki, M. & Kobayashi, K. Heat-induced aggregation of lysozyme with ovotransferrin. *Agric. Biol. Chem.* 55, 1651–1653 (1991).

[44] Mine, Y. Egg proteins. in *Applied Food Protein Chemistry* (ed. Ustunol, Z.) John Wiley & Sons, Ltd. 459–490 (2015).

[45] Handa, A., Takahashi, K., Kuroda, N. & Froning, G. W. Heat-induced egg white gels as affected by pH. *J. Food Sci.* 63, 403–407 (1998).

[46] Totosaus, A., Montejano, J. G., Salazar, J. A. & Guerrero, I. A review of physical and chemical protein-gel induction. *Int. J. Food Sci. Tech.* 37, 589–601 (2002).

Chapter 2 Aggregation of Heteroproteins at High Concentration

Thermal aggregation of hen egg white proteins in the presence of salts

2.1 Introduction

Physiologic fluids in living systems are so crowded with biomacromolecules that a significant fraction of the intracellular space is not available to other macromolecules [1–3]. This crowded environment is known to greatly affect protein stability and aggregation by altering the kinetics and the equilibrium parameters compared to dilute solution [4, 5]. The effect of a crowded environment on protein stability has mainly been described from an excluded volume perspective, in which a solution contains only one kind of protein with a high concentration of inert macromolecules, typically polyethyleneglycol, dextran, or Ficoll as crowders to mimic crowded conditions [6, 7]. However, the environment in living systems is, in fact, highly crowded with the heterogeneous macromolecules, i.e., proteins, nucleic acids, lipids, and polysaccharides [8]. This heterogeneous and highly concentrated condition is also relevant to the food industry [9]. Protein stability and aggregation in this crude environment will be investigated by protein biophysics to understand the intrinsic behaviors in living organisms.

The crowded environment affects protein stability and aggregation by specific interactions between cosolutes and proteins, as well as the excluded volume effect. The specific effect of cosolutes on protein stability has been classically described by Yancey as osmolytic [10]. Such small-molecular-weight cosolutes have been extensively investigated with regard to protein aggregation, such as amino acids [11, 12] and their derivatives [13], arginine [14–17] and its derivatives [18, 19], and amine compounds [20–22]. These data revealed that small organic additives decrease the aggregation rate of protein and increase the solubility of the aggregation-prone unfolded protein. The design rule of aggregation suppressors remained obscure:

(i) multivalent amines decrease the aggregation rate to suppress chemical modification; (ii) the amino acid backbone is an indispensable structure as an additive for heat-induced aggregation; and (iii) the guanidine group increases the solubility of aromatic compounds. However, inorganic salts have comparatively simple rules in terms of their effect on protein aggregation. For example, the surface tension of various kinds of saline describes the thermal aggregation of egg white lysozyme [23].

The Hofmeister series is a well-known index for additive effects on protein aggregation; the propensity of aggregation is as follows [24, 25]:

$$CO_3^{2-} > SO_4^{2-} > S_2O_3^{2-} > H_2PO_4^- > F^- > Cl^- > Br^- \approx NO_3^- > I^- > ClO_4^- > SCN^-$$

In general, chaotropes (typically SCN^- and I^-) show the so-called "salting-in" effect that destabilizes protein tertiary structure, leading to a decrease in the denaturation temperature. In contrast, kosmotropes (typically CO_3^{2-} and SO_4^{2-}) show a "salting-out" effect that stabilizes protein structure [26]. Hofmeister series have been applied in various protein industries and research fields for purification and stabilization in fundamental research, such as the strength of ionic hydration [27, 28], different density of water molecules [29, 30], and accumulation or exclusion of ions from the surface [31, 32].

In this study, I have investigated the thermal aggregation of high and low concentrations of hen egg white proteins with several types of inorganic salts. The egg white proteins were chosen because of the existing protein systems [33]. Egg white from the domestic chicken is one of the most prominent protein source foods. The biophysical structure of egg white plays an important role in the functional properties of food, such as water-holding, emulsifying, foaming, and gelation due to high protein concentration (100 mg/mL) [34–36]. In addition, egg white contains various kinds of proteins with various molecular weights, isoelectric points, and concentrations [37–40]. Ovalbumin, with a molecular weight of 45 kDa, is the most abundant protein, accounting for half the content of egg white proteins. Ovotransferrin and ovomucoid are the next most abundant proteins, with molecular weights of 76 kDa and 28 kDa, respectively. Small amounts of dozens other proteins have been identified, although egg white has the favorable property of no lipid content. This type of crude condition with heterogeneous proteins is common in daily life. Several papers have been reported about the egg white proteins, such as thermal aggregation of egg white proteins [41] and NMR structure of a model protein in the presence of egg white as crowding agent [42]. By contrast, this study provides the first attempt to understand the biophysical aspects of the aggregation highly concentrated protein with Hofmeister salts.

This study provides the first attempt to understand the biophysical aspects of highly concentrated protein aggregation with Hofmeister salts.

2.2 Materials and methods

Materials

Sodium thiocyanate (NaSCN), sodium chloride (NaCl), sodium sulfate (Na_2SO_4), and magnesium chloride ($MgCl_2$) were obtained from Wako Pure Chemical Industries Ltd. (Osaka Japan). 2-[4-(2-Hydroxyethyl)-1-piperazinyl]ethanesulfonic acid (HEPES) was obtained from Nacalai Tesque (Kyoto, Japan). Ficoll 70 with an average molecular weight of 70 kDa and egg white ovalbumin (grade V) were obtained from Sigma Chemical Co. (St. Louis, MO).

Preparation of hen egg white proteins

Hen egg white proteins were prepared by the following procedure to obtain samples for reproducible experiments. Hen egg white protein (EWP) was diluted with an equal volume of distilled water, stirred gently with a magnetic stirrer for 1 hour at 4°C, and then dialyzed using a 1000 MW cut-off dialyzed tube against distilled water with four changes at 4°C to remove small-molecular-weight compounds and salts. The samples were then centrifuged at 10000 × *g* for 30 min to remove undesirable large aggregates for the spectroscopic analysis of the following experiments. It is noted that the protein contents of EWP after the centrifugation is almost identical to that of pristine sample. The supernatant was freeze-dried and then used for further experiments.

Thermal aggregation of hen egg white proteins

The freeze-dried EWP was dissolved in 0.5 M sodium salts (NaSCN, NaCl, and Na_2SO_4), 10 mM $MgCl_2$, and 20 mM HEPES and adjusted to the appropriate protein concentration at pH 7.4. The small amount of divalent ion ($MgCl_2$) was added in all conditions due to the understanding of the structural change of protein under physiological condition. Samples in the presence of 150 mg/mL Ficoll 70 containing 1 mg/mL EWP with 0.5 M sodium salts, 10 mM $MgCl_2$, and 20 mM HEPES were also prepared and adjusted to pH 7.4. Aliquots

of 80 μL of the solutions were added to microfuge tubes. The EWP solutions were heated at various temperatures for 30 min using a temperature control system (GeneAtlasG; Astec, Fukuoka, Japan). After the heat treatment, the samples were stirred with a spatula and centrifuged at 15000 × *g* for 20 min at 25°C. The supernatant concentration of proteins was then analyzed by measuring the absorbance at 280 nm (*A*) using a spectrophotometer (ND-1000, NanoDrop Technologies, Inc., Wilmington, Del, USA). The soluble protein concentration ($A/A_0 \times 100$) was plotted in the figures; *A* and A_0 show the absorbance of the sample in the presence of salt after and before the heat treatment, respectively.

Sodium dodecyl sulfate-polyacrylamide gel electrophoresis

The supernatants of the protein solutions after the heat treatment were dissolved in 62.5 mM Tris-HCl (pH 6.8) loading buffer containing 2% (w/v) SDS, 5% sucrose, 5% β-mercaptoethanol, and 0.01% bromophenol blue. The samples were heated for 5 min in boiling water and then subjected to sodium dodecyl sulfate polyacrylamide gel electrophoresis (SDS-PAGE) using a 5% – 20% gradient gel (e-PAGEL, ATTO Co., Tokyo, Japan) with a molecular weight marker (Precision Plus Protein Dual Xtra Standards; BIO-RAD, Hercules, CA, USA). The gels were then stained using silver nitrate.

2.3 Results

Thermal aggregation of egg white proteins

I investigated the concentration-dependent thermal aggregation of EWP in the presence of the inorganic salts NaSCN, NaCl, and Na_2SO_4. It is noted that NaSCN and Na_2SO_4 are chaotrope and kosmotrope, respectively, with the propensities of salting-in and salting-out at the high salt concentration of 0.5 M. As shown in Figure 2.1, high-concentration EWP was easily gelled by heat treatment. The samples of 100 mg/mL EWPs without salts were visually similar, with white turbidity, after the heat treatment at 60°C – 90°C (Fig. 2.1A). The centrifuged samples were separated from the protein pellet with a clear supernatant in the absence of salts (Fig. 2.1B). It should be noted that $MgCl_2$ slightly accelerates the protein aggregation by the heat treatment.

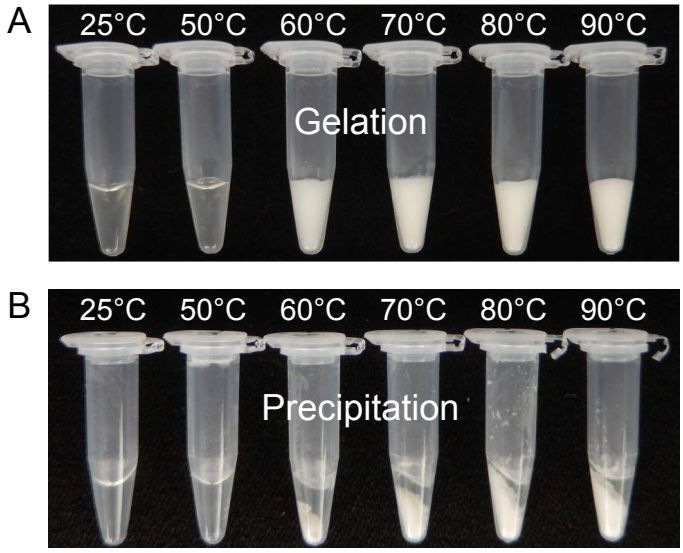

Figure 2.1 Gelation of the EWP solution at 100 mg/mL in the absence of sodium salts. (A) After heat treatment for 30 min. (B) After centrifugation at 15000 × *g* for 20 min.

Figure 2.2 shows the concentration of soluble proteins after heat treatment for 30 min at the respective temperatures. EWP without salt additive began to aggregate at approximately 55°C at all protein concentrations examined (1, 10, and 100 mg/mL). These data were unexpected because highly concentrated proteins are also prone to form aggregates due to the increased probability of protein–protein interaction. However, this independence of protein concentration implies the possibility that the rate-limiting step of aggregation is an unfolding reaction rather than protein–protein interaction, similar to the reaction-limited cluster–cluster aggregation of protein [43].

The addition of 0.5 M salts to 1 mg/mL EWP led to a change in aggregation temperature (Fig. 2.2A). As expected, NaSCN completely inhibited the thermal aggregation of 1 mg/mL EWP even at 90°C. NaCl and Na_2SO_4 resulted in the aggregation of 1 mg/mL EWP above 65°C, and the absorbance decreased to 10% at 90°C. The starting point temperatures of aggregation increased in the order Na_2SO_4 ~ NaCl < NaSCN, which corresponds to the sequence of these salts in the Hofmeister series.

The aggregation tendency of 10 mg/mL EWP with the addition of salt (Fig. 2.2B) was different from the aggregation tendency of 1 mg/mL EWP, especially with NaSCN. EWP at 10 mg/mL with NaSCN showed marked aggregation at 62°C, whereas 1 mg/mL EWP with NaSCN did not aggregate even at 90°C. The aggregation temperature of 10 mg/mL EWP with NaCl was decreased by 8°C compared to 1 mg/mL EWP

with NaCl. However, the results for 10 mg/mL EWP with Na_2SO_4 were almost identical to the results for 1 mg/mL EWP with Na_2SO_4.

The aggregation curves of 100 mg/mL EWP without salt and with NaCl and Na_2SO_4 (Fig. 2.2C) were similar to the aggregation curves of 10 mg/mL EWP with each salt (Fig. 2.2B). However, the aggregation temperature of 100 mg/mL EWP with NaSCN decreased compared to the aggregation temperature for 10 mg/mL EWP with NaSCN. Interestingly, the start point temperatures of aggregation increased in the order NaSCN < NaCl < Na_2SO_4, which was the inverse sequence of the Hofmeister series.

The data shown in Figure 2.2 can be summarized as follows. (i) EWP without salt showed the same aggregation curves regardless of protein concentration from 1 to 100 mg/mL. (ii) EWP with Na_2SO_4 showed similar aggregation curves regardless of protein concentration from 1 to 100 mg/mL. However, EWP with NaSCN showed a decrease in aggregation temperature depending on EWP concentration. (iii) The order of aggregation temperatures was Na_2SO_4 < NaCl < NaSCN at the low concentration (1 mg/mL) of EWP. (iv) In contrast, the order of aggregation temperatures was NaSCN < NaCl < Na_2SO_4 at the high concentration (100 mg/mL) of EWP.

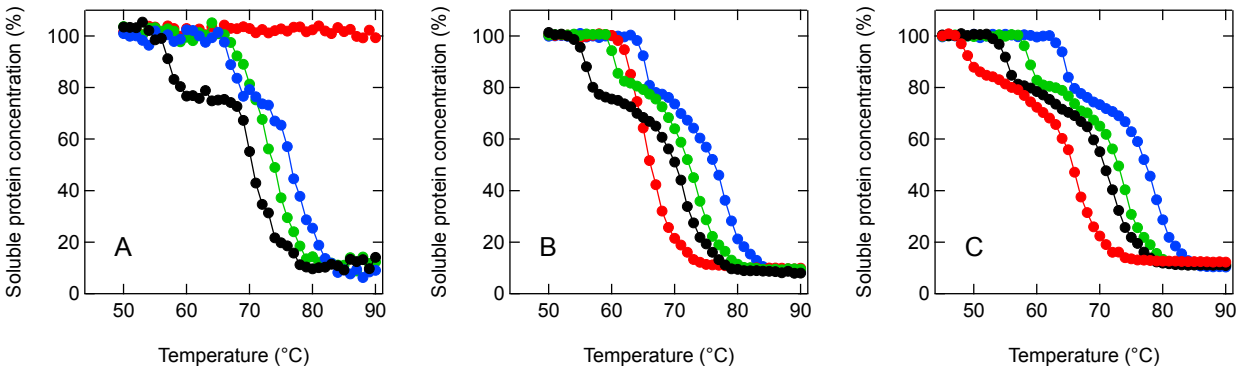

Figure 2.2 Supernatant protein concentration of EWP after heat treatment. The samples containing 0.5 M NaSCN (red), NaCl (green), Na_2SO_4 (blue), and no additive (black) were heat treated for 30 min at the respective temperatures. (A) 1 mg/ mL. (B) 10 mg/mL. (C) 100 mg/mL.

Sodium dodecyl sulfate-polyacrylamide gel electrophoresis of egg white proteins

Table 2.1 shows the properties of the major proteins in EWP, ovalbumin (OVA), ovotransferrin (OVT), ovomucoid, and lysozyme (LYZ). To determine the aggregation propensities of the individual proteins, I performed SDS-PAGE analysis of the EWP after heat treatment. Samples containing 1, 10, and 100 mg/mL EWP in 500 mM salts were prepared and subjected to heat treatment for 30 min at different temperatures; the samples were then centrifuged and the supernatant analyzed by SDS-PAGE (Fig. 2.3). The bands of OVA, OVT, and LYZ were successfully separated at approximately 45, 76, and 14 kDa, respectively. The SDS-PAGE patterns of NaSCN samples at 1 mg/mL EWP did not change even at 90°C for 30 min, while the bands of OVA and OVT in the NaCl and Na_2SO_4 samples decreased with increasing temperature of the heat treatment. To more clearly see this behavior, the aggregation temperatures of OVA, OVT, and LYZ in 1 mg/mL EWP appeared to be in the order Na_2SO_4 ~ NaCl < NaSCN (Table 2.2). EWP at 10 mg/mL sample in the presence of NaSCN decreased the all bands, which was similar pattern to the presence of NaCl and Na_2SO_4. Further increasing concentration of EWP (100 mg/mL) in the presence of NaSCN decreased the overall bands comparing to Na_2SO_4 and NaCl. The aggregation temperatures of OVA, OVT, and LYZ in 10 and 100 mg/mL EWP were in the order NaSCN < NaCl < Na_2SO_4 (Table 2.2). These data can be summarized as follows: the low concentration of EWP was aggregated by the kosmotrope, while the high concentration of EWP was aggregated by the chaotrope, regardless of the kind of protein in EWP.

Table 2.1 Major proteins of EWP

Protein	% of egg white protein[a]	Isoelectric point[a, b, c]	Molecular weight (kDa)[a, b, c]	Denaturation temperature (°C) [a]
Ovalbumin (OVA)	54.0	4.5 (5.19)	45.0 (42.9)	84.0
Ovotransferrin (OVT)	12.0	6.1 (6.30)	76.0 (77.8)	61.0
Ovomucoid	11.0	4.1 [4.82]	28.0 [20.0]	79.0
Lysozyme (LYZ)	3.4	10.7	14.3	75.0

[a]Data are from Qinchun Rao [44].
[b]Data shown in parentheses are from Ning Qiu [40].
[c]Data shown in square brackets are from Catherine Guérin-Dubiard [9].

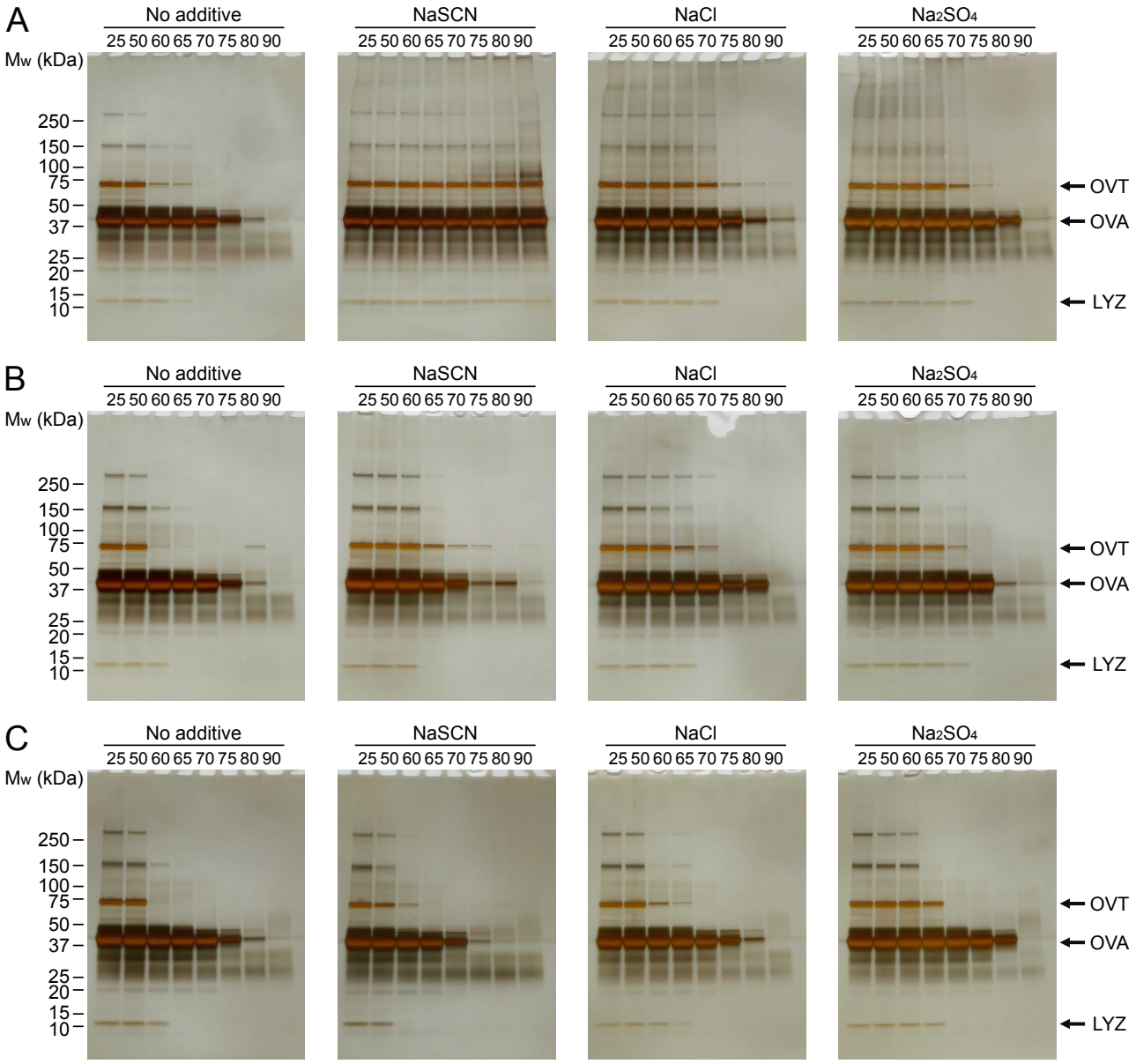

Figure 2.3 SDS-PAGE analyses of heat-induced aggregation of EWP with 0.5 M sodium salts. (A) 1 mg/mL. (B) 10 mg/mL. (C) 100 mg/mL. The numbers in the figures show the temperature of heat treatment (°C). OVT, OVA, and LYZ indicate ovotransferrin, ovalbumin, and lysozyme, respectively.

Table 2.2 Apparent order of the thermal aggregation propensity analyzed by SDS-PAGE

Protein	1 mg/mL	10 mg/mL	100 mg/mL
OVT	Na_2SO_4 ~ NaCl < NaSCN	NaSCN ~ NaCl < Na_2SO_4	NaSCN < NaCl < Na_2SO_4
OVA	Na_2SO_4 ~ NaCl < NaSCN	NaSCN < NaCl < Na_2SO_4	NaSCN < NaCl < Na_2SO_4
LYZ	Na_2SO_4 ~ NaCl < NaSCN	NaSCN < NaCl < Na_2SO_4	NaSCN < NaCl < Na_2SO_4

Excluded volume effect of Ficoll 70

The concentration-dependent behavior of the thermal aggregation of EWP by salts was investigated from the perspective of the excluded volume effect. Ficoll 70 has been used as a hydrophilic polysaccharide for its excluded volume effect with the non-specific steric repulsion of protein molecules [45, 46]. Samples containing 1 mg/mL EWP with 150 mg/mL Ficoll 70 in the presence or absence of salts were prepared and heated for 30 min. Figure 2.4 shows the supernatant concentration of centrifuged protein solutions after the heat treatment. The aggregation curve of 1 mg/mL EWP with 150 mg/mL Ficoll 70 without salt (Fig. 2.4) was similar to 1 mg/mL EWP without Ficoll 70 and salt (Fig. 2.2A). By contrast, the aggregation curve of 1 mg/mL EWP with 150 mg/mL Ficoll 70 with NaSCN (Fig. 2.4) was different from 1 mg/mL EWP without Ficoll 70 and salt (Fig. 2.2A). Accordingly, Ficoll 70 promoted EWP aggregation in the presence of NaSCN. In the presence of NaCl, Ficoll 70 slightly enhanced the aggregation of EWP compared to 1 mg/mL EWP (Figs. 2.2A and 2.4). Interestingly, Ficoll 70 did not affect the thermal aggregation profiles of EWP in the presence of Na_2SO_4 (Figs. 2.2A and 2.4). Thus, the excluded volume effect enhanced aggregation only in the presence of NaSCN.

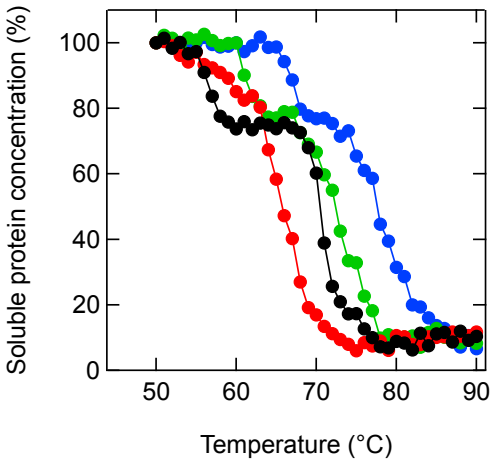

Figure 2.4 Supernatant protein concentration of 1 mg/mL EWP with 150 mg/mL Ficoll 70 after heat treatment. The samples containing 0.5 M NaSCN (red), NaCl (green), Na_2SO_4 (blue), and no additive (black) were heat treated for 30 min at the respective temperatures.

To clarify the crowding effect, I investigated the thermal aggregation of purified OVA alone. Figure 2.5 shows the supernatant concentrations of 1 and 100 mg/mL OVA after heat treatment for 30 min at different temperatures. The sample of OVA without salt aggregated at 60°C – 70°C. In the presence of NaSCN, 1 mg/mL

OVA did not aggregate at 90°C (Fig. 2.5A), which is a similar pattern to the EWP shown in Figure 2A. In contrast, 100 mg/mL OVA was prone to form aggregates (Fig. 2.5B), which was different from the patterns in the presence of NaCl and Na_2SO_4. These data support the hypothesis that chaotropes actually promote protein aggregation by the excluded volume effect.

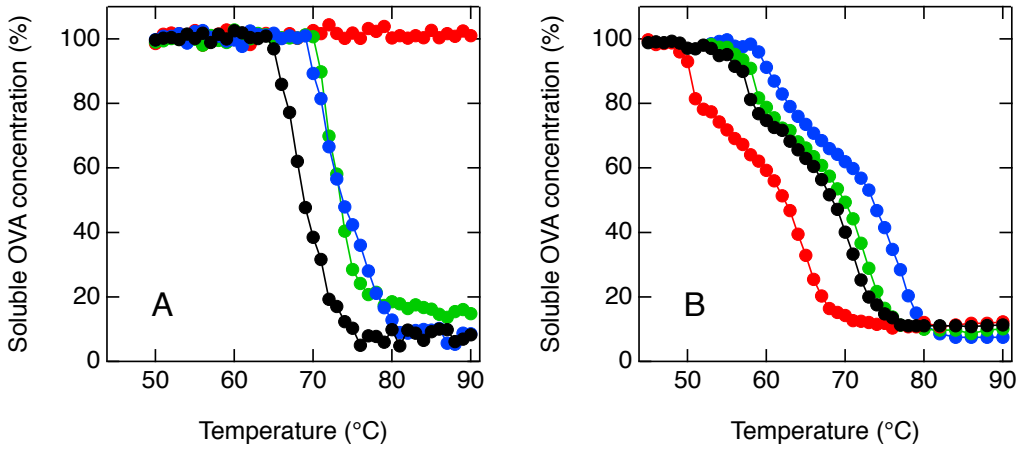

Figure 2.5 Soluble OVA concentration after heat treatment. The samples containing 0.5 M NaSCN (red), NaCl (green), Na_2SO_4 (blue), and no additive (black) were heat treated for 30 min at the respective temperatures. (A) 1 mg/mL. (B) 100 mg/mL.

2.4 Discussion

This study was performed to investigate the thermal aggregation of crude EWP at 100 mg/mL in comparison to 1 mg/mL in the presence of different types of salts. The results can be summarized as follows. (i) The order of the Hofmeister series on thermal aggregation was altered by protein concentration. (ii) The chaotrope NaSCN was unexpectedly the most aggregation-prone additive for the high protein concentration. (iii) The inverse Hofmeister effect was attributed to the macromolecular excluded volume effect.

The most interesting finding of this study is the data regarding the effects of NaSCN on the thermal aggregation of EWP. NaSCN suppressed thermal aggregation at a low concentration of EWP, but not a high concentration (Fig. 2.2). This concentration-dependent aggregation of protein can be discussed in terms of cluster-aggregation theory as follows. Thermal aggregation generally occurs with the initial formation of start

aggregates with a diameter of approximately 50 nm at the initial stage, followed by the growth of the aggregates to large size through association of the start aggregates [43]. This growth of aggregates is classified into diffusion-limited cluster aggregation (DLCA) and reaction-limited cluster aggregation (RLCA); the rate-limiting step of DLCA is the encounter rate of start aggregates, and the rate-limiting step of RLCA is the association and reaction rate of start aggregates [47, 48]. In this situation, it is naturally thought that the crowded environment decreases the diffusion rate, while at the same time, the crowded environment increases the probability of protein-protein interaction [49–51]. Thus, it may be that a chaotrope increases the RLCA-type aggregation in the crowded environment.

Finally, it should be noted that the Hofmeister inverse series has been reported for the cloud-point temperature of lysozyme [52–54]. At a high concentration of salts above 0.5 M, a kosmotrope increases the surface tension of the solution compared to a chaotrope [55], leading to salting-out of protein molecules, which is the direct Hofmeister series effect. At a low concentration of salts, anions bind to the positively-charged surface of lysozyme, leading to increased solubility regardless of the type of ions, which is the inverse Hofmeister series effect. These data show the electrostatic interaction between protein and ions, which affects the solubility of the protein. However, our data describe protein-protein interaction with thermally-unfolded proteins at high ion concentrations. At a high protein concentration, small aggregates are prone to form further aggregates in the presence of a chaotrope, as discussed above. This inverse Hofmeister effect described by RLCA-type aggregation will be found for various proteins at high concentration, as similar data were obtained for both the crude mixture of EWP (Fig. 2.2) and a model crowded environment with albumin and Ficoll 70 (Figs. 2.4 and 2.5).

The thermal aggregation of protein is an important phenomenon in the food industry. However, the control of aggregation is difficult even for pure protein in typical biophysical studies. I believe that this study provides important information on aggregation in high-concentration protein mixtures. Similar data are not expected for biophysical experiments at diluted concentrations of pure protein *in vitro*. In conclusion, the crowded environment unexpectedly increased the probability of protein aggregation in the presence of a chaotrope. The thermal aggregation of highly concentrated protein mixtures is a notable issue in both the food industry and the intercellular environment.

References

[1] Ellis, R. J. Macromolecular crowding: obvious but underappreciated. *Trends Biochem. Sci.* 26, 597–604 (2001).

[2] Minton, A. P. The influence of macromolecular crowding and macromolecular confinement on biochemical reactions in physiological media. *J. Biol. Chem.* 276, 10577–10580 (2001).

[3] Rivas, G., Ferrone, F. & Herzfeld, J. Life in a crowded world. *EMBO Rep.* 5, 23–27 (2004).

[4] Chebotareva, N. A., Kurganov, B. I. & Livanova, N. B. Biochemical effects of molecular crowding. *Biochemistry (Moscow)* 69, 1239–1251 (2004).

[5] Breydo, L., Reddy, K. D., Piai, A., Felli, I. C., Pierattelli, R. & Uversky, V. N. The crowd you're in with: Effects of different types of crowding agents on protein aggregation. *Biochim. Biophys. Acta* 1844, 346–357 (2014).

[6] Perham, M., Stagg, L. & Wittung-Stafshede, P. Macromolecular crowding increases structural content of folded proteins. *FEBS Lett.* 581, 5065–5069 (2007).

[7] Homouz, D., Perham, M., Samiotakis, A., Cheung, M. S. & Wittung-Stafshede, P. Crowded, cell-like environment induces shape changes in aspherical protein. *Proc. Natl. Acad. Sci. U.S.A.* 105, 11754–11759 (2008).

[8] Ellis, R. J. & Minton, A. P. Cell biology: join the crowd. *Nature* 425, 27–28 (2003).

[9] Guerin-Dubiard, C., Pasco, M., Molle, D., Desert, C., Croguennec, T. & Nau, F. Proteomic analysis of hen egg white. *J. Agric. Food Chem.* 54, 3901–3910 (2006).

[10] Yancey, P. H., Clark, M. E., Hand, S. C., Bowlus, R. D. & Somero, G. N. Living with water stress: Evolution of osmolyte systems. *Science* 217, 1214–1222 (1982).

[11] Shiraki, K., Kudou, M., Fujiwara, S., Imanaka, T. & Takagi, M. Biophysical effect of amino acids on the prevention of protein aggregation. *J. Biochem.* 132, 591–595 (2002).

[12] Ito, L., Shiraki, K. & Yamaguchi, H. Comparative analysis of amino acids and amino-acid derivatives in protein crystallization. *Acta Crystallogr. Sect. F Struct. Biol. Cryst. Commun.* 66, 744–749 (2010).

[13] Matsuoka, T., Hamada, H., Matsumoto, K. & Shiraki, K. Indispensable structure of solution additives to prevent inactivation of lysozyme for heating and refolding. *Biotechnol. Prog.* 25, 1515–1524 (2009).

[14] Hirano, A., Arakawa, T. & Shiraki, K. Arginine increases the solubility of coumarin: comparison with salting-in and salting-out additives. *J. Biochem.* 144, 363–369 (2008).

[15] Ariki, R., Hirano, A., Arakawa, T. & Shiraki, K. Arginine increases the solubility of alkyl gallates through interaction with the aromatic ring. *J. Biochem.* 149, 389–394 (2011).

[16] Tomita, S., Nagasaki, Y. & Shiraki, K. Different mechanisms of action of poly(ethylene glycol) and arginine on thermal inactivation of lysozyme and ribonuclease A. *Biotechnol. Bioeng.* 109, 2543–2552 (2012).

[17] Arakawa, T. & Kita, Y. Multi-faceted arginine: mechanism of the effects of arginine on protein. *Curr. Protein Pept. Sci.* 15, 608–620 (2014).

[18] Shiraki, K., Kudou, M., Nishikori, S., Kitagawa, H., Imanaka, T. & Takagi, M. Arginine ethylester prevents thermal inactivation and aggregation of lysozyme. *Eur. J. Biochem.* 271, 3242–3247 (2004).

[19] Hamada, H. & Shiraki, K. L-Argininamide improves the refolding more effectively than L-arginine. *J. Biotechnol.* 130, 153–160 (2007).

[20] Kudou, M., Shiraki, K., Fujiwara, S., Imanaka, T. & Takagi, M. Prevention of thermal inactivation and aggregation of lysozyme by polyamines. *Eur. J. Biochem.* 270, 4547–4554 (2003).

[21] Okanojo, M., Shiraki, K., Kudou, M., Nishikori, S. & Takagi, M. Diamines prevent thermal aggregation and inactivation of lysozyme. *J. Biosci. Bioeng.* 100, 556–561 (2005).

[22] Hamada, H., Takahashi, R., Noguchi, T. & Shiraki, K. Differences in the effects of solution additives on heat- and refolding-induced aggregation. *Biotechnol. Prog.* 24, 436–443 (2008).

[23] Hirano, A., Hamada, H., Okubo, T., Noguchi, T., Higashibata, H. & Shiraki, K. Correlation between thermal aggregation and stability of lysozyme with salts described by molar surface tension increment: an exceptional propensity of ammonium salts as aggregation suppressor. *Protein J.* 26, 423–433 (2007).

[24] Kunz, W., Henle, J. & Ninham, B. W. 'Zur Lehre von der Wirkung der Salze' (about the science of the effect of salts): Franz Hofmeister's historical papers. *Curr. Opin. Colloid Interface Sci.* 9, 19–37 (2004).

[25] Lo Nostro, P. & Ninham, B. W. Hofmeister phenomena: an update on ion specificity in biology. *Chem. Rev.* 112, 2286–2322 (2012).

[26] Jungwirth, P. & Cremer, P. S. Beyond Hofmeister. *Nat. Chem.* 6, 261–263 (2014).

[27] Kunz, W. Specific ion effects in colloidal and biological systems. *Curr. Opin. Colloid Interface Sci.* 15, 34–39 (2010).

[28] Schwierz, N., Horinek, D. & Netz, R. R. Anionic and cationic Hofmeister effects on hydrophobic and hydrophilic surfaces. *Langmuir* 29, 2602–2614 (2013).

[29] Zhang, Y. & Cremer, P. S. Interactions between macromolecules and ions: The Hofmeister series. *Curr. Opin. Chem. Biol.* 10, 658–663 (2006).

[30] López-León, T., Santander-Ortega, M. J., Ortega-Vinuesa, J. L. & Bastos-González, D. Hofmeister effects in colloidal systems: Influence of the surface nature. *J. Phys. Chem. C* 112, 16060–16069 (2008).

[31] Pegram, L. M. & Record, M. T. Quantifying accumulation or exclusion of H^+, HO^-, and Hofmeister salt ions near interfaces. *Chem. Phys. Lett.* 467, 1–8 (2008).

[32] Nihonyanagi, S., Yamaguchi, S. & Tahara, T. Counterion effect on interfacial water at charged interfaces and its relevance to the Hofmeister series. *J. Am. Chem. Soc.* 136, 6155–6158 (2014).

[33] Abeyrathne, E. D. N. S., Lee, H. Y. & Ahn, D. U. Egg white proteins and their potential use in food processing or as nutraceutical and pharmaceutical agents—A review. *Poult. Sci.* 92, 3292–3299 (2013).

[34] Handa, A., Takahashi, K., Kuroda, N. & Froning, G. W. Heat-induced egg white gels as affected by pH. *J. Food Sci.* 63, 403–407 (1998).

[35] Croguennec, T., Nau, F. & Brule, G. Influence of pH and salts on egg white gelation. *J. Food Sci.* 67, 608–614 (2002).

[36] Sun, Y. & Hayakawa, S. Heat-induced gels of egg white/ovalbumins from five avian species: Thermal aggregation, molecular forces involved, and rheological properties. *J. Agric. Food Chem.* 50, 1636–1642 (2002).

[37] Mann, K. The chicken egg white proteome. *Proteomics* 7, 3558–3568 (2007).

[38] Qiu, N., Ma, M., Zhao, L., Liu, W., Li, Y. & Mine, Y. Comparative proteomic analysis of egg white proteins under various storage temperatures. *J. Agric. Food Chem.* 60, 7746–7753 (2012).

[39] Wang, J. & Wu, J. Proteomic analysis of fertilized egg white during early incubation. *EuPA Open Proteom.* 2, 38–59 (2014).

[40] Qiu, N., Ma, M., Cai, Z., Jin, Y., Huang, X., Huang, Q. & Sun, S. Proteomic analysis of egg white proteins during the early phase of embryonic development. *J. Proteom.* 75, 1895–1905 (2012).

[41] Mine, Y., Noutomi, T. & Haga, N. Thermally induced changes in egg white proteins. *J. Agric. Food Chem.* 38, 2122–2125 (1990).

[42] Sanfelice, D., Adrover, M., Martorell, G., Pastore, A. & Temussi, P. A. Crowding versus molecular seeding: NMR studies of protein aggregation in hen egg white. *J. Phys.: Condens. Matter* 24, 244107 (2012).

[43] Tomita, S., Yoshikawa, H. & Shiraki, K. Arginine controls heat-induced cluster–cluster aggregation of lysozyme at around the isoelectric point. *Biopolymers* 95, 695–701 (2011).

[44] Rao, Q., Rocca-Smith, J. R. & Labuza, T. P. Moisture-induced quality changes of hen egg white proteins in a protein/water model system. *J. Agric. Food Chem.* 60, 10625–10633 (2012).

[45] van den Berg, B. Effects of macromolecular crowding on protein folding and aggregation. *EMBO J.* 18, 6927–6933 (1999).

[46] Sarkar, M., Li, C. & Pielak, G. J. Soft interactions and crowding. *Biophys. Rev.* 5, 187–194 (2013).

[47] Lin, M. Y., Lindsay, H. M., Weitz, D. A., Ball, R. C., Klein, R. & Meakin, P. Universality in colloid aggregation. *Nature* 339, 360–362 (1989).

[48] Markossian, K., Yudin, I. & Kurganov, B. Mechanism of suppression of protein aggregation by α-crystallin. *Int. J. Mol. Sci.* 10, 1314–1345 (2009).

[49] Ellis, R. J. Macromolecular crowding: an important but neglected aspect of the intracellular environment. *Curr. Opin. Struct. Biol.* 11, 114–119 (2001).

[50] Kozer, N. & Schreiber, G. Effect of crowding on protein–protein association rates: Fundamental differences between low and high mass crowding agents. *J. Mol. Biol.* 336, 763–774 (2004).

[51] Wang, Y., Li, C. & Pielak, G. J. Effects of proteins on protein diffusion. *J. Am. Chem. Soc.* 132, 9392–9397 (2010).

[52] Wang, Y., Benton, L. A., Singh, V. & Pielak, G. J. Disordered protein diffusion under crowded conditions. *J. Phys. Chem. Lett.* 3, 2703–2706 (2012).

[53] Zhang, Y. & Cremer, P. S. The inverse and direct hofmeister series for lysozyme. *Proc. Natl. Acad. Sci. U.S.A.* 106, 15249–15253 (2009).

[54] Schwierz, N., Horinek, D. & Netz, R. R. Reversed anionic Hofmeister series: The interplay of surface charge and surface polarity. *Langmuir* 26, 7370–7379 (2010).

[55] Pegram, L. M. & Record, M. T., Jr. Hofmeister salt effects on surface tension arise from partitioning of anions and cations between bulk water and the air−water interface. *J. Phys. Chem. B* 111, 5411–5417 (2007).

Chapter 3 Coaggregation of Heteroproteins in a Binary System

3.1 Coaggregation of ovotransferrin and lysozyme

3.1.1 Introduction

Hen egg white is an excellent source of high-quality proteins that can be used as ingredients in protein-enriched foods [1–3]. Food industrial egg white undergoes many aggregation processing such as heating, alkali treatment, and pulsed electric field [4]. Heat pasteurization of raw liquid egg white is required to eliminate pathogenic bacteria and reduce the spoilage bacteria, which cause food poisoning in humans. However, due to the susceptibility of egg white proteins to aggregation upon heating, the physicochemical properties of proteins are perturbed leading to changes in the functional properties of foods, such as gelling and foaming [5]. Therefore, control of thermal aggregation is important for pasteurization and processing of egg white [6].

The aggregation of egg white proteins has been studied extensively [7, 8]. Thermal aggregation of egg white proteins is mediated by disulfide bonds, hydrophobic interactions, and electrostatic interactions [9]. Disulfide bonds, which involve crosslinkage of sulfhydryl groups, play a crucial role in stabilizing the gel structure [10, 11]. Non-covalent hydrophobic and electrostatic interactions initiate gel network formation after the heat-induced denaturation of proteins. The precise measurement of egg white thermal aggregation showed a step-wise behavior as a function of temperature [12, 13]. Decreases in protein solubility occur in two steps with increasing temperature at around 55°C and 70°C due to denaturation and aggregation of ovotransferrin and ovalbumin, respectively, which are the main components of egg white proteins [14].

The apo- (iron-free) form of ovotransferrin (OVT) is the most thermolabile protein in egg [15]. OVT is the second most abundant component accounting for 12% of the total egg white protein with a molecular mass of 76 kDa. Therefore, OVT plays a major role in the initiation of egg white protein aggregation. In addition to its inherent thermodynamic properties, the thermal aggregation behavior of OVT depends on the presence of other proteins. Ovalbumin has an inhibitory effect on the thermal aggregation of OVT by suppressing the

interaction between OVT molecules at temperatures higher than the denaturation temperature of OVT but lower than that of ovalbumin [16]. Some combinations of proteins have been shown to promote aggregation with each other. Specifically, in egg white, OVT tends to aggregate with lysozyme (LYZ) during heating at moderate temperatures [17–19]. LYZ is the most alkaline protein in egg white and has high thermal stability. It has been reported that the aggregation of OVT with LYZ occurs through electrostatic attraction and disulfide bond formation [20]. Although the interactions occurring in coaggregation have been reported, the processes underlying coaggregate formation remain unclear. Determination of the coaggregation mechanism of OVT and LYZ would provide information central to understand the thermal aggregation of egg white proteins by moderate heat treatment for pasteurization.

Here, I investigated the mechanism of thermal aggregation in an OVT–LYZ binary system in terms of protein structures, aggregation rates, aggregation forces, and aggregate morphology. The heat-induced interaction between OVT and LYZ is influenced by the presence of salts and the solution pH [20]. Therefore, I adopted condition without co-solute at weak basic pH when processing egg white to clarify the fundamental tendencies of aggregation. Natural egg white releases dissolved carbon dioxide resulting in an increase in pH up to 8.5–9.2 depending on the temperature during storage [21, 22]. Moreover, total protein concentration in hen egg white is close to 10%. Thus, the aggregation experiment in this paper was investigated under the 10-fold diluted condition of pristine egg white proteins. It is worth investigating the aggregation at a diluted condition for understanding gelation of egg white, although the crowding effect is involved in the aggregation behavior at high protein concentration of the pristine egg white [12]. Establishing the mechanisms to describe this will allow control of heat treatment for pasteurization more precisely and facilitate the development of food processing methods suitable to obtain the desired product properties.

3.1.2 Materials and methods

Materials

Hen egg white ovotransferrin (iron-free) and lysozyme (six times crystallized and lyophilized) were obtained from Sigma Chemical Co. (St. Louis, MO), and were used without further purification. Glycine, Na-phosphate, Na-hydroxide, and guanidine hydrochloride were obtained from Wako Pure Chemical Inc. Ltd. (Osaka, Japan).

Preparation and thermal treatment of hen egg white proteins

A solution of hen egg white proteins was prepared according to the following procedure at ambient temperature. Hen egg white was diluted with an equal volume of 100 mM glycine buffer (pH 9.0), stirred gently with a magnetic stirrer for 1 hour, and then dialyzed using a 3000 MW cut-off dialyzed tube against 50 mM glycine buffer (pH 9.0) with four changes to remove small-molecular-weight compounds and salts. The samples were then centrifuged at 10000 × *g* for 20 min to remove undesirable large aggregates. The egg white protein contents after centrifugation were almost identical to those of the pristine sample. The supernatant diluted 5-fold with the same buffer was heated at various temperatures for 20 min. The samples were centrifuged at 15000 × *g* for 20 min, and then the supernatant was analyzed by electrophoresis.

Preparation for thermal aggregation of ovotransferrin and lysozyme mixtures

Ovotransferrin (OVT) and lysozyme (LYZ) were dissolved individually at 40 μM in 50 mM glycine buffer (pH 9.0). The protein concentration was determined by measuring the absorbance at 280 nm based on the following extinction coefficients: $E_{280\,\mathrm{nm}}^{1\%} = 12.3\ \mathrm{cm}^{-1}$ for OVT and 26.4 cm^{-1} for LYZ calculated from those amino acid sequences [23]. The following experiments were conducted by mixing these solutions.

To investigate the aggregation temperature depending on the presence of the opposite protein, a mixture of 20 μM OVT and 20 μM LYZ was heated at various temperatures for 30 min. To investigate the aggregation rate depending on the co-existing opposite protein concentration, the solutions of 20 μM OVT with 0 – 20 μM LYZ, and those of 20 μM LYZ with 0 – 20 μM OVT were heated at 55°C for various periods. To investigate the amount of aggregate and morphology depending on the mixing ratio, a mixture of OVT and LYZ with a total protein concentration of 40 μM in molar fractions of 0 – 1 was heated at 55°C for various periods. After heat treatment, the samples were centrifuged at 15000 × *g* for 20 min, and then the soluble protein concentration in the supernatant was determined by size exclusion chromatography. The sample solution before centrifugation was imaged by electron microscopy.

The affinities of OVT and LYZ were investigated as follows. Individual solutions of 40 μM OVT and LYZ were heated at 55°C for 30 min. The sample solutions were diluted 2-fold with buffer solution or mixed with the other protein solution at a ratio of 1:1 at room temperature. After 30 min, the samples were centrifuged at 15000 × *g* for 20 min, and then 80% of supernatant was replaced with 50 mM glycine buffer solution (pH 9.0). The soluble protein concentration in the supernatant was determined by size exclusion

chromatography. These centrifugation and supernatant-exchange processes were repeated three times. Finally, the precipitate was suspended in the same amount of buffer solution as before centrifugation.

Determination of soluble protein concentration using size exclusion chromatography

Soluble protein concentration was determined by high-performance liquid chromatography (HPLC) (Shimadzu, Kyoto, Japan) using a system consisting of a degasser (DGU-20A_3), a pump (LC-10AT), an auto injector (SIL-10A_{XL}), a column oven (CTO-10A), a UV–vis detector (SPD-10AV), and a system controller (SCL-10Avp) with a size exclusion column (3 μm, 300 mm × 7.8 mm i.d., Yarra SEC 3000; Phenomenex, Torrance, CA). Isocratic HPLC was performed with a flow rate of 1.0 mL/min at 30°C using 150 mM Na-phosphate buffer (pH 7.0). Aliquots of 40 μL of samples were loaded into the column. The absorbance was monitored at 280 nm. Three independent experiments were performed to determine soluble protein concentration; that was calculated from the chromatogram peak area.

Circular dichroism

Circular dichroism (CD) measurements were performed on a spectropolarimeter (J-720W; Japan Spectroscopic Co. Ltd., Tokyo, Japan) using a Peltier cell holder with a temperature controller (PTC-348W; Japan Spectroscopic Co. Ltd.). A solution of 0.5 mg/mL ovotransferrin (OVT) and lysozyme (LYZ) dissolved in 50 mM glycine buffer (pH 9.0) was prepared. The CD spectra of solutions were measured using a 1-mm path-length quartz cell for far-UV in the wavelength range of 205 – 250 nm or a 10-mm path-length quartz cell for near-UV in the wavelength range of 250 – 320 nm at room temperature. Thermal unfolding of OVT and LYZ was monitored by CD intensity change with an increasing temperature rate of 1.0°C/min.

Sodium dodecyl sulfate-polyacrylamide gel electrophoresis

The protein solutions were subjected to heat treatment and mixing, and were then mixed with 125 mM Tris-HCl (pH 6.8) loading buffer solution containing 4% (w/v) sodium dodecyl sulfate (SDS), 10% (w/v) sucrose, and 0.01% (w/v) bromophenol blue with or without 10% (v/v) β-mercaptoethanol at a ratio of 1:1. The samples were incubated for 24 hours at 25°C and then subjected to SDS-polyacrylamide gel electrophoresis (SDS-PAGE) using a 5% – 20% gradient gel (e-PAGEL; ATTO Co., Tokyo, Japan) with molecular weight marker

(Precision Plus Protein Dual Xtra Standards; Bio-Rad, Hercules, CA). The gels were then stained using Coomassie Brilliant Blue R-250.

Imaging of aggregates by transmission electron microscopy

Aliquots of 4 μL of protein solution was placed on a 150-mesh copper grid covered with a carbon-coated hydrophilic film, then the grid was dipped into pure water to wash non-adsorbed protein. Subsequently, 1% (w/v) tungstosilicic acid solution was placed on a grid in order to stain adsorbed aggregates, and then the grid was dipped in pure water again. Finally, the grid was dried for a few minutes. The samples were observed by transmission electron microscopy (TEM) (H7650; Hitachi, Tokyo, Japan) with an acceleration voltage of 80 keV.

Imaging of aggregates by optical microscopy

Aliquots of 20 μL of the heated OVT–LYZ mixtures containing 50 mM glycine (pH 9.0) were placed on a 96-well plate (Costar, Corning Inc., Lowell, MA, USA). The samples were observed using an optical microscope (BZ-X710; Keyence, Osaka, Japan).

Measurement of ζ-potential

Samples of 1 mg/mL OVT or LYZ diluted in 50 mM glycine buffer (pH 9.0) were heated at 55°C for 30 min. The surface charges of proteins before and after heating were measured at 25°C using a Zetasizer Nano Z (Malvern Instruments, Worcestershire, UK). Three runs were performed for each measurement.

GdnHCl titration and stability curve data analysis

Guanidine hydrochloride (GdnHCl) induced unfolding was described previously [24]. A solution of 0.5 mg/mL LYZ containing guanidine hydrochloride (GdnHCl) at various concentrations in 50 mM glycine buffer (pH 9.0) was prepared. GdnHCl-induced unfolding was monitored by CD at 222 nm using a 1-mm path-length quartz cell at 55°C. The conformational free energy change (ΔG) at 55°C was determined by a two-state folding mechanism. A two-state unfolding model can assume a linear dependence between ΔG and the denaturant concentration as shown in equation,

$$\Delta G = \Delta G_{H_2O} - m[\text{denaturant}]$$

where m value represents the dependence of the ΔG on denaturant.

3.1.3 Results

Thermal susceptibility to aggregation of OVT and LYZ in egg white

First, I clarified the thermal susceptibility of proteins in egg white by SDS-PAGE. Briefly, egg white protein dialyzed against 50 mM glycine buffer (pH 9.0) was heated at various temperatures for 20 min. The heated samples were analyzed by SDS-PAGE under reducing and non-reducing conditions (Fig. 3.1.1). Under reducing conditions, the gel patterns showed clear bands of OVT at 76 kDa, ovalbumin at 45 kDa, and LYZ at 14 kDa with minor bands of ovoinhibitor and ovoglobulin at approximately 50 kDa under reducing conditions. With the exception of these proteins, bands of minor proteins in egg white were not observed under these conditions. OVT and LYZ bands were faint in the samples heated at temperatures above 60°C. Even with heating to 80°C, there were no changes in the compositions of other proteins. Under non-reducing conditions, another band was observed at 90 kDa corresponding to dimeric ovalbumin. The band of aggregates appeared in samples heated at 55°C, and those of OVT and LYZ disappeared at 60°C. The bands of ovoinhibitor and ovoglobulin became obscure with heating to temperatures above 60°C. At an even higher temperature of 75°C, the monomeric ovalbumin band decreased, and a smear band appeared that was assumed to be comprised of multimeric ovalbumin. These results indicated that OVT and LYZ were heat-susceptible to aggregation compared to the other major egg white proteins, consistent with many previous reports [17, 25, 26]. Liu *et al.* have demonstrated that OVT and LYZ mainly aggregate by heating at above 60°C not 55°C at pH 9 [17, 25]. Their results have a slight difference from the results presented here. The differences are derived from coexisting low-molecular-weight compounds. They did not remove low-molecular-weight compounds originally included in egg white and excessive ions for pH adjustment by dialysis. The protein aggregation also depends on pH and salt concentration [12]. The solution used in this study was at weak basic pH, without any other salts except for a buffer-agent. Thus, differences in the preparation of egg white proteins can lead to different behavior of the aggregation.

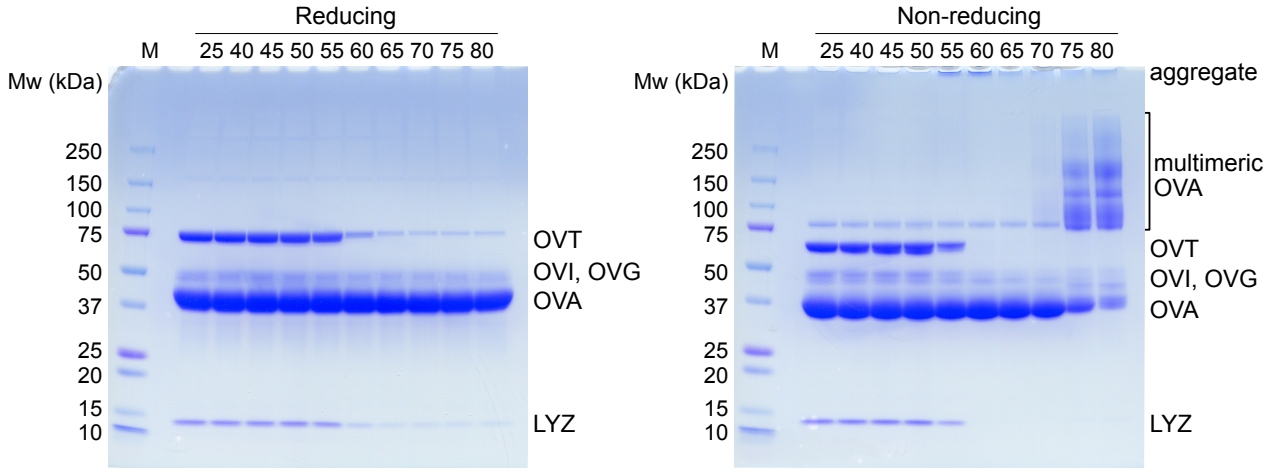

Figure 3.1.1 SDS-PAGE analyses of heat-induced aggregation of egg white proteins under reducing and non-reducing conditions. The numbers in the upper part of the figures indicate the temperatures of heat treatment (°C). OVT, OVI, OVG, OVA, and LYZ indicate ovotransferrin, ovoinhibitor, ovoglobulin, ovalbumin, and lysozyme, respectively. Lane M, Standard molecular weight marker.

Inclusion of LYZ in aggregates of OVT

To understand the cooperative aggregation between OVT and LYZ, a simple system was prepared using purified OVT and LYZ. Three types of samples were prepared (20 μM OVT, 20 μM LYZ, and 20 μM OVT + 20 μM LYZ), and heated at various temperatures for 30 min. The supernatant concentrations of OVT and LYZ were measured by size exclusion chromatography. Figure 3.1.2 shows the soluble concentrations of OVT (Fig. 3.1.2A) and LYZ (Fig. 3.1.2B). OVT formed aggregates at temperatures above 50°C regardless of the presence or absence of LYZ, and completely formed aggregates at temperatures of 60°C or higher (Fig. 3.1.2A). In contrast, LYZ alone required a temperature higher than 65°C for aggregation. However, LYZ formed aggregates in the presence of OVT even at 50°C (Fig. 3.1.2B). The aggregation ability of LYZ was remarkably enhanced by the presence of OVT, while that of OVT was not altered by the presence of LYZ as a function of temperature.

Protein unfolding is responsible for the first step of thermal aggregation. Therefore, protein unfolding was monitored by circular dichroism spectroscopy (Fig. 3.1.3). The melting temperature of OVT was defined as 64.0°C for far-UV and 59.8°C for near-UV, indicating that the tertiary structure monitored by near-UV was more susceptible than the secondary structure monitored by far-UV. The melting temperature of LYZ was defined as 72.7°C for far-UV and 73.5°C for near-UV. The secondary and tertiary structures of LYZ were perturbed at a similar temperature. These data indicated that OVT is partially unfolded by heat treatment, while

LYZ retains the native structure at ~55°C. Therefore, the aggregation of LYZ at 50°C – 60°C, as shown in Figure 3.1.2B, was suggested to be caused by the unfolding and/or aggregation of OVT. That is, LYZ molecules were included in the aggregates of OVT. Therefore, I focused on the coaggregation of OVT and LYZ at 55°C for further analyses.

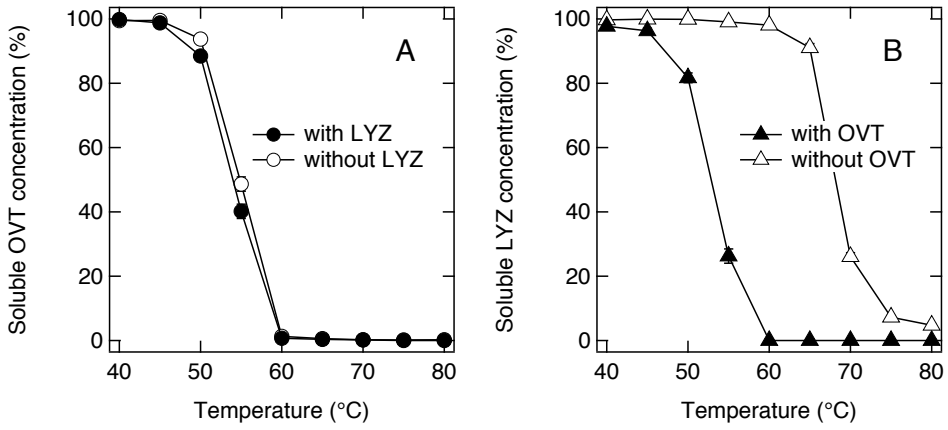

Figure 3.1.2 Soluble protein concentration of OVT–LYZ mixture after heating at various temperatures for 30 min. (A) Samples contained 20 μM OVT in the presence (closed circles) or absence (open circles) of 20 μM LYZ. (B) Samples contained 20 μM LYZ in the presence (closed triangles) or absence (open triangles) of 20 μM OVT.

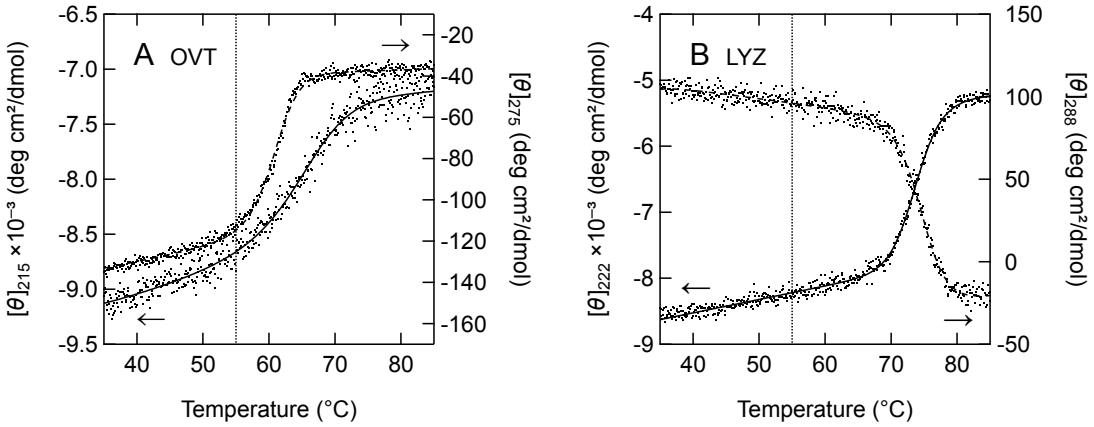

Figure 3.1.3 Thermal unfolding curves of OVT (A) and LYZ (B) monitored by far-UV CD (left axis, solid line) and near-UV CD (right axis, broken line). The dotted lines at 55°C indicate the temperature of heat treatment in this study.

To elucidate the dependence of OVT and LYZ aggregation rate on the opposite protein concentration (i.e., LYZ and OVT, respectively), the heat-induced aggregation of protein mixtures was measured by size exclusion chromatography. Briefly, solutions containing 20 μM OVT with 0 – 20 μM LYZ, and *vice versa*, were heated at 55°C for various periods. The concentrations of the soluble protein are plotted in Figure 3.1.4. OVT was prone to form aggregates without LYZ; 52% of OVT molecules formed aggregates during heating for 30 min (Fig. 3.1.4A). With increasing concentration of LYZ, the aggregation rate of OVT increased for the initial several min. This tendency suggested that the unfolded but not yet aggregated OVT molecules were promoted to undergo aggregation by the interaction with native LYZ molecules. Soluble OVT concentration decreased by 61% when mixed with an equimolar amount of LYZ after heating for 30 min. On the other hand, LYZ did not form aggregates by heat treatment at 55°C for 30 min. However, LYZ was prone to form aggregates depending on the increase in OVT concentration (Fig. 3.1.4B). These data indicate that the aggregation of OVT and LYZ affected each other. Based on these results, it is important to track the time course of changes in protein concentration during heating to gain an understanding of the overall picture of the phenomenon.

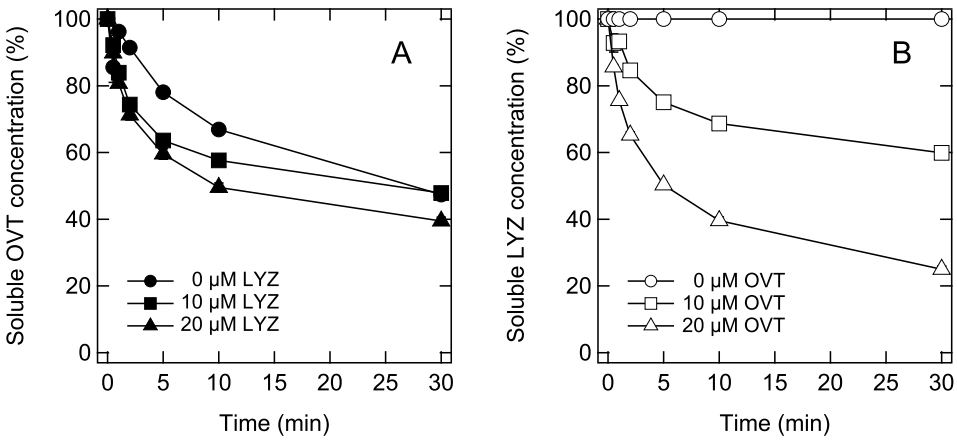

Figure 3.1.4 Soluble protein concentration of OVT–LYZ mixture after heating at 55°C for various periods. (A) Samples contained 20 μM OVT and 0 (closed circles), 10 (closed squares), or 20 (closed triangles) μM LYZ. (B) Samples contained 20 μM LYZ and 0 (open circles), 10 (open squares), or 20 (open triangles) μM OVT.

Subsequently, I investigated the protein compositions of OVT and LYZ for collaborative aggregation. Briefly, mixtures of OVT and LYZ with a total protein concentration of 40 μM in molar ratios of 2:8, 4:6, 5:5, 6:4, and 8:2 were heated at 55°C for various periods, and the residual soluble protein concentration was then

determined by size exclusion chromatography (Fig. 3.1.5). The amount of aggregate was calculated from the difference between initial and residual soluble concentrations after heating. Figure 3.1.5A shows the profiles of the samples [OVT:LYZ = 2:8] of soluble LYZ, aggregated LYZ, aggregated OVT, and soluble OVT during heat treatment. The amount of aggregated LYZ increased during heat treatment, while that of soluble LYZ decreased. Similarly, the amount of aggregated OVT increased during heat treatment, while the amount of soluble OVT decreased. The amount of OVT aggregate increased with increasing fraction of OVT, and the profiles were similar at all mixing ratios of the samples from [OVT:LYZ = 2:8] to [OVT:LYZ = 8:2]. In contrast, the amount of LYZ aggregate increased proportionally with the OVT fraction. The aggregated ratio of OVT and LYZ was constantly 5:6 throughout heating at mixing molar ratios from [OVT:LYZ = 2:8] to [OVT:LYZ = 6:4] (Figs. 3.1.5A – 3.1.5D). The sample of [OVT:LYZ = 8:2] was depleted of soluble LYZ during heating, and then OVT alone formed aggregates (Fig. 3.1.5E). The amount of aggregated LYZ was dependent on the amount of aggregated OVT.

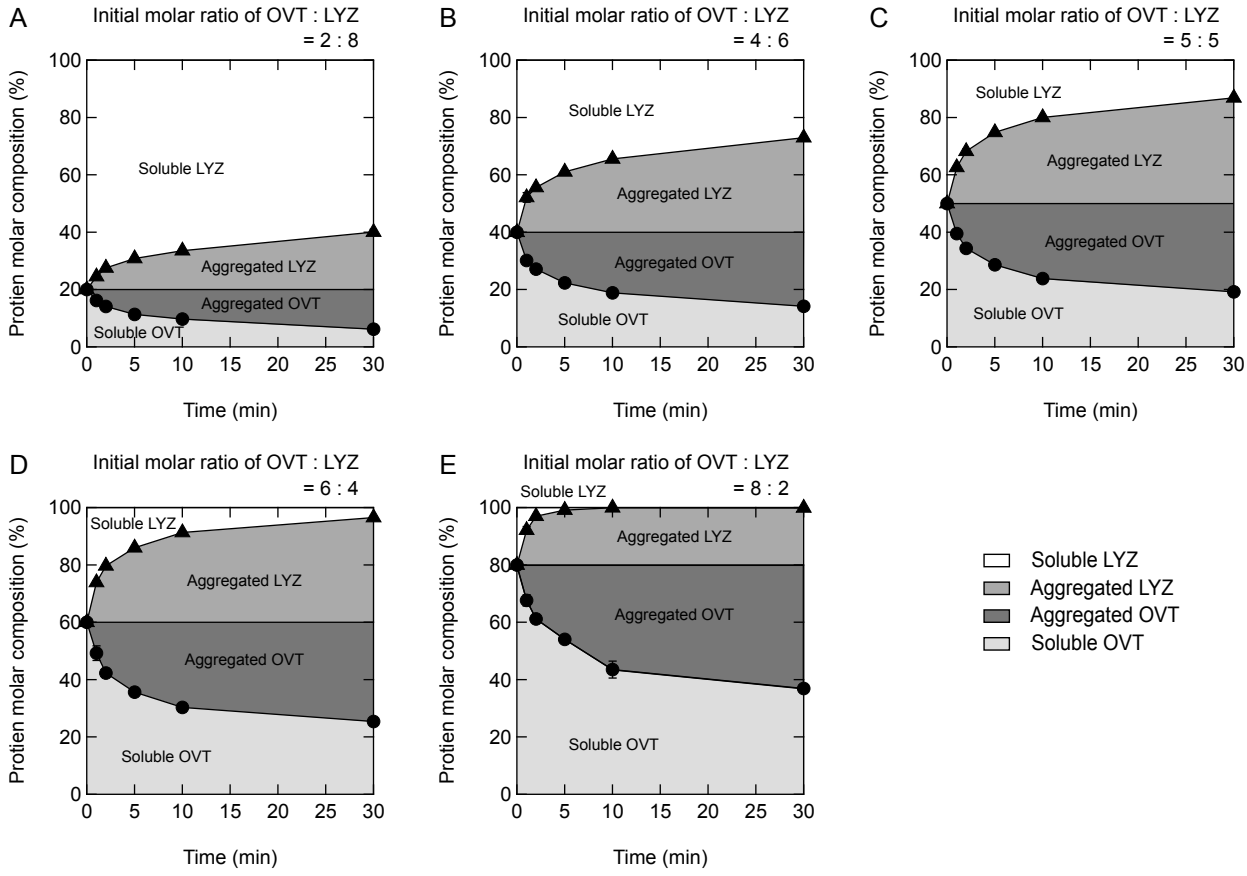

Figure 3.1.5 Time course of changes in protein composition in OVT–LYZ coaggregation at 55°C with various mixture ratios. Mixtures of OVT and LYZ with total protein concentration of 40 μM in molar ratios of 2:8 (A), 4:6 (B), 5:5 (C), 6:4 (D), and 8:2 (E) were heated at 55°C for various periods.

To summarize these results, coaggregation of OVT and LYZ occurs with thermal unfolded OVT as a trigger. OVT forms aggregate spontaneously at 55°C, which is accelerated with increasing LYZ concentration. In contrast, LYZ is passively aggregated by inclusion in OVT aggregates. Before depletion of soluble LYZ, the coaggregation reaction occurs uniformly throughout the heating process regardless of the initial mixing molar ratio.

Morphology of coaggregates of OVT and LYZ

The morphology of protein aggregates is thought to depend on the aggregated protein composition. Mixtures of OVT and LYZ with a total protein concentration of 40 μM in various mixing molar ratios were heated at 55°C for 30 min, and the morphologies of the aggregates were then imaged by optical microscopy (Fig. 3.1.6) and TEM (inset in Fig. 3.1.6). No aggregate observed in the samples of LYZ alone (Fig. 3.1.6A) and OVT alone (Fig. 3.1.6K). OVT and LYZ have negative and positive charges, respectively, at pH 9. Thus, the sample of OVT and LYZ alone did not form large aggregates due to the electrostatic repulsion (Figs. 3.1.6A and 3.1.6K).

In contrast, the samples of OVT–LYZ mixtures formed aggregates in all mixture ratios. The aggregates have a hierarchical structure with a macroscopic network observed by optical microscope composed of submicron colloids with a microscopic network observed by TEM. More specifically, the network structures of the aggregates differed according to the mixing ratio. The aggregates in [OVT:LYZ = 1:9] to [OVT:LYZ = 7:3] showed a similar micro-network structure composed of small submicron colloids (Figs. 3.1.6B – 3.1.6H inset). The colloids in [OVT:LYZ = 1:9] to [OVT:LYZ = 7:3] formed a coarse macro-network structure (Figs. 3.1.6B – 3.1.6G). Although the submicron colloids in [OVT:LYZ = 7:3] showed a micro-network structure, the aggregates were dispersed macroscopically (Fig. 3.1.6H). The aggregates of [OVT:LYZ = 8:2] was similar to that of [OVT:LYZ = 7:3] (Fig. 3.1.6I). The aggregates of [OVT:LYZ = 9:1] decreased comparing to that of [OVT:LYZ = 8:2] (Fig. 3.1.6J). The difference of the aggregate structure results from the electrostatic repulsion between small colloids. The insufficient amount of positively LYZ against negatively OVT in the solution increases the proportion of OVT in the coaggregates, leading to the inhibition of large network due to the electrostatic repulsion between negatively-charged colloids.

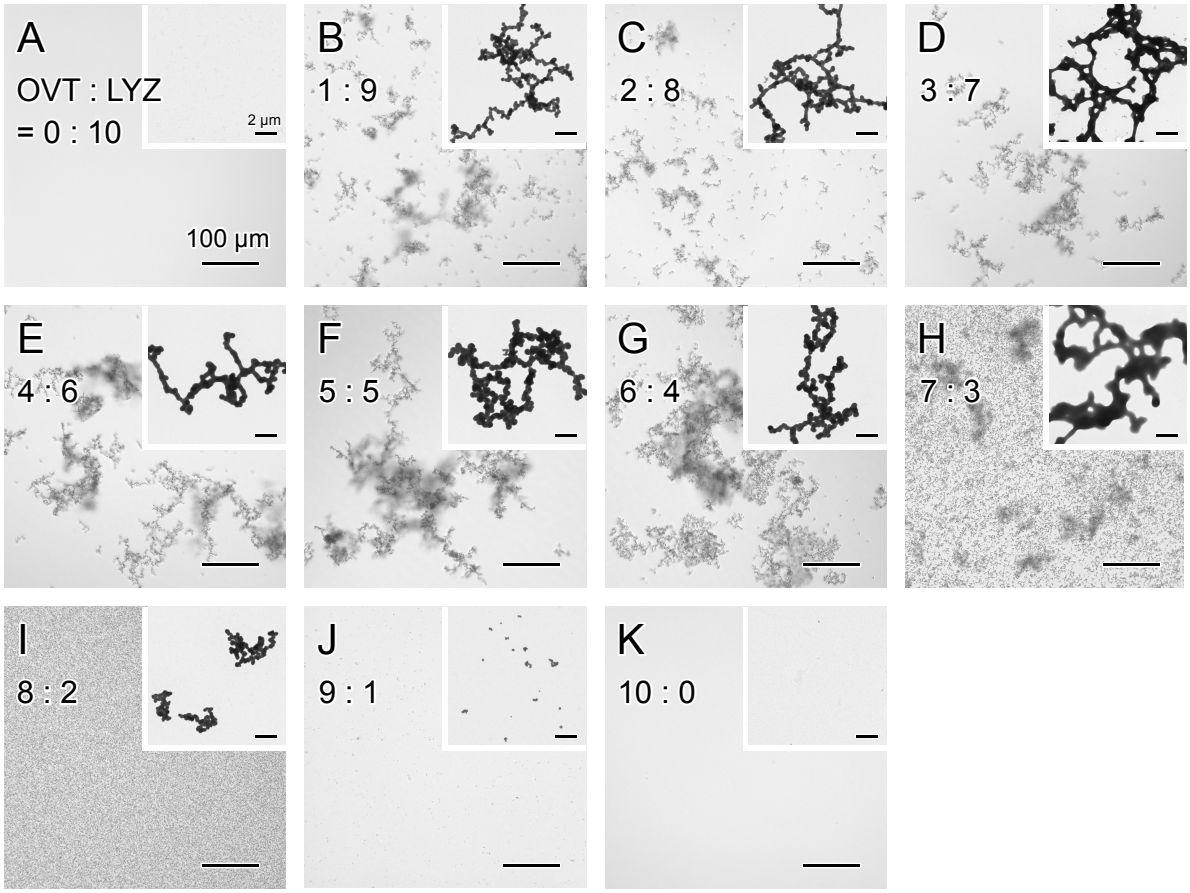

Figure 3.1.6 Morphology of OVT–LYZ aggregates by optical microscopy and TEM (inset). Mixtures of OVT and LYZ with total protein concentration of 40 μM in molar ratios of 0:10 (A), 1:9 (B), 2:8 (C), 3:4 (D), 4:6 (E), 5:5 (F), 6:4 (G), 7:3 (H), 8:2 (I), 9:1 (J), and 10:0 (K) were heated at 55°C for 30 min. The scale bars represent 100 μm for optical microscopy and 2 μm for TEM image.

Association of native LYZ with OVT aggregates

To evaluate the association of OVT and LYZ during the growth of coaggregates, I prepared proteins in both native and heated states and analyzed the affinity between native OVT (nOVT), native LYZ (nLYZ), heated OVT (hOVT), and heated LYZ (hLYZ). Briefly, solutions of 40 μM OVT and LYZ were individually heated at 55°C for 30 min. Subsequently, the native or heated OVT and LYZ solutions were mixed with each other at a ratio of 1:1 at 25°C. In addition, nOVT and nLYZ were mixed and then heated at 55°C for 30 min, which was designated as "co-hOVT–LYZ." Then, soluble proteins in the samples were analyzed by size exclusion chromatography (Fig. 3.1.7 A).

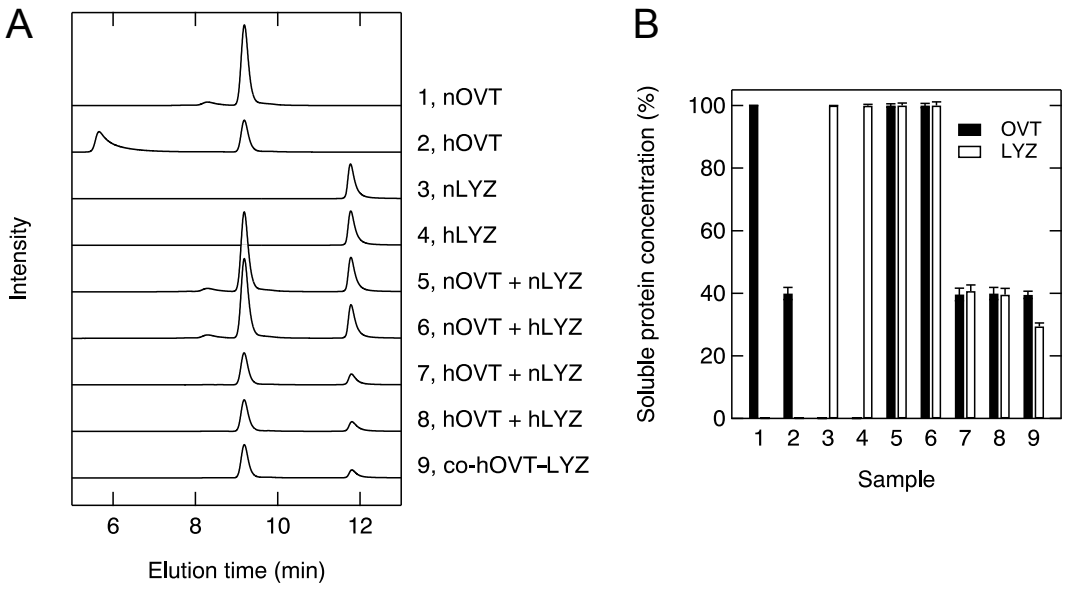

Figure 3.1.7 Size exclusion chromatograms (A) and soluble protein concentrations (B) of the supernatants of OVT–LYZ mixtures. nOVT, native OVT. hOVT, OVT heated at 55°C for 30 min nLYZ, native LYZ. hLYZ, LYZ heated at 55°C for 30 min. The + symbols indicate mixtures of native protein or heat-treated protein. "co-hOVT–LYZ" indicates the sample in which nOVT and nLYZ mixture was heated at 55°C for 30 min.

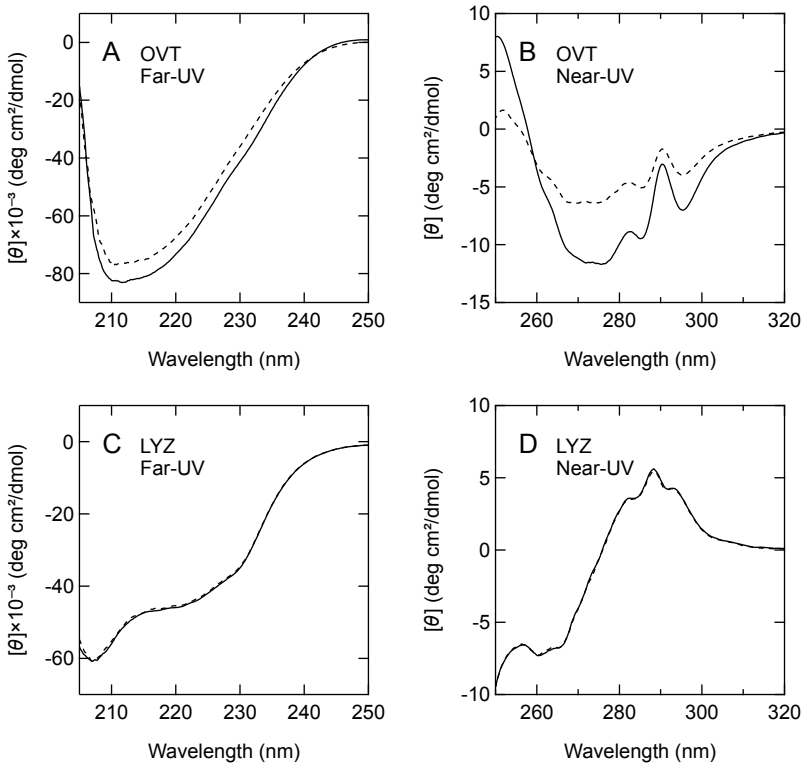

Figure 3.1.8 Circular dichroism spectra. Samples of OVT (A and B) and LYZ (C and D) were heated at 55°C for 30 min. The protein structure was monitored by far-UV (A and C) and near-UV (B and D) before (solid lines) and after (broken lines) heating.

The sample of nOVT showed two peaks at elution times of around 8 min and 9 min, which corresponded to dimer and monomer, respectively. In contrast, the sample of hOVT showed a further peak at around 6 min corresponding to soluble aggregates. Circular dichroism spectroscopy showed that hOVT had a partially denatured conformation (Figs. 3.1.8A and 3.1.8B). Thus, the soluble aggregates contained in the sample of hOVT were considered to be composed of denatured OVT. The sample of nLYZ showed only one peak at 12 min as a monomeric form. On the other hand, the peak of hLYZ on the chromatogram was identical to that of nLYZ. Circular dichroism spectra indicated that LYZ retained the native three-dimensional structure even after heating at 55°C (Figs. 3.1.8C and 3.1.8D).

The peaks of "nOVT + nLYZ" and "nOVT + hLYZ" samples on the chromatogram showed the addition of those of nOVT and nLYZ or nOVT and hLYZ, respectively. These results indicated that native OVT did not interact with LYZ. In contrast, the "hOVT + nLYZ" and "hOVT + hLYZ" samples showed two peaks of monomeric OVT and LYZ, rather than the soluble aggregates of hOVT. The native LYZ peak area of "hOVT + hLYZ" was simultaneously lower than that of "nOVT + hLYZ." These results suggest that the soluble aggregates of OVT formed insoluble precipitates with LYZ molecules. Note that the chromatograms of "co-hOVT–LYZ" showed two peaks of monomeric OVT and LYZ, which was similar to the sample of "hOVT + hLYZ."

For quantitative comparison, I calculated the protein concentrations from the chromatograms (Fig. 3.1.7B). After heat treatment, the concentration of soluble OVT decreased to 40%, while that of LYZ remained at 100%. The soluble protein concentrations of OVT and LYZ in "nOVT + nLYZ" and "nOVT + hLYZ" samples remained constant corresponding to the control samples. On the other hand, the soluble LYZ concentrations in "hOVT + nLYZ" and "hOVT + hLYZ" samples decreased to 40%, while the soluble OVT concentration was identical regardless of nLYZ and hLYZ. These results indicated that monomeric LYZ has affinity for soluble aggregates composed of unfolded OVT rather than native OVT.

Furthermore, the identical concentrations of soluble OVT and LYZ indicated that the precipitates formed in "hOVT + nLYZ" and "hOVT + hLYZ" samples were composed of equimolar amounts of OVT and LYZ. Importantly, the ratio of the amount of precipitated LYZ and OVT was not dependent on the mixing ratio in the "hOVT + nLYZ" samples (Fig. 3.1.9), indicating that the association reaction of native LYZ onto the aggregates of OVT reached saturation. However, the precipitates formed by mixing after heating did not correspond to the aggregates formed by co-heating in terms of protein composition, i.e., the coaggregates

formed in “co-hOVT–LYZ” samples were composed of OVT and LYZ at a molar ratio of 5:6 as shown in Figure 3.1.5. Assuming that the amount of LYZ involved in aggregation of OVT was dependent on the accessible surface area of OVT aggregates, due to the lack of possibility for LYZ to come into contact with internal OVT molecules, the amount of LYZ contained in the precipitates of the “hOVT + nLYZ” samples was less than that in the coaggregates of “co-hOVT–LYZ” samples.

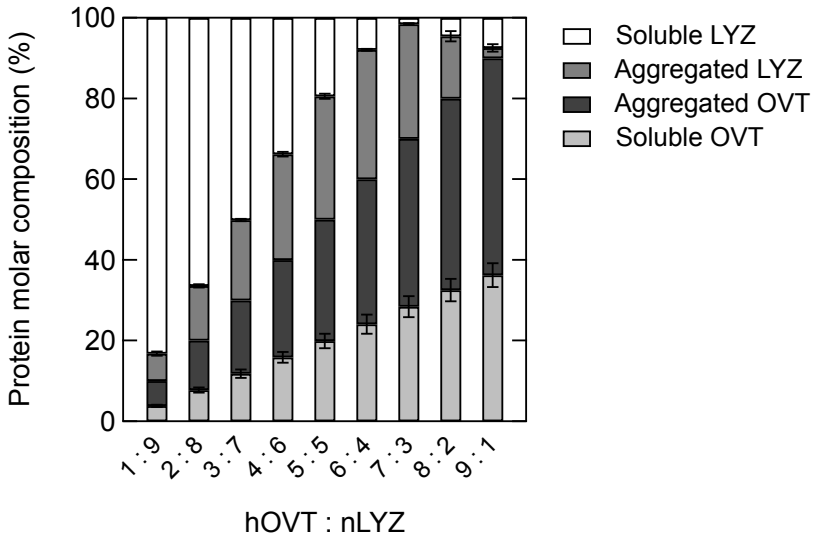

Figure 3.1.9 Protein compositions in “hOVT + nLYZ” samples at various mixture ratios. The soluble protein concentration was determined by size exclusion chromatography. The amounts of aggregates were calculated from the difference between initial and residual soluble concentrations after heating.

Neutralization of surface charge of OVT aggregates with LYZ

As electrostatic interaction between OVT and LYZ is thought to play an important role in coaggregation, I investigated the ζ-potentials of OVT and LYZ in 50 mM glycine buffer (pH 9.0) and then examined the relationship between the charged state and the aggregation ratio of OVT and LYZ (Table 3.1.1). The ζ-potential was –12 mV for nOVT, while that for hOVT was more negative at –16 mV. This difference in ζ-potential before and after heating may have been due to thermal unfolding and misfolding during heating and cooling. The ζ-potentials of nLYZ and hLYZ showed the same value of +7 mV, indicating that the native structure was retained even after heat treatment.

Table 3.1.1 ζ-Potentials of OVT and LYZ in 50 mM glycine (pH 9).

Sample	ζ-Potential (mV)
Native OVT (nOVT)	–11.9 ± 0.4
55°C-heated OVT (hOVT)	–16.3 ± 0.3
Native LYZ (nLYZ)	+7.1 ± 0.3
55°C-heated LYZ (hLYZ)	+7.0 ± 0.6

To evaluate the contribution of electrostatic interaction between OVT and LYZ to coaggregation, it is reasonable to compare the ζ-potentials of unfolded OVT and native LYZ. The absolute value of the ζ-potential of nLYZ was less than half that of hOVT (Table 3.1.1). The soluble protein concentration as shown in Figure 3.1.7B indicated that the coaggregates in the "co-hOVT–LYZ" sample and the precipitates in the "hOVT + nLYZ" and "hOVT + hLYZ" samples consisted of OVT and LYZ at molar ratios of 5:6 and 5:5, respectively. These results suggested that the net charges of the coaggregates and precipitates were negative. Nevertheless, LYZ molecules included in the coaggregates were sufficient to suppress the electrostatic repulsion between OVT soluble aggregates due to neutralization of charge on the surface. That is, LYZ molecules decreased the colloidal stability of the OVT soluble aggregates, leading to growth into large precipitates by hydrophobic attraction. Therefore, the interaction of native LYZ with OVT aggregates is thought to facilitate the formation of their insoluble aggregates.

Non-covalent and covalent bonding between native LYZ and aggregated OVT

Disulfide bond exchange is generally one of the most important reactions in the thermal aggregates of proteins. To investigate the disulfide bond exchange reaction, I performed SDS-PAGE analyses of reduced or non-reduced samples of OVT–LYZ aggregates (Fig. 3.1.10). Solutions of nOVT, hOVT, nLYZ, and hLYZ were loaded as controls. Under reducing conditions, nOVT and hOVT solutions showed a clear band corresponding to monomer with numerous smaller molecular weight bands. As these minor bands were not observed in pristine egg white proteins, it was assumed that they were derived from peptide fragments of OVT. Under non-reducing conditions, the aggregates were observed in hOVT in addition to the monomer, which corresponded to the results of size exclusion chromatography (Fig. 3.1.7A). These results indicated that OVT soluble

aggregates were formed by covalent bonds. The nLYZ and hLYZ solutions showed a monomer band under reducing and non-reducing conditions.

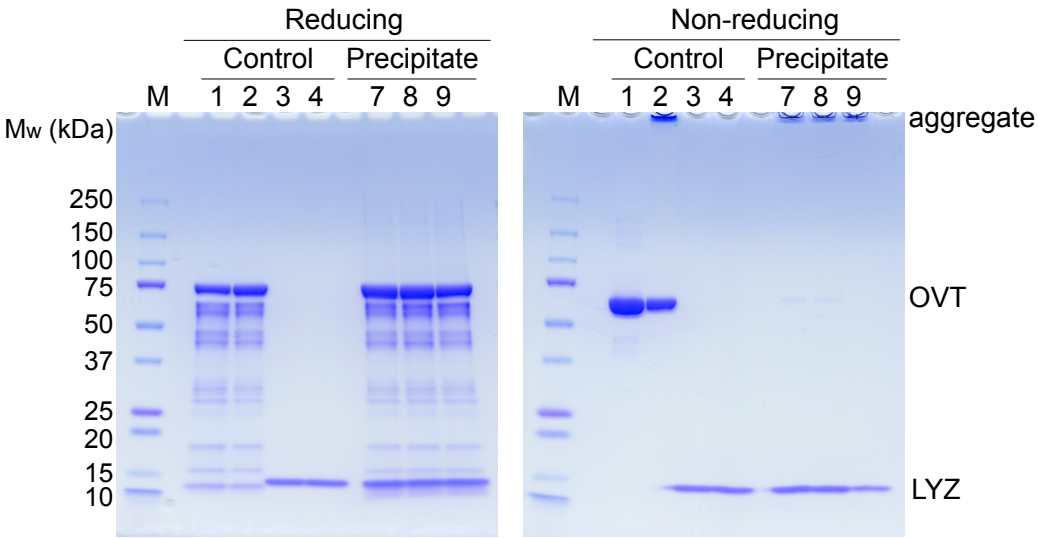

Figure 3.1.10 SDS-PAGE analysis of precipitate formed in OVT–LYZ mixtures. The entire solutions of nOVT (Lane 1), hOVT (Lane 2), nLYZ (Lane 3), and hLYZ (Lane 4) were loaded as controls. The precipitates of "hOVT + nLYZ" (Lane 7), "hOVT + hLYZ" (Lane 8), and "co-hOVT–LYZ" (Lane 9) were washed and then loaded on the gel. Lane M, Standard molecular weight marker.

The precipitates of the samples of "hOVT + nLYZ," "hOVT + hLYZ," and "co-hOVT–LYZ" were analyzed by SDS-PAGE (Fig. 3.1.10). The protein compositions of the precipitates formed in the three samples showed similar patterns. No monomeric OVT band was observed in the precipitates under non-reducing conditions, caused by the interaction between OVT aggregates and native LYZ for the formation of precipitates. The intensities of the LYZ band observed in "hOVT + nLYZ" and "hOVT + hLYZ" were similar under reducing and non-reducing conditions, indicating that the soluble aggregates of OVT and monomers of LYZ formed precipitates via non-covalent interactions. In contrast, the intensity of the LYZ band in the "co-hOVT–LYZ" sample was weaker under non-reducing than reducing conditions, indicating that LYZ partially formed aggregates via formation of both covalent bonds and non-covalent interactions with unfolded OVT. Therefore, intermolecular disulfide bond exchange plays a key role in the interactions involved in the formation of insoluble aggregates of "co-hOVT–LYZ" samples during heat treatment.

3.1.4 Discussion

Egg white is a complex mixture containing various kinds of proteins. This heterogeneous mixture of proteins is common in foods. Protein aggregation increases in complexity with increasing heterogeneity of protein composition. The results presented here suggest the coaggregation of OVT and LYZ with heating at low temperatures for pasteurization.

Initiation of OVT–LYZ coaggregation by aggregation of OVT

The simple process of thermal aggregation of a protein generally follows three steps: the initial unfolding, the formation of aggregates via hydrophobic interactions, and crosslinking between aggregates through disulfide exchange reaction [2]. The coaggregation of egg white proteins is thought to be initiated by OVT aggregates according to the above process. OVT was unfolded into the molten globule state by heat treatment at 55°C, which perturbed the tertiary structure, resulting in the formation of soluble aggregates [27]. However, Matsudomi *et al.* reported that OVT did not form aggregates at 65°C at pH 9 [20]. This discrepancy may be explained by differences between the experimental methods used in these studies; the aggregates were detected only by turbidity measurement rather than chromatography in these previous studies. In contrast, we showed here that OVT formed soluble aggregates while the solution remained transparent. The coaggregation was then promoted by binding between OVT aggregates and LYZ molecules.

Association of native LYZ with OVT aggregates

The presence of proteins with the opposite net charge promotes protein–protein interactions, which impacts the aggregate networks [28]. The electrostatic interaction between OVT and LYZ plays an important role in the coaggregation observed in this study. In fact, the coaggregation of OVT and LYZ in egg white has been confirmed only at pH between the isoelectric points of the proteins [17]. The association of proteins with opposite net charges via electrostatic interaction, called coacervation, is often seen in extremely low ionic strength environments [29]. Positively charged LYZ has reported to undergo coacervation with negatively charged proteins, such as ovalbumin, β-lactoglobulin, and bovine serum albumin in the native state [30–32]. In addition, protein–poly(amino acid) complexes involve similar aggregative associations mainly by electrostatic interactions [33, 34]. These coacervates and aggregative complexes are stabilized mainly by

electrostatic attraction under conditions of low ionic strength. Association of ovalbumin and LYZ via non-covalent interaction is reported in Chapter 4 [35]. Native ovalbumin and native LYZ associate via mainly electrostatic attraction; hence, the association is easily inhibited in the presence of 25 mM NaCl. In contrast, partially unfolded ovalbumin and native LYZ associate via hydrophobic interaction in addition to electrostatic attraction. In the presence study, OVT–LYZ coaggregates are stabilized by an electrostatic attraction and other processes, including hydrophobic and covalent interactions. It has been reported that LYZ is not involved in thermal aggregation of OVT as ion concentrations increased [20]. The electrostatic interactions between proteins are weakened by the electrostatic shielding by the addition of ions [36]. From another perspective, coaggregation can be controlled by the choice of solution additives, typically arginine, for thermal aggregation of egg white proteins [6].

Crosslinkage of disulfide bonds

The sulfhydryl–disulfide exchange reaction occurs between proteins after they come into contact via non-covalent bonds. A previous study of the coaggregation of ovalbumin and LYZ at 70°C indicated that LYZ completely aggregated with equimolar ovalbumin due to crosslinking between disulfide bonds of LYZ and sulfhydryl groups of ovalbumin [28]. As LYZ partially unfolded at 70°C, the four intramolecular disulfide bonds of LYZ would have a probability of coming into contact with the exposed free sulfhydryl groups of unfolded ovalbumin. In contrast, a heating temperature of 55°C was selected in this study, which is markedly lower than the melting temperature of LYZ at 73°C (Fig. 3.1.11). The guanidine hydrochloride titration experiment showed that the stability (ΔG) of LYZ at 55°C was approximately 20 kJ/mol, indicating that almost all of the LYZ molecules retained the native folded state (Fig. 3.1.11 and Table 3.1.2) [37]. However, the one disulfide bridge, C6–C127, which combines the C-terminus with the N-terminus, is partially exposed to the solvent [38]. Native LYZ associated with the OVT aggregates via electrostatic and hydrophobic interactions may crosslink with the aggregates via the C6–C127 disulfide bond. Some LYZ molecules heated with OVT were observed to form covalent bonds within the aggregates (Fig. 3.1.10). The formation of disulfide bonds is attributed to the aggregate network. However, it was not plausible that a single disulfide bond in the LYZ molecule contributed significantly to the structure of the aggregate network.

The network of protein aggregates and gels formed by thermal treatment exhibits a fractal microstructure stiffened with disulfide bonds [39, 40]. This study showed a similar fractal network structure of coaggregates

formed by OVT and LYZ (Fig. 3.1.6). LYZ binds to the soluble aggregates of OVT, leading to insolubilization, followed by the formation of disulfide bonds of OVT–LYZ aggregates between themselves, which contributes to the formation of a rigid network structure.

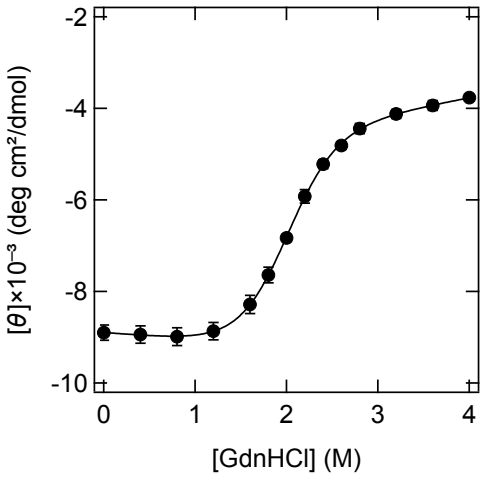

Figure 3.1.11 GdnHCl titration curve of LYZ with 50 mM glycine (pH 9.0) at 55°C. The solid line shows the two-state theoretical curve of LYZ.

Table 3.1.2 ΔG values of LYZ in 50 mM glycine (pH 9.0).

ΔG_{H_2O} at 55°C (kJ/mol)	m (kJ/mol/M)	$[GdnHCl]_{50\%}$ (M)
20.1 ± 0.7	10.1 ± 0.4	1.98 ± 0.01

Coaggregation process of OVT and LYZ

Here, I propose a molecular mechanism of coaggregation between OVT and LYZ considering the results of this study (Fig. 3.1.12). The process of coaggregation can be divided into the following steps: (i) unfolding, and then aggregation of OVT itself via hydrophobic interactions and disulfide bond formation; (ii) the association of native LYZ with the aggregates of OVT via electrostatic and hydrophobic interactions; (iii) the insolubilization of the aggregates of OVT with native LYZ due to colloidal instability; (iv) the crosslinking of disulfide bonds between adjacent aggregates of OVT, and secondarily across native LYZ and aggregated OVT in the inside; and finally (v) growth of the aggregates with a fractal structure. OVT alone formed stable soluble

aggregates due to the dominance of long-range electrostatic repulsion over short-range attraction [41]. The association of LYZ suppressed the electrostatic repulsion between soluble aggregates of OVT leading to insolubilization. Since electrostatic interaction is a considerable driving force in the coaggregation, the protein composition ratio is thought to be influenced by the protein charge state depended on the solution pH and the presence of ions. Subsequently, OVT aggregates could come into contact with each other, with further crosslinking of disulfide bonds resulting in the formation of a large network.

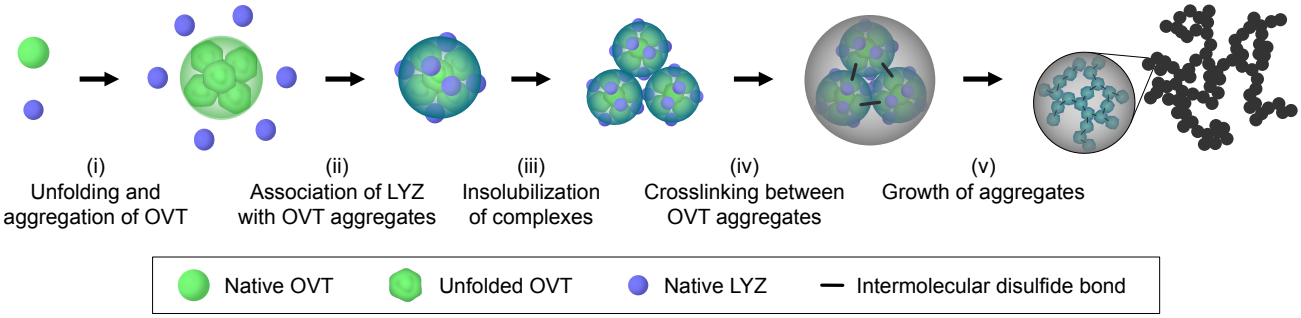

Figure 3.1.12 Schematic diagram of coaggregation process of OVT and LYZ.

3.1.5 Conclusion

Here, I elucidated the coaggregation process of OVT and LYZ at pH 9 at a moderate temperature, which was higher than the melting temperature of OVT but lower than that of LYZ. Thermally unfolded OVT aggregated with the inclusion of native LYZ. Native LYZ promoted the aggregation of unfolded OVT, and the precipitation of soluble OVT aggregates by association via non-covalent interactions. Some of the LYZ included in the aggregates formed intermolecular disulfide bonds, although it was considered to be in the native state. The association of native LYZ with OVT aggregates decreased the colloidal stability due to the suppression of electrostatic repulsion, which allowed the formation of crosslinking by disulfide bonds between OVT aggregates, leading to growth to a large network with a fractal structure. These results represent valuable information to allow optimal heat treatment for pasteurization and gelation of egg white. For example, egg white contains almost the same molar amounts of OVT and LYZ. Accordingly, the removal of LYZ from egg white may inhibit the overgrowth of aggregates by coaggregation, which would affect the value of final

marketable egg products. In the actual processing of food in general, interactions with unexpected ingredients play key roles in the behavior of protein aggregation.

References

[1] Abeyrathne, E. D. N. S., Lee, H. Y. & Ahn, D. U. Egg white proteins and their potential use in food processing or as nutraceutical and pharmaceutical agents—A review. *Poult. Sci.* 92, 3292–3299 (2013).

[2] Mine, Y. Recent advances in the understanding of egg white protein functionality. *Trends Food Sci. Technol.* 6, 225–232 (1995).

[3] Mine, Y. Egg proteins. in *Applied Food Protein Chemistry* (ed. Ustunol, Z.) John Wiley & Sons, Ltd. 459–490 (2015).

[4] Gharbi, N. & Labbafi, M. Effect of processing on aggregation mechanism of egg white proteins. *Food Chem.* 252, 126–133 (2018).

[5] Van der Plancken, I., Van Loey, A. & Hendrickx, M. E. Effect of heat-treatment on the physico-chemical properties of egg white proteins: A kinetic study. *J. Food Eng.* 75, 316–326 (2006).

[6] Hong, T., Iwashita, K., Handa, A. & Shiraki, K. Arginine prevents thermal aggregation of hen egg white proteins. *Food Res. Int.* 97, 272–279 (2017).

[7] Handa, A., Hayashi, K., Shidara, H. & Kuroda, N. Correlation of the protein structure and gelling properties in dried egg white products. *J. Agric. Food Chem.* 49, 3957–3964 (2001).

[8] Handa, A., Takahashi, K., Kuroda, N. & Froning, G. W. Heat-induced egg white gels as affected by pH. *J. Food Sci.* 63, 403–407 (1998).

[9] Hamada, H., Arakawa, T. & Shiraki, K. Effect of additives on protein aggregation. *Curr. Pharm. Biotechnol.* 10, 400–407 (2009).

[10] Totosaus, A., Montejano, J. G., Salazar, J. A. & Guerrero, I. A review of physical and chemical protein-gel induction. *Int. J. Food Sci. Tech.* 37, 589–601 (2002).

[11] Van der Plancken, I., Van Loey, A. & Hendrickx, M. E. Changes in sulfhydryl content of egg white proteins due to heat and pressure treatment. *J. Agric. Food Chem.* 53, 5726–5733 (2005).

[12] Iwashita, K., Inoue, N., Handa, A. & Shiraki, K. Thermal aggregation of hen egg white proteins in the presence of salts. *Protein J.* 34, 212–219 (2015).

[13] Matsuda, T., Watanabe, K. & Sato, Y. Heat-induced aggregation of egg white proteins as studied by vertical flat-sheet polyacrylamide gel electrophoresis. *J. Food Sci.* 46, 1829–1834 (1981).

[14] Kovacs-Nolan, J., Phillips, M. & Mine, Y. Advances in the value of eggs and egg components for human health. *J. Agric. Food Chem.* 53, 8421–8431 (2005).

[15] Mizutani, K., Chen, Y., Yamashita, H., Hirose, M. & Aibara, S. Thermostabilization of ovotransferrin by anions for pasteurization of liquid egg white. *Biosci. Biotechnol. Biochem.* 70, 1839–1845 (2006).

[16] Matsudomi, N., Oka, H. & Sonoda, M. Inhibition against heat coagulation of ovotransferrin by ovalbumin in relation to its molecular structure. *Food Res. Int.* 35, 821–827 (2002).

[17] Liu, Y.-F., Oey, I., Bremer, P., Carne, A. & Silcock, P. Effects of pH, temperature and pulsed electric fields on the turbidity and protein aggregation of ovomucin-depleted egg white. *Food Res. Int.* 91, 161–170 (2017).

[18] Matsudomi, N. Significance of lysozyme in heat-induced aggregation of egg white protein. in *Interactions of Food Proteins* (ed. Parris, N. & Barford, R.) American Chemical Society 73–90 (1991).

[19] Yamashita, H., Ishibashi, J., Hong, Y.-H. & Hirose, M. Involvement of ovotransferrin in the thermally induced gelation of egg white at around 65°C. *Biosci., Biotechnol., Biochem.* 62, 593–595 (1998).

[20] Matsudomi, N., Takasaki, M. & Kobayashi, K. Heat-induced aggregation of lysozyme with ovotransferrin. *Agric. Biol. Chem.* 55, 1651–1653 (1991).

[21] Samli, H. E., Agma, A. & Senkoylu, N. Effects of storage time and temperature on egg quality in old laying hens. *J. Appl. Poult. Res.* 14, 548–553 (2005).

[22] Wang, J. & Wu, J. Proteomic analysis of fertilized egg white during early incubation. *EuPA Open Proteom.* 2, 38–59 (2014).

[23] Pace, C. N., Vajdos, F., Fee, L., Grimsley, G. & Gray, T. How to measure and predict the molar absorption coefficient of a protein. *Protein Sci.* 4, 2411–2423 (1995).

[24] Shiraki, K., Nishikori, S., Fujiwara, S., Hashimoto, H., Kai, Y., Takagi, M. & Imanaka, T. Comparative analyses of the conformational stability of a hyperthermophilic protein and its mesophilic counterpart. *Eur. J. Biochem.* 268, 4144–4150 (2001).

[25] Liu, Y. F., Oey, I., Bremer, P., Silcock, P. & Carne, A. Proteolytic pattern, protein breakdown and peptide production of ovomucin-depleted egg white processed with heat or pulsed electric fields at different pH. *Food Res. Int.* 108, 465–474 (2018).

[26] Watanabe, K., Xu, J. Q. & Shimoyamada, M. Inhibiting effects of egg white dry-heated at 120°C on heat aggregation and coagulation of egg white and characteristics of dry-heated egg white. *J. Agric. Food Chem.* 47, 4083–4088 (1999).

[27] Hirose, M. Molten globule state of food proteins. *Trends Food Sci. Technol.* 4, 48–51 (1993).

[28] Iwashita, K., Handa, A. & Shiraki, K. Co-aggregation of ovalbumin and lysozyme. *Food Hydrocolloids* 67, 206–215 (2017).

[29] Croguennec, T., Tavares, G. M. & Bouhallab, S. Heteroprotein complex coacervation: A generic process. *Adv. Colloid Interface Sci.* 239, 115–126 (2017).

[30] Diarrassouba, F., Remondetto, G., Garrait, G., Alvarez, P., Beyssac, E. & Subirade, M. Self-assembly of β-lactoglobulin and egg white lysozyme as a potential carrier for nutraceuticals. *Food Chem.* 173, 203–209 (2015).

[31] Santos, M. B., Costa, A. R. D. & Garcia-Rojas, E. E. Heteroprotein complex coacervates of ovalbumin and lysozyme: Formation and thermodynamic characterization. *Int. J. Biol. Macromol.* 106, 1323–1329 (2018).

[32] Santos, M. B., de Carvalho, C. W. P. & Garcia-Rojas, E. E. Heteroprotein complex formation of bovine serum albumin and lysozyme: Structure and thermal stability. *Food Hydrocolloids* 74, 267–274 (2018).

[33] Kurinomaru, T., Maruyama, T., Izaki, S., Handa, K., Kimoto, T. & Shiraki, K. Protein–poly(amino acid) complex precipitation for high-concentration protein formulation. *J. Pharm. Sci.* 103, 2248–2254 (2014).

[34] Kurinomaru, T. & Shiraki, K. Aggregative protein-polyelectrolyte complex for high-concentration formulation of protein drugs. *Int. J. Biol. Macromol.* 100, 11–17 (2017).

[35] Iwashita, K., Handa, A. & Shiraki, K. Coacervates and coaggregates: Liquid–liquid and liquid–solid phase transitions by native and unfolded protein complexes. *Int. J. Biol. Macromol.* 120, 10–18 (2018).

[36] Oki, S., Iwashita, K., Kimura, M., Kano, H. & Shiraki, K. Mechanism of co-aggregation in a protein mixture with small additives. *Int. J. Biol. Macromol.* 107, 1428–1437 (2018).

[37] Clarkson, B. R., Schön, A. & Freire, E. Conformational stability and self-association equilibrium in biologics. *Drug Discov. Today* 21, 342–347 (2016).

[38] Guez, V., Roux, P., Navon, A. & Goldberg, M. E. Role of individual disulfide bonds in hen lysozyme early folding steps. *Protein Sci.* 11, 1136–1151 (2002).

[39] Alting, A. C., Hamer, R. J., de Kruif, C. G. & Visschers, R. W. Cold-set globular protein gels: Interactions, structure and rheology as a function of protein concentration. *J. Agric. Food Chem.* 51, 3150–3156 (2003).

[40] Marangoni, A. On the structure of particulate gels—the case of salt-induced cold gelation of heat-denatured whey protein isolate. *Food Hydrocolloids* 14, 61–74 (2000).

[41] Campbell, A. I., Anderson, V. J., van Duijneveldt, J. S. & Bartlett, P. Dynamical arrest in attractive colloids: the effect of long-range repulsion. *Phys. Rev. Lett.* 94, 208301 (2005).

3.2 Coaggregation of ovalbumin and lysozyme

3.2.1 Introduction

Hen egg white is one of the most prominent protein source foods used as an ingredient by many food industries because of its functional properties: emulsification, foaming, and gelation. Heat coagulation is an especially important functional property of egg white protein [1, 2]. The physical attributes of a heat-induced gel are highly dependent on the microstructure [3]. The network in the microstructure determines the appearance and texture of egg white gels by entrapping water [4, 5] and modulating viscoelasticity [6].

The protein network is mainly mediated by crosslinkage of disulfide bonds, and non-covalent hydrophobic and electrostatic interactions [7]. The disulfide bonds and sulfhydryl groups play a crucial role in covalent crosslinking and stabilizing the gel structure of proteins [8]. In addition, the hydrophobic and electrostatic interactions control the physical characteristics of protein gels [9]. These intermolecular forces are attributed to solution pH, ionic strength, and co-solvents leading to promotion of protein unfolding, enhancement of hydrophobic interactions, decrease in number of ionic bonds, and destruction of disulfide bonds [3, 10]. The mechanisms underlying thermal gelation and aggregation of egg white proteins have been investigated using isolated components, such as ovalbumin [4, 11–13], ovotransferrin [14, 15], lysozyme [16–18], and ovomucin [19]. However, analysis of a single protein alone isolated from egg white is too simple to gain an understanding of the molecular mechanisms occurring in egg white aggregation. On the other hand, whole egg white is too complex to understand the aggregation process of respective proteins [20, 21] because it contains various kinds of proteins with various molecular weights, isoelectric points, and concentrations [22]. To understand the structural changes occurring in egg white by heat treatment, it is necessary to elucidate the intermolecular interactions between heterogeneous proteins.

Ovalbumin (OVA) is a major protein comprising 54% of total egg white proteins. OVA is a globular protein with molecular mass of 45.5 kDa containing one disulfide bond, four sulfhydryl groups, and zero to two phosphoryl groups with a carbohydrate chain [23]. OVA is a dominant factor in the heat-induced gel formation of egg white that forms amorphous or linear aggregates [15, 24]. Lysozyme (LYZ) is one of the most abundant basic proteins in egg white with molecular mass of 14.3 kDa comprising 3.5% of total egg white proteins; Another basic protein is avidin of 0.05%. The tertiary structure of LYZ is stabilized by four disulfide

bonds [25]. LYZ has a melting temperature of around 80°C at neutral pH and forms aggregates irreversibly with a single exponential process during heat treatment [26]. Thus, the thermal aggregation of LYZ has been used as a model system to develop suppressors of protein aggregation, such as amino acid derivatives [27, 28], amine compounds [29], and ammonium ions [30]. LYZ is a basic protein, and therefore it tends to associate electrostatically with other acidic proteins, such as α-lactalbumin [31], ovomucin [32], ovotransferrin [33], and OVA [34, 35].

Here, I investigated the coaggregation reaction steps of an OVA–LYZ binary system. Egg white is composed of many complex constituents, containing hundreds of proteins [36, 37]. Thus, heat-induced gel formation of egg white is quite difficult to understand, although the boiled egg is a familiar food. OVA and LYZ are known to spontaneously associate with each other at extremely low ionic strength even at room temperature [34, 35]. In response to this fact, I selected two important proteins, OVA that is the main component of egg white and LYZ that is the most studied protein in the aggregation process. Bouhallab and Croguennec reported an overview of the induced aggregation and spontaneous reversible assembly of food proteins [38]. By contrast, I investigated irreversible thermal aggregation of OVA–LYZ binary system by focused dynamics in the aggregation process. The coaggregation of OVA and LYZ was reported 30 years ago [39, 40], and the results showed that the heat-induced aggregation between OVA and LYZ is due to electrostatic interaction and disulfide bond exchange. However, the dynamics in the coaggregation processes is still not revealed in detail. Inspired by the pioneering work of Matsudomi and coworkers, I analyzed the quantitative compositions of proteins to explore the role played by each protein during the hierarchical processes of thermal aggregation using the combination of current techniques. The interactions of proteins during heat treatment should let us control network formation of heat-induced egg white gels and aggregates. The aggregation process of OVA and LYZ was identified in terms of aggregation rates, aggregation forces, and aggregate morphology.

3.2.2 Materials and methods

Materials

Hen egg white ovalbumin (grade V), lysozyme (six times crystallized and lyophilized), and bovine serum albumin were obtained from Sigma Chemical Co. (St. Louis, MO). The proteins were used without further purification. Na-phosphate, Na-hydroxide, and *Micrococcus luteus* were obtained from Wako Pure Chemical Inc. Ltd. (Osaka, Japan).

Sample preparation for thermal aggregation of ovalbumin and lysozyme mixtures

Sample preparation for investigation of the aggregation rate depending on the co-existing opposite protein concentration was as follows. A solution of 50 μM ovalbumin (OVA) and lysozyme (LYZ) with 0 – 50 μM LYZ and OVA, respectively, in 50 mM Na-phosphate buffer (pH 7.0) was heated at 70°C for various periods. The samples were centrifuged at 15000 × *g* for 20 min, and then the soluble protein concentration in the supernatant was determined by size exclusion chromatography.

The sample preparation for investigation of the affinity of OVA and LYZ was performed as follows. A solution of 100 μM OVA and LYZ containing 50 mM Na-phosphate buffer (pH 7.0) was heated at 70°C for 30 min. The sample solution was diluted 2-fold with buffer solution or mixed with another protein solution at a ratio of 1:1 at room temperature. Immediately, the sample was centrifuged at 15000 × *g* for 20 min, and then the soluble protein concentration in the supernatant was determined by size exclusion chromatography. The sample solution before centrifugation was analyzed by electrophoresis and enzyme assay.

The sample preparation for investigation of the protein composition and morphology of aggregates was performed as follows. A mixture of OVA and LYZ with total protein concentration of 100 μM in the molar fraction of 0 – 1 in 50 mM Na-phosphate buffer (pH 7.0) was heated at 70°C for 30 min. The samples were centrifuged at 15000 × *g* for 20 min for determination of protein concentration by size exclusion chromatography. The sample solution before centrifugation was diluted 10-fold with pure water for imaging by electron microscopy.

A solution of 100 μM OVA, LYZ, and bovine serum albumin (BSA) containing 50 mM Na-phosphate buffer (pH 7.0) was heated at 70°C for 30 min. The sample solution was diluted 2-fold with buffer solution or mixed with another protein solution at a ratio of 1:1 at room temperature. The sample was immediately

centrifuged at 15000 × *g* for 20 min, and then soluble protein concentration in the supernatant was determined by size exclusion chromatography. The sample solution before centrifugation was analyzed by electrophoresis.

Circular dichroism

Circular dichroism (CD) measurements were performed on a spectropolarimeter (J-720W; Japan Spectroscopic Co. Ltd., Tokyo, Japan) using a Peltier cell holder with a temperature controller (PTC-348W; Japan Spectroscopic Co. Ltd.). A solution of 0.5 mg/mL OVA, LYZ, and BSA dissolved in 50 mM Na-phosphate buffer (pH 7.0) was measured by CD 222 nm intensity change with an increasing temperature rate of 1.0°C/min using a 1-mm path-length quartz cell.

Determination of soluble protein concentration using size exclusion chromatography

Soluble protein concentration was determined by high-performance liquid chromatography (HPLC) (Shimadzu, Kyoto, Japan) using a system comprised of a degasser (DGU-20A_3), a pump (LC-10AT), an auto injector (SIL-10A_{XL}), a column oven (CTO-10A), a UV–vis detector (SPD-10AV), and a system controller (SCL-10Avp) with a size exclusion column (3 μm, 300 mm × 7.8 mm i.d., Yarra SEC 3000; Phenomenex, Torrance, CA). Isocratic HPLC was conducted with a flow rate of 1.0 mg/mL at 30°C using 150 mM Na-phosphate buffer (pH 7.0). Aliquots of 30 μL of samples were loaded into the column. The absorbance was monitored at 280 nm. All soluble protein concentrations were determined as the averages of three experiments.

Sodium dodecyl sulfate-polyacrylamide gel electrophoresis

The protein solutions were subjected to heat treatment and mixing, and were then mixed with 125 mM Tris-HCl (pH 6.8) loading buffer solution containing 4% (w/v) sodium dodecyl sulfate (SDS), 10% (w/v) sucrose, and 0.01% (w/v) bromophenol blue with or without 10% (v/v) β-mercaptoethanol at a ratio of 1:1. The samples were incubated for 20 hours at 25°C and then subjected to SDS-polyacrylamide gel electrophoresis (SDS-PAGE) using a 5% – 20% gradient gel (e-PAGEL; ATTO Co., Tokyo, Japan) with a molecular weight marker (Precision Plus Protein Dual Xtra Standards; Bio-Rad, Hercules, CA). The gels were then stained using Coomassie Brilliant Blue R-250.

Lysozyme enzyme assay

Lysozyme activities catalyze the cleavage of the β-1,4-glycosidic linkages between *N*-acetylmuramic acid and *N*-acetyl-D-glucosamine, which are in peptidoglycan cell wall of Gram-positive bacteria. A substrate solution of 1990 μL containing 0.3 mg/mL *M. luteus* in 50 mM Na-phosphate buffer (pH 7.0) was mixed with 10 μL of protein solution. The enzymatic reaction rate was estimated from the slope of the initial decrease in the absorbance at 600 nm using a spectrophotometer (V-630; Japan Spectroscopic Co. Ltd., Tokyo, Japan)

Imaging of aggregates by transmission electron microscopy

Aliquots of 4 μL of protein solution were negatively stained with 4 μL of 1% (w/v) tungstosilicic acid solution. Then, 4 μL of the stained solution was placed on a 150-mesh copper grid covered with a carbon-coated hydrophilic film. The solution on the grid was dried for a few minutes. The samples were observed using a transmission microscope (H7650; Hitachi, Tokyo, Japan) with an acceleration voltage of 80 keV.

Distribution of aggregate size

The size distributions were analyzed using a laser diffraction particle sizer (SALD-2300; Shimadzu, Kyoto, Japan).

3.2.3 Results

Condition of OVA and LYZ

Before the main experiment, I confirmed the solution structure of OVA dissolved in 50 mM Na-phosphate buffer solution at pH 7.0 where is the pH of fresh egg white. Size exclusion chromatography showed that the OVA solution contained mainly the monomeric form with small amounts of dimers, trimers, and tetramers at the elution point around 10 min (Fig. 3.2.1). In addition, soluble aggregates were observed at an elution time of around 5 min. The amount of soluble aggregates was about 14%, as calculated from the chromatogram peak area. The polydispersed OVA molecules were observed as expected in the crude state of egg white proteins, as described previously [41]. According to the data, it is estimated that 50 μM OVA solution contains 43.2 ± 1.0% soluble molecules in monomeric to tetrameric forms.

Protein unfolding was monitored by the ellipticity at 222 nm that indicates a content of α-helix structure. Far-UV CD analysis showed that the secondary structures of OVA and LYZ were slightly perturbed at 70°C (Fig. 3.2.2). Accordingly, a small amount of heat-induced unfolded molecules was thought to be present during heat treatment at 70°C. Heat treatment at 70°C was adopted in this investigation because aggregation reaction is not too fast to analyze coaggregation of OVA and LYZ.

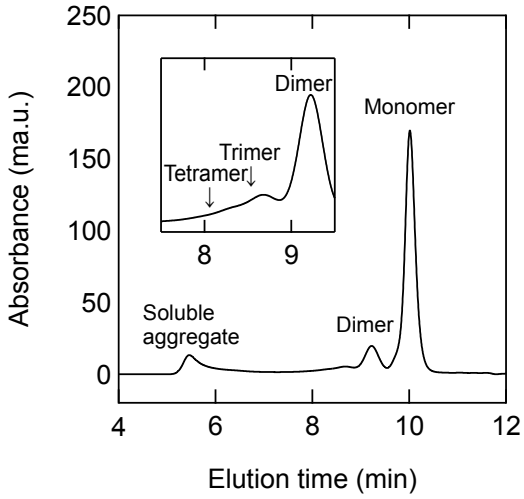

Figure 3.2.1 Size exclusion chromatogram of OVA solution before heat treatment.

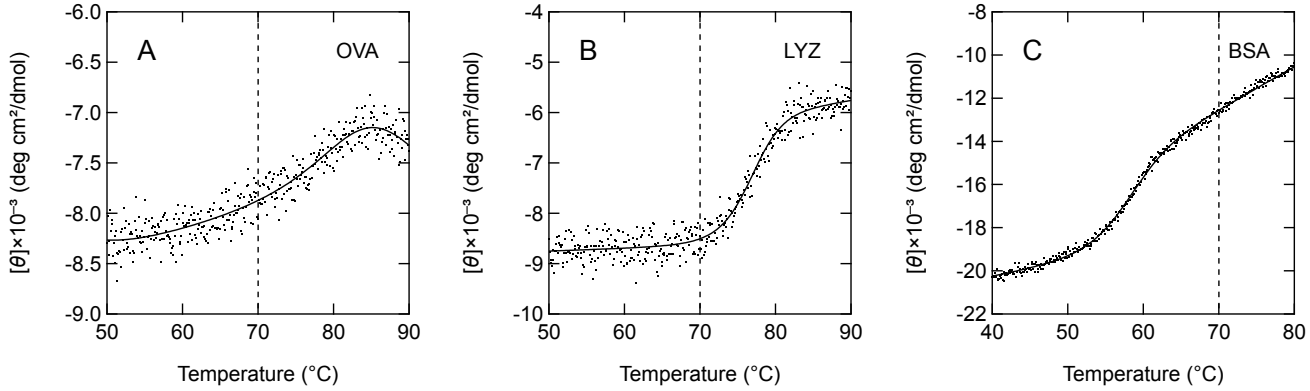

Figure 3.2.2 Thermal unfolding curves of OVA (A), LYZ (B), and BSA (C).

Coaggregation of OVA and LYZ

To understand the coaggregation of OVA and LYZ, I investigated the heat-induced aggregation of protein mixtures measured by size exclusion chromatography. Briefly, solutions containing 50 μM OVA with 0–50 μM LYZ, and *vice versa*, were heated at 70°C for various periods. The concentrations of soluble protein are plotted in Figure 3.2.3. The soluble OVA concentration decreased from 100% to 50% during heat treatment for 30 min in the presence or absence of LYZ at any concentration (Fig. 3.2.3A). As shown in the figure, the aggregation of OVA was not affected by the presence of LYZ. In contrast, the soluble concentration of LYZ depended on the concentration of OVA (Fig. 3.2.3B). In the absence of OVA, almost all of the LYZ remained in the soluble fraction after heat treatment for 30 min. In contrast, the aggregation rate of LYZ increased with increasing concentration of mixed OVA (Fig. 3.2.3B). For example, 50 μM LYZ added over 30 μM OVA showed complete aggregation with heat treatment for 30 min. For quantitative comparison, the rate constants of aggregation were determined by fitting to the exponential function. Figure 3.2.4 shows the rate constant of the aggregation processes of OVA mixed with LYZ, and *vice versa*. The aggregation-rate constants of OVA remained constant at about 0.12 min^{-1} regardless of the co-existence of LYZ (Fig. 3.2.4A). In contrast, the aggregation-rate constants of LYZ increased monotonically from 0.01 min^{-1} to 0.64 min^{-1} with increasing amount of coexisting OVA (Fig. 3.2.4B). The aggregation rate constant of LYZ with equimolar OVA was 64-fold higher than that of LYZ alone.

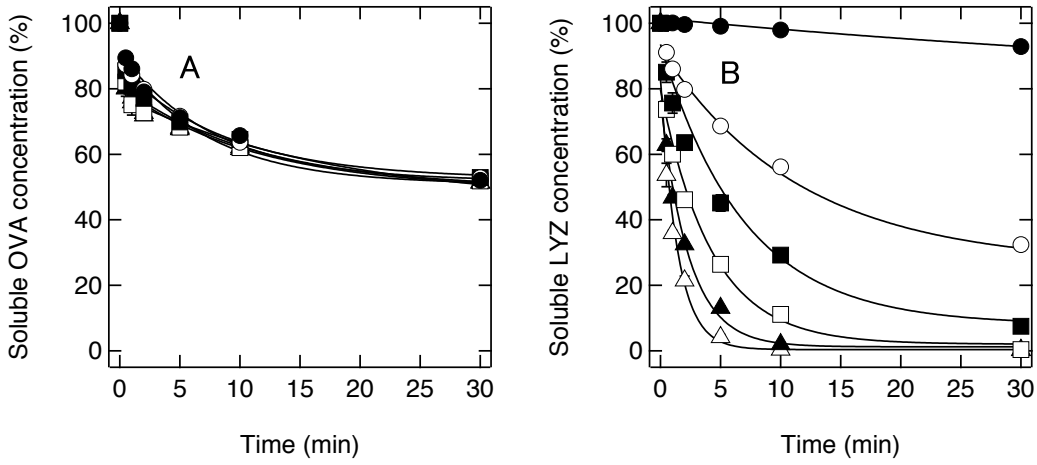

Figure 3.2.3 Soluble protein concentration of OVA–LYZ mixture after heating at 70°C for various periods. (A) Samples contained 50 μM OVA and 0 (closed circles), 10 (open circles), 20 (closed squares), 30 (open squares), 40 (closed triangles), and 50 (open triangles) μM LYZ. (B) Samples contained 50 μM LYZ with 0 (closed circles), 10 (open circles), 20 (closed squares), 30 (open squares), 40 (closed triangles), and 50 (open triangles) μM OVA.

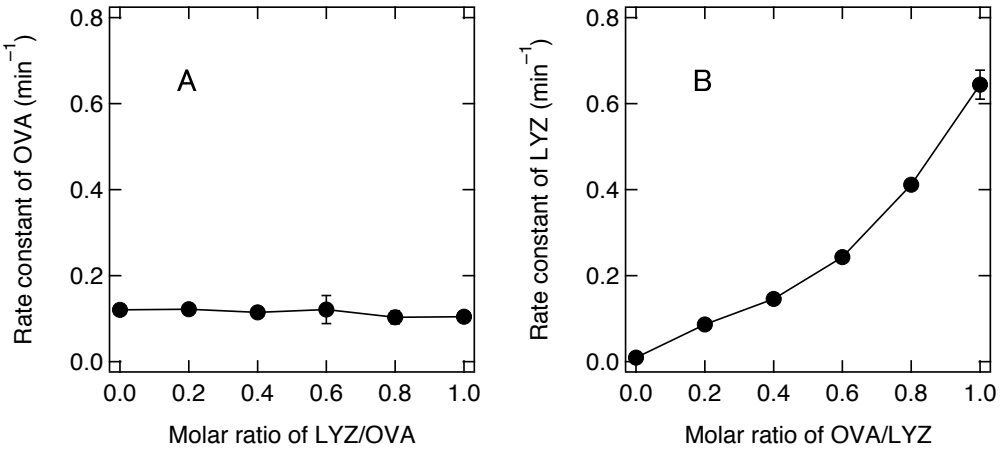

Figure 3.2.4 Aggregation rate constants of OVA and LYZ. (A) The aggregation rate constants of OVA in the presence of various ratios of LYZ. (B) The aggregation rate constants of LYZ in the presence of various ratios of OVA.

Affinity between OVA and LYZ

To understand the structures of LYZ and OVA during coaggregation, I prepared proteins in the native state and heated state, and analyzed the affinity between native OVA (nOVA), native LYZ (nLYZ), heated OVA (hOVA), and heated LYZ (hLYZ) by evaluating instant association of OVA and LYZ. Briefly, solutions of 100 μM OVA and LYZ in 50 mM Na-phosphate buffer (pH 7.0) were individually heated at 70°C for 30 min. Subsequently, the native or heated OVA and LYZ solutions were mixed with each other at a ratio of 1:1 at room temperature, and then soluble proteins in the mixed samples and control samples were analyzed by size exclusion chromatography. In addition, nOVA and nLYZ were mixed and then heated at 70°C for 30 min, which was designated as "co-hOVA–LYZ." The samples were centrifuged at 15000 × *g* for 20 min, and then the soluble fraction was subjected to size exclusion chromatography.

Figure 3.2.5 shows the size exclusion chromatograms of the various combinations of native and heated OVA and LYZ. First, I compared the single samples of OVA and LYZ. The chromatogram peaks of nOVA appeared at around 5 min, 9 min, and 10 min, which corresponded to soluble aggregates, oligomer, and monomer, respectively. The chromatogram peak of nLYZ was observed only at 12 min as a monomeric form of LYZ. The amount of soluble aggregates of hOVA was increased compared to that of nOVA. The peak area at 12 min of hLYZ was decreased compared to nLYZ, but no other peaks were observed corresponding to soluble aggregates.

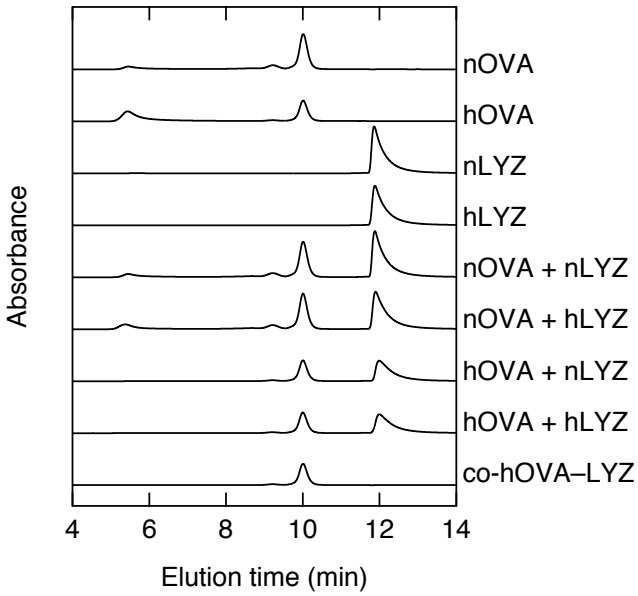

Figure 3.2.5 Size exclusion chromatograms of the supernatant of OVA–LYZ mixture. nOVA, native OVA. hOVA, OVA heated at 70°C for 30 min nLYZ, native LYZ. hLYZ, LYZ heated at 70°C for 30 min. The + symbol denotes the mixed sample of the native protein or the heat-treated protein. "co-hOVA–LYZ" indicates the sample in which nOVA and nLYZ mixture was heated at 70°C for 30 min.

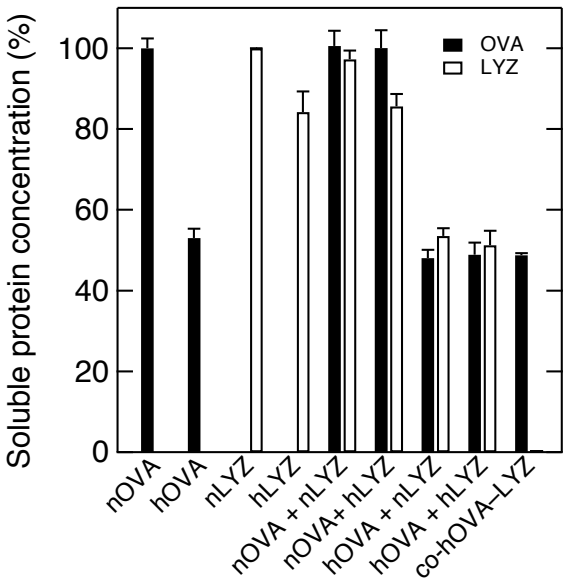

Figure 3.2.6 Soluble protein concentration determined by the chromatograms in Figure 3.2.5.

Next, I compare the mixed samples. The sample “nOVA + nLYZ” showed simple peaks composed of the peaks of nOVA and nLYZ. Similar data were obtained for “nOVA + hLYZ”; i.e., the peaks of this sample were identical to the addition of the peaks of nOVA and hLYZ. These results indicate that native OVA did not interact with native LYZ or heated LYZ. In contrast, the “hOVA + nLYZ” and “hOVA + hLYZ” samples showed two peaks of monomeric OVA and LYZ, and the soluble aggregate peak vanished. These results suggest that the soluble aggregates of OVA formed insoluble precipitates with LYZ molecules. Finally, the chromatograms of “co-hOVA–LYZ” showed only a single peak of monomeric OVA.

For quantitative comparison, I calculated the protein concentrations from the chromatograms (Fig. 3.2.6). After heat treatment, the soluble concentrations of OVA and LYZ decreased to 53% and 84%, respectively. The soluble protein concentrations of OVA and LYZ in “nOVA + nLYZ” and “nOVA + hLYZ” samples remained constant. In contrast, the soluble protein concentrations in “hOVA + nLYZ” and “hOVA + hLYZ” samples were clearly decreased; the concentrations of both proteins were about 50%. The identical concentrations of soluble LYZ and OVA indicated that the precipitates were composed of equimolar amounts of LYZ and OVA. This result indicated that both nLYZ and hLYZ have specific affinity for the unfolded OVA rather than native OVA. Note that the specific affinity of LYZ toward hOVA was not observed for bovine serum albumin (BSA) (Figs. 3.2.7 and 3.2.8). However, as shown in the “co-hOVA–LYZ” sample, LYZ aggregated completely on co-heating with OVA, forming aggregates at a ratio of 1:2 of OVA and LYZ. These results indicate that the specific affinity of LYZ for the heat-induced unfolded OVA could not be fully described by OVA–LYZ coaggregation. The mechanisms were investigated as follows.

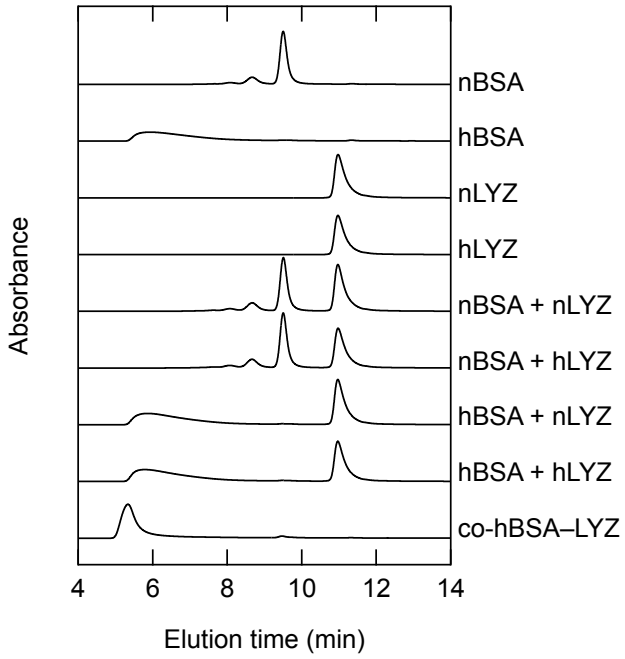

Figure 3.2.7 Size exclusion chromatograms of the supernatant of BSA–LYZ mixture. nBSA, native BSA. hBSA, BSA heated at 70°C for 30 min. nLYZ, native LYZ. hLYZ, LYZ heated at 70°C for 30 min. The + symbol denotes the mixed sample of the native protein or the heat-treated protein. "co-hBSA–LYZ" indicates the sample in which nBSA and nLYZ mixture was heated at 70°C for 30 min.

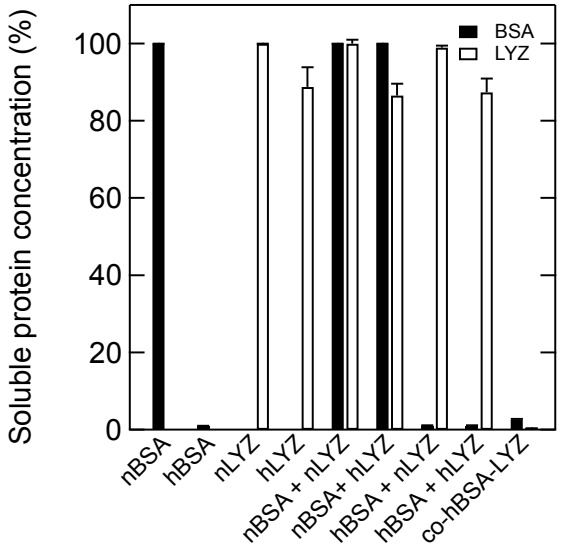

Figure 3.2.8 Soluble protein concentration determined by the chromatograms in Figure 3.2.7.

Non-covalent and covalent bonding between LYZ and unfolded OVA

Disulfide bond exchange is one of the most important reactions in the thermal aggregation of proteins [42, 43]. To investigate the disulfide bond exchange reaction, I performed SDS-PAGE analyses of reduced or non-reduced samples of OVA–LYZ mixture using β-mercaptoethanol (Fig. 3.2.9). Clear bands were obtained with monomeric OVA (45 kDa) and monomeric LYZ (14 kDa). Other minor bands were observed with dimeric (90 kDa) and trimeric (135 kDa) OVA. For the samples except for "co-hOVA–LYZ," all bands in mixtures of OVA and LYZ under reducing and non-reducing conditions were identical to the control samples. The broad band observed in hOVA-containing sample under non-reducing condition seems to be corresponding to denatured multimeric OVA with disulfide crosslinkage, containing in a soluble aggregate fraction from HPLC (Fig. 3.2.5). The data indicated that disulfide bond exchange between OVA and LYZ does not occur under conditions of ambient temperature, and that binding between hOVA and nLYZ or hLYZ is stabilized by non-covalent interactions. In contrast, the bands of the "co-hOVA–LYZ" sample under non-reducing conditions were different from those under reducing conditions; the monomeric LYZ band and a broad band of over 100 kDa corresponding to soluble large aggregates disappeared. Note that similar intermolecular disulfide bonds were also observed between BSA and LYZ during heat treatment (Fig. 3.2.10). Therefore, intermolecular disulfide bond exchange is one of the key interactions to form insoluble aggregates of "co-hOVA–LYZ" samples during heat treatment.

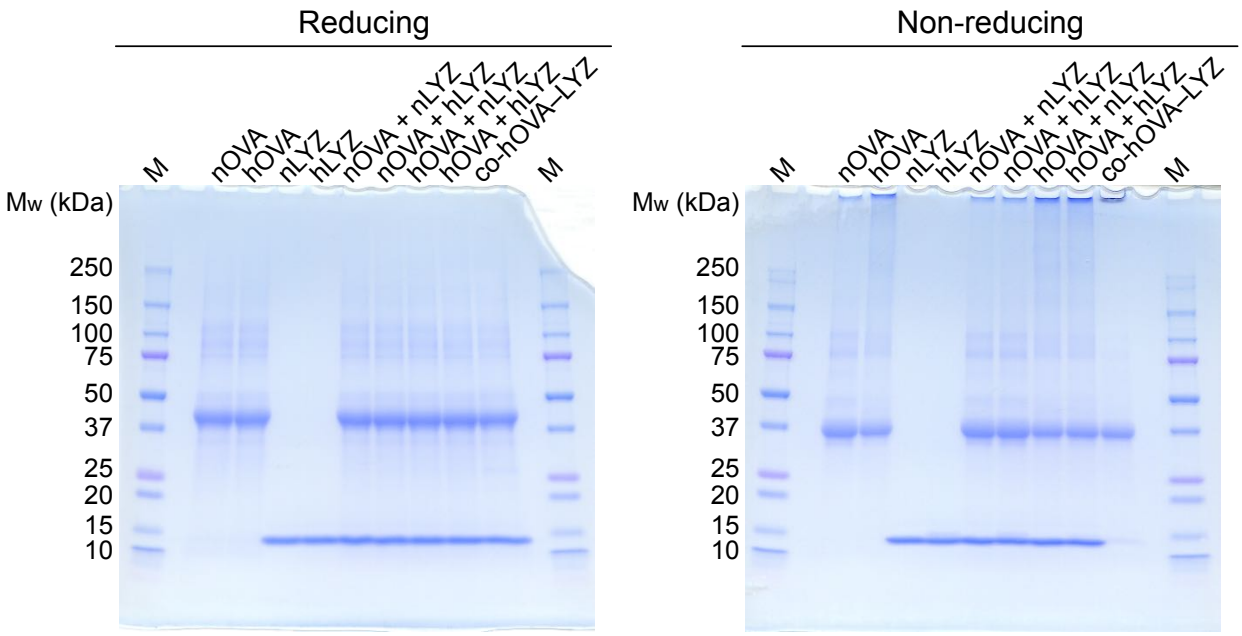

Figure 3.2.9 SDS-PAGE analysis of reduced and non-reduced OVA–LYZ mixtures. nOVA, native OVA. hOVA, OVA heated at 70°C for 30 min nLYZ, native LYZ. hLYZ, LYZ heated at 70°C for 30 min. The + symbol denotes the mixed sample of the native protein or the heat-treated protein. "co-hOVA–LYZ" indicates the sample in which nOVA and nLYZ mixture was heated at 70°C for 30 min. Lane M shows standard ladder marker.

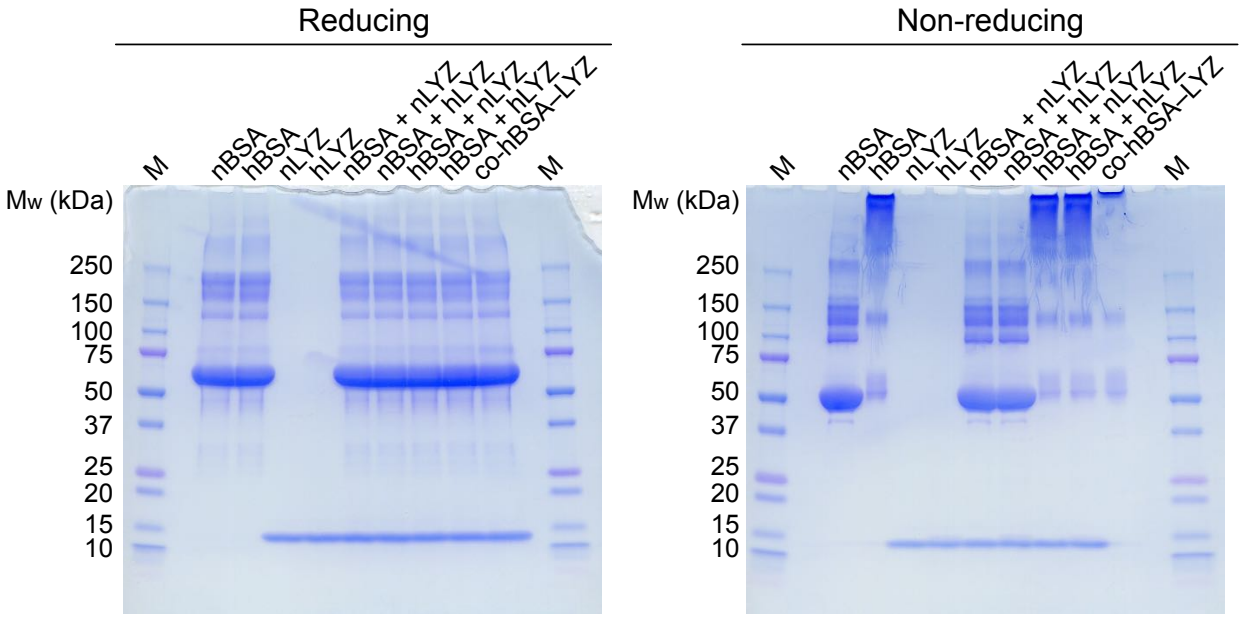

Figure 3.2.10 SDS-PAGE analysis of reduced and non-reduced BSA–LYZ mixtures. nBSA, native BSA. hBSA, BSA heated at 70°C for 30 min. nLYZ, native LYZ. hLYZ, LYZ heated at 70°C for 30 min. The + symbol denotes the mixed sample of the native protein or the heat-treated protein. "co-hBSA–LYZ" indicates the sample in which nBSA and nLYZ mixture was heated at 70°C for 30 min. Lane M shows standard ladder marker.

Enzyme activity of LYZ associated with OVA

The chromatograms and SDS-PAGE analyses showed that the native state of LYZ has the ability to associate with the heat-induced unfolded state of OVA. To confirm the tertiary structure of LYZ associated with OVA, the enzyme reaction of LYZ mixed with OVA was measured. Figure 3.2.11 shows the enzyme reaction rate of LYZ. As expected, the enzyme-reaction rate of "nOVA + nLYZ" did not change compared with that of LYZ alone. Surprisingly, the enzyme reaction rate of "hOVA + nLYZ" remained at 92%, while the soluble concentration of LYZ decreased to 52% (Fig. 3.2.8). Note that the enzyme reaction rate was measured by using the mixture solution containing the insoluble fraction, while the soluble protein concentration was determined from the supernatant of the mixture after centrifugation. Under conditions similar to those used for determination of soluble protein concentration, the enzyme-reaction rate of LYZ in the soluble fraction of "hOVA + nLYZ" obtained by a centrifugation was 50% corresponding to soluble protein concentration. Thus, the native LYZ appeared to contain insoluble aggregates in the "hOVA + nLYZ" sample.

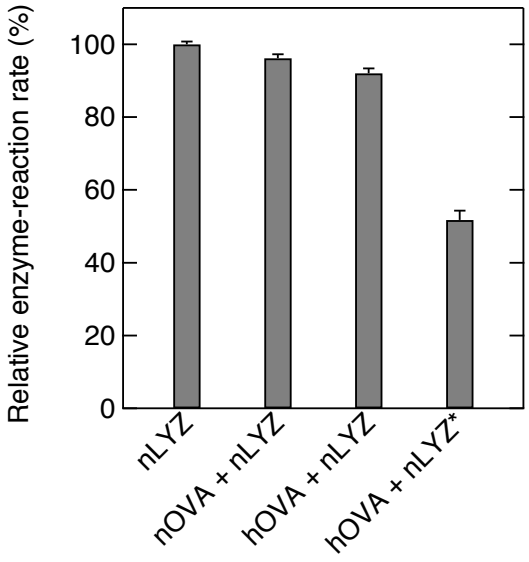

Figure 3.2.11 Enzyme-reaction rate of LYZ with or without OVA. nLYZ, native LYZ. nOVA + nLYZ, native LYZ with native OVA. hOVA + nLYZ, native LYZ with OVA heated at 70°C for 30 min hOVA + nLYZ*, soluble fraction of "hOVA + nLYZ" obtained by centrifugation at 15000 × *g* for 20 min.

Composition and morphology of coheated OVA–LYZ aggregates

Subsequently, I investigated the protein compositions of OVA and LYZ for collaborative aggregation. Briefly, mixtures of OVA and LYZ with total protein concentration of 100 μM in molar fractions of 0.0 – 1.0 were heated at 70°C for 30 min, and the residual soluble protein concentration was then determined by size exclusion chromatography (Fig. 3.2.11A). The soluble OVA concentration after heating was directly proportional to the initial OVA concentration. In contrast, the soluble LYZ concentration decreased markedly with increasing molar fraction of OVA. At OVA molar fraction > 0.3, LYZ was completely aggregated. To present the data more clearly, the protein compositions of OVA and LYZ in aggregates are plotted (Fig. 3.2.11B). The composition of LYZ was abundant in aggregates under all conditions. In particular, when the overall molar fraction of OVA was 0.5, the protein composition in aggregates showed 30% OVA. Therefore, LYZ heated with OVA was prone to form aggregates due to intermolecular disulfide bonds, resulting in high proportions of LYZ in aggregates.

The morphologies of the aggregates formed in OVA–LYZ mixtures at various molar ratios were examined by TEM (Fig. 3.2.12). The aggregates of LYZ alone ($X = 0.0$) were small and amorphous, ranging in size from 10 nm to 100 nm (Fig. 3.2.12A). At $X = 0.1$, large aggregates were observed in TEM images with a size range from 10 nm to 1 μm (Fig. 3.2.12B). With increasing molar fraction of OVA at $X = 0.3$, the small aggregates were not observed, but large aggregates of few μm in size were found in TEM images (Fig. 3.2.12C). In the solution containing equimolar amounts of OVA and LYZ at $X = 0.5$, the aggregates apparently grew to above several dozens μm with a large network (Fig. 3.2.12D). With further increases in the ratio of OVA, the smaller aggregates increased with a spherical shape (Figs. 3.2.12E – 3.2.12G). The aggregate size formed at $X = 0.7 – 0.9$, which is similar ratio to the actual egg white protein composition, was a little larger than at $X = 1.0$. Judging from the morphology, the aggregation mode of OVA–LYZ mixtures was probably dominated by (i) LYZ aggregate-driven amorphous shapes when $X < 0.5$ or (ii) OVA aggregate-driven spherical shapes when $X > 0.5$. In summary, OVA alone and LYZ alone are prone to form small aggregates due to itself electrostatic repulsion resulting in soluble state, while OVA and LYZ mixtures form large aggregates with a hierarchical network between small aggregates. As described above, the large aggregates were attributed to the affinity of LYZ with unfolded OVA and intermolecular disulfide bonds between LYZ and OVA molecules.

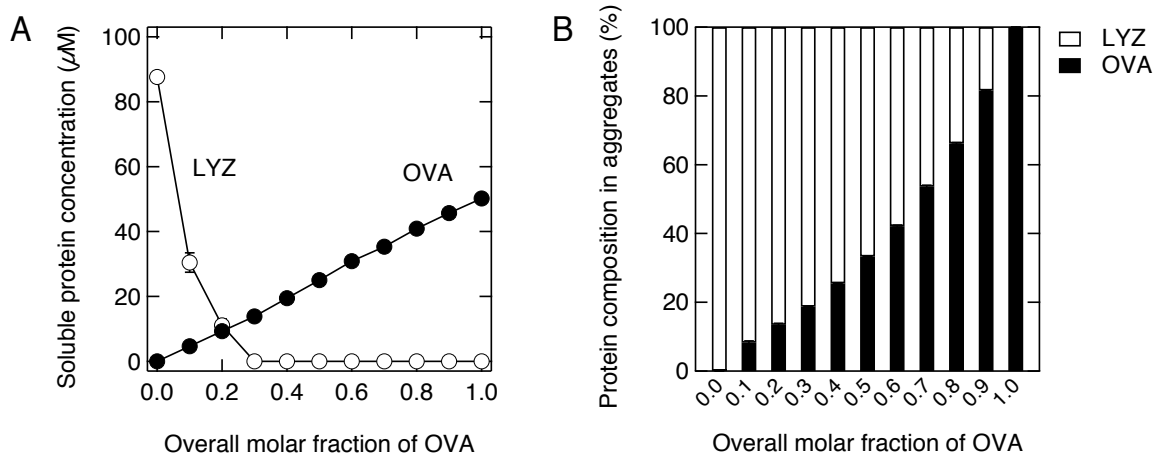

Figure 3.2.11 (A) Soluble protein concentration of OVA–LYZ mixture after heat treatment. (B) Composition of aggregates in the formed OVA–LYZ mixture. The initial concentration of total protein was 100 μM. Molar fraction of OVA was [OVA]/([LYZ] + [OVA]).

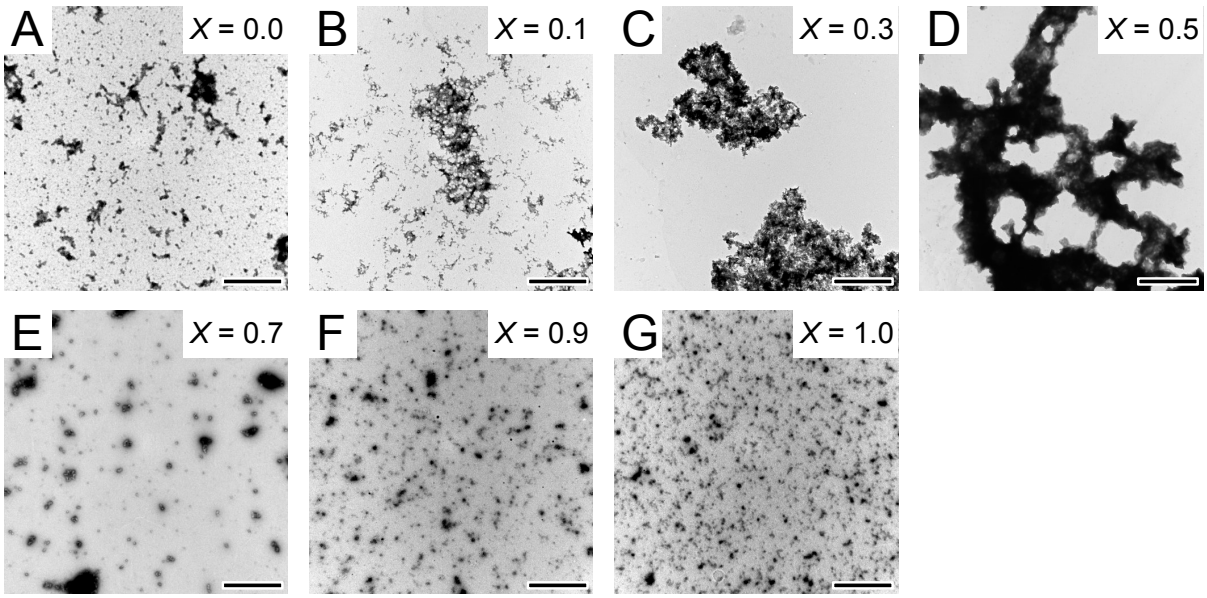

Figure 3.2.12 Morphology of OVA–LYZ mixture aggregation in the molar fraction monitored by TEM. X = [OVA]/([LYZ] + [OVA]). The scale bars represent 1 μm.

3.2.4 Discussion

Driving forces for coaggregation

First, I discuss the simplest case of aggregates between native OVA (nOVA) and native LYZ (nLYZ). Negatively charged OVA and positively charged LYZ at physiological pH are known to spontaneously associate with each other via electrostatic interactions at extremely low ionic strength even at room temperature [35]. Such aggregates, called coacervates, can be reversibly dissolved at increasing ionic concentration above 50 mM [44, 45]. Thus, under our experimental conditions, nOVA and nLYZ did not form precipitates only by mixing because the solutions contained 50 mM Na-phosphate as a buffer.

On the other hand, aggregates were observed when nOVA and nLYZ were mixed and heated at 70°C. At this temperature, both OVA and LYZ were slightly unfolded (Fig. 3.2.2). Note that the mixing of OVA and LYZ does not influence their unfolding temperature [46]. In saline at 70°C, aggregates were formed through hydrophobic interactions rather than through only electrostatic interactions, followed by crosslinking between OVA and LYZ molecules by disulfide bond exchange. Coaggregation of OVA and LYZ was sensitive to thermal unfolding compared with single protein system of OVA or LYZ. Weak hydrophobic interaction induced by partial unfolding may be amplified by electrostatic attraction between OVA and LYZ. Therefore, the pH is an important property for coaggregation such as oppositely charged OVA and LYZ system. In addition, our data indicated that the aggregation of OVA is not affected by the presence of LYZ. Thus, OVA plays a role as a trigger for the start of coaggregation by unfolding itself.

Binding region of unfolded OVA and native LYZ

Heated OVA (hOVA) showed affinity with native LYZ (nLYZ) via non-covalent interactions. The complex of hOVA with nLYZ formed insoluble precipitates. These results indicated that an internal hydrophobic region of OVA exposed by unfolding had affinity for the surface of nLYZ. In fact, the intramolecular hydrophobic region of OVA was identified as ILELPFASGT MSMLVLLPDE VSGLEQLESIINFEK (residues 229 – 263), named S-peptide, which is capable of binding strongly to the LYZ molecule [47]. Sugimoto *et al*. concluded that S-peptide enhances the formation of LYZ aggregation. It should be noted that S-peptide has no cysteine residues, suggesting that non-covalent interactions between unfolded OVA and native LYZ trigger aggregate formation.

In addition, LYZ has a binding site with OVA [47]. The amino acid sequences of the peptides were identified as RNRCKGTDVQAW (residues 112 – 123), named M-peptide, which is located in the LYZ surface, and GILQINSRW (residues 54 – 62), named K-peptide, which is located in the inside near the active site of LYZ. Considering the association between OVA and LYZ at room temperature, S-peptide of the unfolded OVA was exposed on the protein surface, leading to binding to M-peptide of native LYZ.

Residual enzyme reaction rate of LYZ

The enzyme-reaction rate of LYZ of "hOVA + nLYZ" remained at about 90% (Fig. 3.2.11). This raised the following possibilities: (i) the interaction occurred between a non-active site of LYZ and hOVA, and (ii) LYZ sufficiently dissolved from aggregates due to dilution for the enzyme assay. The two cases are discussed below.

(i) The LYZ molecule mostly adopts the native conformation even at 70°C (Fig. 3.2.2). In addition, the active site residues of LYZ are negatively charged Glu35 and Asp52. Therefore, K-peptide of LYZ, which is located in the inside of the molecule near the active site, cannot approach the OVA surface. In fact, the binding of M-peptide to OVA is more favorable than K-peptide to OVA for the detection of OVA [48]. Furthermore, K-peptide of LYZ is known to be a core region of amyloid fibrils [49]; this peptide is prone to form aggregates itself rather than to bind to OVA due to its high hydrophobicity [47]. Thus, LYZ is thought to bind to OVA via the M-peptide.

(ii) The chromatogram of "hOVA + nLYZ" solution shown in Figure 3.2.5 indicated that all of the soluble OVA aggregates were associated with LYZ, leading to formation of precipitates. If Case (ii) is correct, the precipitates dissociate immediately at the time of dilution with substrate solution during the enzyme assay. I investigated the particle size using a laser diffraction particle sizer, showing that the diameter of the "hOVA + nLYZ" sample was actually decreased by > 10-fold dilution (Fig. 3.2.13). The size distribution in 100-fold diluted "hOVA + nLYZ" solution was the same as that of "hOVA" solution. Therefore, it was concluded that the precipitates between hOVA and nLYZ are dissociated by dilution, resulting in reactivation of LYZ (Fig. 3.2.11). That is, the precipitates were in an unstable colloidal state.

Intermolecular disulfide bond exchange during co-heating

As shown in SDS-PAGE analyses (Fig. 3.2.9), the disulfide bonds were formed between OVA and LYZ molecules during heat treatment. The OVA molecule has four sulfhydryl groups and one disulfide bond buried in the intramolecular core. LYZ has four disulfide bonds in the inside. A previous study indicated that heat treatment at 70°C exposed free sulfhydryl groups of OVA to the solvent resulting in induction of a sulfhydryl–disulfide exchange reaction between OVA and LYZ, which caused irreversible aggregate formation [39]. As shown in Figure 3.2.11, the abundant LYZ in coaggregates may be attributed to the exchange reaction between a sulfhydryl group of OVA and a disulfide bond of LYZ. The many disulfide bonds in LYZ play a key role in connection of soluble OVA aggregates. Sulfhydryl–disulfide exchange reaction between OVA and LYZ propagates new sulfhydryl group of LYZ, leading to formation of large aggregates with crosslinked network.

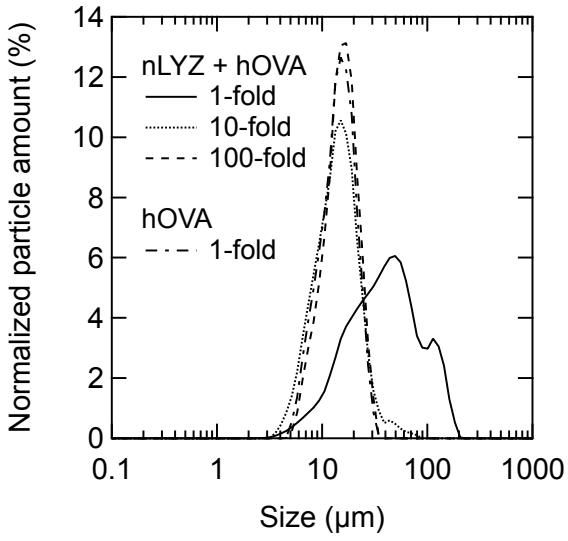

Figure 3.2.13 Size distribution of particles dissolved in the 1-, 10-, and 100-fold diluted "hOVA + nLYZ" and 1-fold "hOVA" solution.

Process of coaggregation

Figure 3.2.14 shows the molecular mechanism of coaggregation between OVA and LYZ. The process of coaggregation includes the following steps: (i) the unfolding of OVA, (ii) the association of unfolded OVA and LYZ via non-covalent interaction, (iii) the insolubilization of the complexes due to the colloidal instability, (iv) the additional binding of LYZ induced by exchange reaction between sulfhydryl groups of unfolded OVA

and disulfide bonds of LYZ, and (v) the growth of aggregates due to the formation of intermolecular disulfide bonds across the OVA–LYZ colloids. Sulfhydryl–disulfide exchange reaction between OVA and LYZ in the step (iv) generated new sulfhydryl groups of LYZ. Sulfhydryl groups were propagated by the exchange reaction and contributed to the growth of the aggregate by the formation of intermolecular disulfide bonds in the step (v). The hierarchical aggregation was important for understanding of coaggregation by OVA and LYZ. For example, if the solution contained LYZ or OVA alone, small aggregates were observed. These small aggregates cannot grow due to the balance between short-range attraction and long-range electrostatic repulsion [50, 51]. It is important to note that the thermal unfolding of OVA itself does not influence the mixture with LYZ, while that of LYZ markedly facilitates mixture with OVA. This is because aggregation occurs by both sulfhydryl–disulfide exchange reaction and affinity via non-covalent interactions with unfolded OVA.

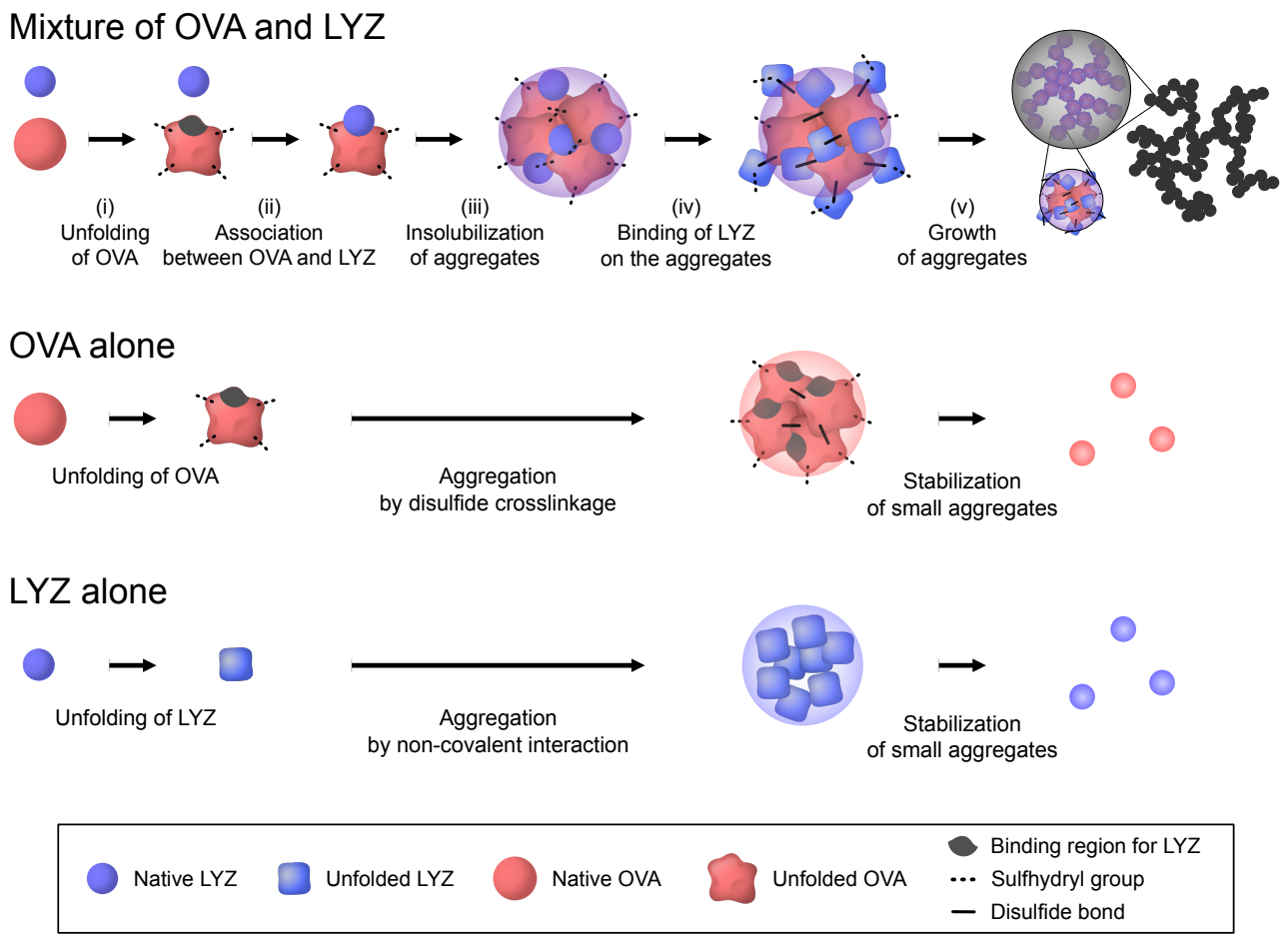

Figure 3.2.14 Schematic diagram of coaggregation process of OVA and LYZ.

3.2.5 Conclusion

The thermal aggregation rate of OVA was not dependent on coexisting LYZ concentration. In contrast, the thermal aggregation rate of LYZ was enhanced by increases in the co-existing OVA concentration. Native LYZ formed precipitates with unfolded OVA by non-covalent interactions even at room temperature. The precipitates were labile and unstable, and could be dissociated by 10-fold dilution. In addition to the affinity of unfolded OVA for native LYZ, intermolecular disulfide bonds were formed between OVA and LYZ during co-heating. These results indicated that the unfolding of OVA triggered the collaborative aggregation of OVA and LYZ via the affinity of unfolded OVA for LYZ and sulfhydryl–disulfide exchange reaction between OVA and LYZ. The unfolded OVA plays a crucial role in the nucleus of LYZ aggregation before the growth of large aggregates. The precise mechanism of coaggregation provides information on control of aggregation and gelation of egg white proteins. It will be future issues to clarify relations of this coaggregation phenomenon and gel properties of egg white protein. Finally, I would like to emphasize that the molecular mechanism of coaggregation between heterogeneous proteins cannot be extrapolated by investigation of the aggregation of a single protein.

References

[1] Mine, Y. Recent advances in the understanding of egg white protein functionality. *Trends Food Sci. Technol.* 6, 225–232 (1995).

[2] Mine, Y. Egg proteins. in *Applied Food Protein Chemistry* (ed. Ustunol, Z.) John Wiley & Sons, Ltd. 459–490 (2015).

[3] Handa, A., Takahashi, K., Kuroda, N. & Froning, G. W. Heat-induced egg white gels as affected by pH. *J. Food Sci.* 63, 403–407 (1998).

[4] Nieuwland, M., Bouwman, W. G., Pouvreau, L., Martin, A. H. & de Jongh, H. H. J. Relating water holding of ovalbumin gels to aggregate structure. *Food Hydrocolloids* 52, 87–94 (2016).

[5] Urbonaite, V., de Jongh, H. H., van der Linden, E. & Pouvreau, L. Protein aggregates may differ in water entrapment but are comparable in water confinement. *J. Agric. Food Chem.* 63, 8912–8920 (2015).

[6] Tomczyńska-Mleko, M., Nishinari, K. & Handa, A. Ca^{2+}-induced egg white isolate gels with various microstructure. *Food Sci. Technol. Res.* 20, 1207–1212 (2014).

[7] Campbell, L., Raikos, V. & Euston, S. R. Modification of functional properties of egg-white proteins. *Food/Nahrung* 47, 369–376 (2003).

[8] Van der Plancken, I., Van Loey, A. & Hendrickx, M. E. Changes in sulfhydryl content of egg white proteins due to heat and pressure treatment. *J. Agric. Food Chem.* 53, 5726–5733 (2005).

[9] Sun, Y. & Hayakawa, S. Heat-induced gels of egg white/ovalbumins from five avian species: Thermal aggregation, molecular forces involved, and rheological properties. *J. Agric. Food Chem.* 50, 1636–1642 (2002).

[10] Mine, Y., Noutomi, T. & Haga, N. Thermally induced changes in egg white proteins. *J. Agric. Food Chem.* 38, 2122–2125 (1990).

[11] Croguennec, T., Renault, A., Beaufils, S., Dubois, J. J. & Pezennec, S. Interfacial properties of heat-treated ovalbumin. *J. Colloid Interface Sci.* 315, 627–636 (2007).

[12] Tani, F., Shirai, N., Onishi, T., Venelle, F., Yasumoto, K. & Doi, E. Temperature control for kinetic refolding of heat-denatured ovalbumin. *Protein Sci.* 6, 1491–1502 (1997).

[13] Weijers, M., Barneveld, P. A., Cohen Stuart, M. A. & Visschers, R. W. Heat-induced denaturation and aggregation of ovalbumin at neutral pH described by irreversible first-order kinetics. *Protein Sci.* 12, 2693–2703 (2003).

[14] Mizutani, K., Chen, Y., Yamashita, H., Hirose, M. & Aibara, S. Thermostabilization of ovotransferrin by anions for pasteurization of liquid egg white. *Biosci. Biotechnol. Biochem.* 70, 1839–1845 (2006).

[15] Yamashita, H., Ishibashi, J., Hong, Y.-H. & Hirose, M. Involvement of ovotransferrin in the thermally induced gelation of egg white at around 65°C. *Biosci., Biotechnol., Biochem.* 62, 593–595 (1998).

[16] Matsuoka, T., Tomita, S., Hamada, H. & Shiraki, K. Amidated amino acids are prominent additives for preventing heat-induced aggregation of lysozyme. *J. Biosci. Bioeng.* 103, 440–443 (2007).

[17] Matsuoka, T., Hamada, H., Matsumoto, K. & Shiraki, K. Indispensable structure of solution additives to prevent inactivation of lysozyme for heating and refolding. *Biotechnol. Prog.* 25, 1515–1524 (2009).

[18] Shiraki, K., Kudou, M., Fujiwara, S., Imanaka, T. & Takagi, M. Biophysical effect of amino acids on the prevention of protein aggregation. *J. Biochem.* 132, 591–595 (2002).

[19] Offengenden, M. & Wu, J. Egg white ovomucin gels: structured fluids with weak polyelectrolyte properties. *RSC Adv.* 3, 910–917 (2013).

[20] Handa, A., Hayashi, K., Shidara, H. & Kuroda, N. Correlation of the protein structure and gelling properties in dried egg white products. *J. Agric. Food Chem.* 49, 3957–3964 (2001).

[21] Iwashita, K., Inoue, N., Handa, A. & Shiraki, K. Thermal aggregation of hen egg white proteins in the presence of salts. *Protein J.* 34, 212–219 (2015).

[22] Guerin-Dubiard, C., Pasco, M., Molle, D., Desert, C., Croguennec, T. & Nau, F. Proteomic analysis of hen egg white. *J. Agric. Food Chem.* 54, 3901–3910 (2006).

[23] Huntington, J. A. & Stein, P. E. Structure and properties of ovalbumin. *J. Chrom. B Biomed. Sci. Appl.* 756, 189–198 (2001).

[24] Kawachi, Y., Kameyama, R., Handa, A., Takahashi, N. & Tanaka, N. Role of the N-terminal amphiphilic region of ovalbumin during heat-induced aggregation and gelation. *J. Agric. Food Chem.* 61, 8668–8675 (2013).

[25] De Bernardez Clark, E., Hevehan, D., Szela, S. & Maachupalli-Reddy, J. Oxidative renaturation of hen egg-white lysozyme. Folding vs aggregation. *Biotechnol. Prog.* 14, 47–54 (1998).

[26] Kudou, M., Shiraki, K., Fujiwara, S., Imanaka, T. & Takagi, M. Prevention of thermal inactivation and aggregation of lysozyme by polyamines. *Eur. J. Biochem.* 270, 4547–4554 (2003).

[27] Shiraki, K., Kudou, M., Nishikori, S., Kitagawa, H., Imanaka, T. & Takagi, M. Arginine ethylester prevents thermal inactivation and aggregation of lysozyme. *Eur. J. Biochem.* 271, 3242–3247 (2004).

[28] Shiraki, K., Kudou, M., Sakamoto, R., Yanagihara, I. & Takagi, M. Amino acid esters prevent thermal inactivation and aggregation of lysozyme. *Biotechnol. Prog.* 21, 640–643 (2005).

[29] Okanojo, M., Shiraki, K., Kudou, M., Nishikori, S. & Takagi, M. Diamines prevent thermal aggregation and inactivation of lysozyme. *J. Biosci. Bioeng.* 100, 556–561 (2005).

[30] Hirano, A., Hamada, H., Okubo, T., Noguchi, T., Higashibata, H. & Shiraki, K. Correlation between thermal aggregation and stability of lysozyme with salts described by molar surface tension increment: An exceptional propensity of ammonium salts as aggregation suppressor. *Protein J.* 26, 423–433 (2007).

[31] Nigen, M., Croguennec, T. & Bouhallab, S. Formation and stability of α-lactalbumin–lysozyme spherical particles: Involvement of electrostatic forces. *Food Hydrocolloids* 23, 510–518 (2009).

[32] Matsuda, T., Watanabe, K. & Sato, Y. Interaction between ovomucoid and lysozyme. *J. Food Sci.* 47, 637–641 (1982).

[33] Lechevalier, V., Croguennec, T., Pezennec, S., Guérin-Dubiard, C., Pasco, M. & Nau, F. Ovalbumin, ovotransferrin, lysozyme: Three model proteins for structural modifications at the air−water interface. *J. Agric. Food Chem.* 51, 6354–6361 (2003).

[34] Le Floch-Fouéré, C., Pezennec, S., Lechevalier, V., Beaufils, S., Desbat, B., Pézolet, M. & Renault, A. Synergy between ovalbumin and lysozyme leads to non-additive interfacial and foaming properties of mixtures. *Food Hydrocolloids* 23, 352–365 (2009).

[35] Yu, S., Yao, P., Jiang, M. & Zhang, G. Nanogels prepared by self-assembly of oppositely charged globular proteins. *Biopolymers* 83, 148–158 (2006).

[36] Stevens, L. Egg white proteins. *Comp. Biochem. Physiol. B* 100, 1–9 (1991).

[37] Mann, K. The chicken egg white proteome. *Proteomics* 7, 3558–3568 (2007).

[38] Bouhallab, S. & Croguennec, T. Spontaneous assembly and induced aggregation of food proteins. in *Polyelectrolyte Complexes in the Dispersed and Solid State II Advances in Polymer Science* 67–101 (2013).

[39] Matsudomi, N., Yamamura, Y. & Kobayashi, K. Heat-induced aggregation between ovalbumin and lysozyme. *Agric. Biol. Chem.* 50, 1389–1395 (1986).

[40] Matsudomi, N., Yamamura, Y. & Kobayashi, K. Aggregation between lysozyme and heat-denatured ovalbumin. *Agric. Biol. Chem.* 51, 1811–1817 (2014).

[41] Campanella, B., Onor, M., D'Ulivo, A., Giannarelli, S. & Bramanti, E. Impact of protein concentration on the determination of thiolic groups of ovalbumin: A size exclusion chromatography–chemical vapor generation–atomic fluorescence spectrometry study via mercury labeling. *Anal. Chem.* 86, 2251–2256 (2014).

[42] Tomita, S. & Shiraki, K. Why do solution additives suppress the heat-induced inactivation of proteins? inhibition of chemical modifications. *Biotechnol. Prog.* 27, 855–862 (2011).

[43] Shiraki, K., Tomita, S. & Inoue, N. Small amine molecules: Solvent design toward facile improvement of protein stability against aggregation and inactivation. *Curr. Pharm. Biotechnol.* 17, 116–125 (2016).

[44] Croguennec, T., Tavares, G. M. & Bouhallab, S. Heteroprotein complex coacervation: A generic process. *Adv. Colloid Interface Sci.* 239, 115–126 (2017).

[45] Salvatore, D., Croguennec, T., Bouhallab, S., Forge, V. & Nicolai, T. Kinetics and structure during self-assembly of oppositely charged proteins in aqueous solution. *Biomacromolecules* 12, 1920–1926 (2011).

[46] Arntfield, S. D. & Bernatsky, A. Characteristics of heat-induced networks for mixtures of ovalbumin and lysozyme. *J. Agric. Food Chem.* 41, 2291–2295 (1993).

[47] Sugimoto, Y., Kamada, Y., Tokunaga, Y., Shinohara, H., Matsumoto, M., Kusakabe, T., Ohkuri, T. & Ueda, T. Aggregates with lysozyme and ovalbumin show features of amyloid-like fibrils. *Biochem. Cell Biol.* 89, 533–544 (2011).

[48] Sugawara, K., Kadoya, T., Kuramitz, H. & Tanaka, S. Voltammetric detection of ovalbumin using a peptide labeled with an electroactive compound. *Anal. Chim. Acta* 834, 37–44 (2014).

[49] Tokunaga, Y., Sakakibara, Y., Kamada, Y., Watanabe, K. & Sugimoto, Y. Analysis of core region from egg white lysozyme forming amyloid fibrils. *Int. J. Biol. Sci.* 9, 219–227 (2013).

[50] Campbell, A. I., Anderson, V. J., van Duijneveldt, J. S. & Bartlett, P. Dynamical arrest in attractive colloids: the effect of long-range repulsion. *Phys. Rev. Lett.* 94, 208301 (2005).

[51] Mossa, S., Sciortino, F., Tartaglia, P. & Zaccarelli, E. Ground-state clusters for short-range attractive and long-range repulsive potentials. *Langmuir* 20, 10756–10763 (2004).

Chapter 4 Onset Process of Coaggregation

Coacervates and coaggregates: Liquid–liquid and liquid–solid phase transitions by native and unfolded protein complexes

4.1 Introduction

Self-assemblies of macromolecules have attracted attention as new materials with potential applications as functional foods and drug delivery carriers because of their suitability for the delivery and sustained release of active substances, promoting progress in food science and pharmacology [1]. Food proteins are particularly interesting biocompatible and biodegradable matrices beyond their nutritional value [2]. They can encapsulate and protect bioactive ingredients during storage and passage through digestive organs [3]. Additionally, protein particles influence the perception of sensations within the mouth [4]. Since the assembly from food proteins was first proposed by Howell [5], numerous efforts have been devoted to understanding the formation mechanisms [6, 7]. The heterogeneous interactions behind the mechanisms lead to a diversity of supramolecular structures, such as particles, fibers, ribbons, and hydrogels [8]. Coacervate is an assembly with a dense protein-rich phase in which a dilute phase coexists, and this assembly is driven by liquid–liquid phase separation throughout the electrostatic attraction between oppositely charged biomacromolecules [1, 7]. Coacervates generally have a well-defined spherical shape with fluidity. However, the morphology of coacervates often becomes irregular similarly as that of aggregates depending on the composition of the coacervate and solution conditions [9, 10]. Consequently, the desired functions and characteristics of the unexpected structures are impaired. Precise information about protein structures plays an important role in controlling the structure of coacervates.

The mechanism and shape of spontaneous protein assembly depend on the mode and balance of interactions between proteins, e.g., electrostatic interactions, hydrogen bonding, van der Waals forces, and hydrophobic interactions [11]. The interactions between protein molecules are also strongly influenced by the protein structure, such as native, unfolded, oligomer, and various types of aggregated states. This diversity of

protein structure differs markedly from that of synthetic polymers. Changes in the three-dimensional structure of protein is probable to perturb the interactions that play indispensable roles in the association between protein molecules. One of the main obstacles to predicting such associations is the absence of knowledge regarding the protein structure, molecular interactions, and structural hierarchy of complexes.

In this report, I aim to clarify the differences in molecular mechanisms between the liquid–liquid phase separation of coacervates and liquid–solid precipitation of coaggregates. Ovalbumin (OVA) and hen egg-white lysozyme (LYZ), which are the major components of egg white, were selected as the model proteins. OVA is known as the most advanced protein material for food applications because of its abundance and versatility [12]. OVA, with a molecular weight of 45 kDa, isoelectric point of 4.5, denaturation temperature of 77.5°C, also comprises 54% of egg white proteins [13, 14]. LYZ is a basic protein that is rare among food proteins, and it has a molecular weight of 14.3 kDa and isoelectric point of 10.7. LYZ is a stable protein with a denaturation temperature of 75.0°C [15, 16]. The investigation of coacervates and aggregates of OVA and LYZ will provide important information for managing the large diversity of supramolecular structures derived from globular proteins for the food industry as well as biophysical science.

4.2 Materials and methods

Materials

Hen egg white OVA (grade VI) and LYZ (six times crystallized and lyophilized) were obtained from Sigma Chemical Co. (St. Louis, MO, USA). The proteins were used without further purification. Sodium fluoride (NaF), sodium chloride (NaCl), arginine hydrochloride (ArgHCl), urea, sodium phosphate, sodium hydroxide, and hydrochloric acid were obtained from Wako Pure Chemical Inc. Ltd. (Osaka, Japan).

Preparation for unfolded state and complexation of OVA and LYZ

OVA and LYZ were dissolved at 1.5 mg/mL in pure water, and then the solution pH was adjusted to 8.0 using NaOH. Unfolded proteins were prepared as follows. Each solution was heated at 80°C for 30 min using a water bath, immediately cooled to 4°C, and finally incubated at room temperature. The unheated and heated OVA solutions were denoted pristine OVA (pOVA) and heated OVA (hOVA) solution, respectively. In the same

manner, the unheated and heated LYZ solutions were denoted pristine LYZ (pLYZ) and heated LYZ (hLYZ) solution, respectively. Aliquots of 200 μL of the OVA and LYZ solutions were mixed with water or additive solution (NaF, NaCl, ArgHCl, and urea) adjusted to pH 8 at the equivalent volume ratio at ambient temperature. Instantly, the pH of the mixture was adjusted to 3 – 12 for pH-dependent experiments or 8 for additive concentration-dependent experiments by dropping 0.01 – 0.1 M HCl or 0.01 – 1 M NaOH, followed by incubation for 30 min.

Circular dichroism

Circular dichroism (CD) spectra of 3-fold diluted solutions of pOVA, hOVA, pLYZ, and hLYZ were measured using a 1-mm path-length quartz cell for far-UV in the wavelength range of 200 – 250 nm and a 10-mm path-length quartz cell for near-UV in the wavelength range of 250 – 320 nm at room temperature using a spectropolarimeter (J-720W; Japan Spectroscopic Co. Ltd., Tokyo, Japan).

Sodium dodecyl sulfate-polyacrylamide gel electrophoresis

The OVA/LYZ mixtures were centrifuged at 10000 × *g* for 20 min. Subsequently, 500 μL of supernatant were replaced with pure water. Centrifugation and supernatant exchange were repeated three times. Finally, 500-μL aliquots of supernatant were replaced with loading buffer solution (pH 6.8) containing 75 mM Tris-HCl, 2.4% (w/v) sodium dodecyl sulfate (SDS), 6% (w/v) sucrose, and 0.01% (w/v) bromophenol blue. The samples were incubated for 24 h at room temperature and then subjected to SDS-polyacrylamide gel electrophoresis (SDS-PAGE) using a 5% – 20% gradient gel (e-PAGEL; ATTO Co., Tokyo, Japan) with the entire solutions of pOVA, hOVA, pLYZ, and hLYZ as controls. The gels were then stained using Coomassie Brilliant Blue R-250.

Fluorescence assay

To measure intrinsic fluorescence spectra, the pOVA, hOVA, pLYZ, and hLYZ solutions were diluted 10-fold with pure water. To measure ANS fluorescence spectra, the solutions were diluted 10-fold with pure water containing 10 μM ANS, and then each sample was incubated for 30 min at room temperature in the dark. The fluorescence spectra were determined at 25°C using a spectrofluorometer (FP-6500; Japan Spectroscopic) with a 1-cm path-length quartz cuvette. The emission spectra were recorded with excitation at 280 nm for intrinsic

and 380 nm for ANS fluorescence. The slit width was 3 nm for intrinsic fluorescence and 5 nm for ANS fluorescence on both emission and excitation sides.

Size exclusion chromatography

pOVA, hOVA, pLYZ, hLYZ, and mixtures of these solutions were centrifuged at 10000 × *g* for 20 min, and then the soluble protein concentrations in the supernatant were determined via high-performance liquid chromatography (Shimadzu, Kyoto, Japan) using a system consisting of a degasser (DGU-20A_3), pump (LC-10AT), auto injector (SIL-10A_{XL}), column oven (CTO-10A), UV–vis detector (SPD-10AV), and system controller (SCL-10Avp) with a size exclusion column (3 μm, 300 mm × 7.8 mm i.d., Yarra SEC 3000; Phenomenex, Torrance, CA, USA). Isocratic HPLC was performed with a flow rate of 1.0 mL/min at 30°C using 150 mM sodium phosphate buffer (pH 7.0). Sample aliquots of 40 μL were loaded into the column. The absorbance was monitored at 280 nm. All soluble protein concentrations were determined as the averages of three experiments.

ζ-potential

The pH value of the pOVA, hOVA, pLYZ, and hLYZ solutions at protein concentrations of 1.5 mg/mL was adjusted to 3 – 12 by dropping 0.01 – 0.1 M HC1 or 0.01 – 1 M NaOH. The surface charges of proteins were measured at 25°C using a Zetasizer Nano Z (Malvern Instruments, Worcestershire, UK). Three runs were performed for each measurement.

Turbidity measurement

The solutions of OVA/LYZ mixtures were added into a 1-cm path-length disposable PMMA cell. The turbidity at 600 nm was measured using a Jasco spectrophotometer model V-630 (Japan Spectroscopic).

Imaging of complexes via phase contrast microscopy

Aliquots of 1 μL of the OVA/LYZ mixtures were placed on a 96-well plate (Costar, Corning Inc., Lowell, MA, USA). The samples were observed using a phase contrast microscope (BZ-X710; Keyence, Osaka, Japan).

4.3 Results and discussion

Physicochemical properties of native and heated OVA and LYZ

Figure 4.1A shows the far-UV CD spectra of OVA and LYZ before and after heating. The far-UV CD spectrum of pOVA had an α-helix–rich shape with minima at 208 and 222 nm, which is typical of the native form of OVA. On the contrary, the far-UV CD spectrum of hOVA exhibited decreased intensity compared with that of pOVA, indicating a markedly decreased amount of the α-helix. Likewise, the far-UV CD spectrum of hLYZ had decreased intensity compared with that of pLYZ. The near-UV CD spectra of OVA and LYZ also represented the different spectral shapes between before and after heating (Fig. 4.2). These data showed that heat treatment disrupted the secondary and tertiary structures of the proteins. The structures of hOVA and hLYZ did not undergo additional changes at ambient temperature for one day.

Figure 4.1B shows the SDS-PAGE data of pOVA, hOVA, pLYZ, and hLYZ under non-reducing conditions. The pOVA solution contained a monomeric form divided into two bands, and a small amount of dimer was observed on SDS-PAGE, which is similar to previous findings that OVA has multiple molecular species due to phosphorylation and glycosylation [14]. Levels of the multimers of hOVA were increased compared with those of pOVA. pLYZ solution contained only a monomer observed by SDS-PAGE. By contrast, the hLYZ solution contained multimers as observed via SDS-PAGE.

Figure 4.1C and 4.1D shows the size exclusion chromatograms (SEC) of the soluble fractions of pOVA, hOVA, pLYZ, and hLYZ. Similar to SDS-PAGE, monomers and multimers were observed in both pOVA and hOVA via SEC. The chromatogram for hOVA revealed a broad peak at 7–11 min for unfolded OVA and a sharp peak around 10 min for native OVA. An analysis of the peak area of the chromatogram showed that the hOVA solution consisted of the native, soluble unfolded, and aggregated states at 10, 75, and 15%, respectively. In the chromatogram for hLYZ, the monomer peak dramatically decreased to 5% compared with that of pLYZ. The monomer was clearly observed via SDS-PAGE (Fig. 4.1B). This inconsistency is not surprising because the unfolded LYZ molecules adsorb onto the matrices in the column due to surface hydrophobicity, making them undetectable by SEC.

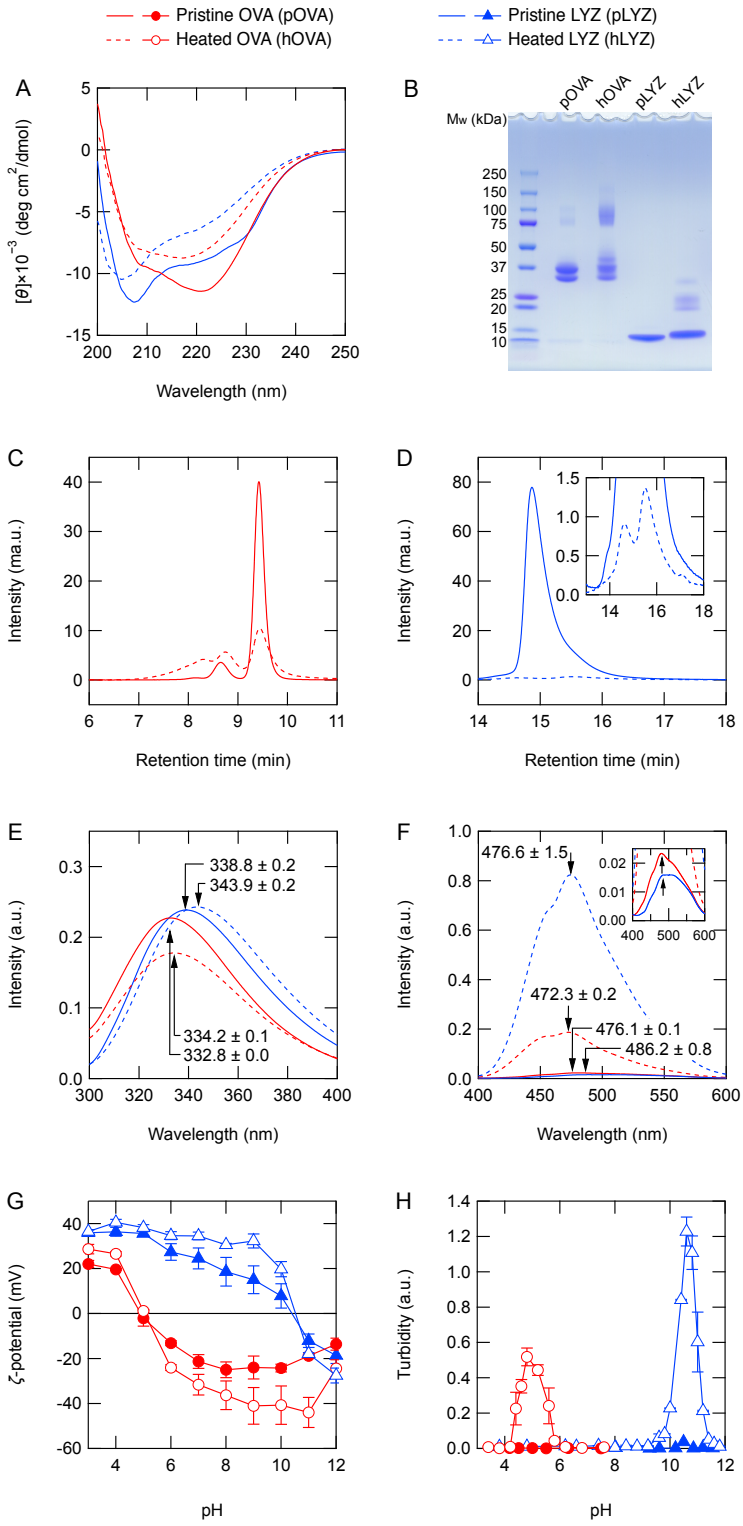

Figure 4.1 Physicochemical properties of the solutions of pristine ovalbumin (pOVA), heated ovalbumin (hOVA), pristine lysozyme (pLYZ), and heated lysozyme (hLYZ). (A) The far-UV circular dichroism spectra. (B) Sodium dodecyl sulfate-polyacrylamide gel electrophoresis under non-reducing conditions. (C and D) Size exclusion chromatograms of the soluble fractions of the samples. (E) Intrinsic fluorescence. (F) ANS fluorescence. (G) ζ-potential. (H) Turbidity. The hOVA (broken red line or open squares) and hLYZ (broken blue line or open circles) solutions were generated by heating the pOVA (solid red line or closed squares) and pLYZ solutions (solid blue line or closed circles), respectively, at 80°C for 30 min.

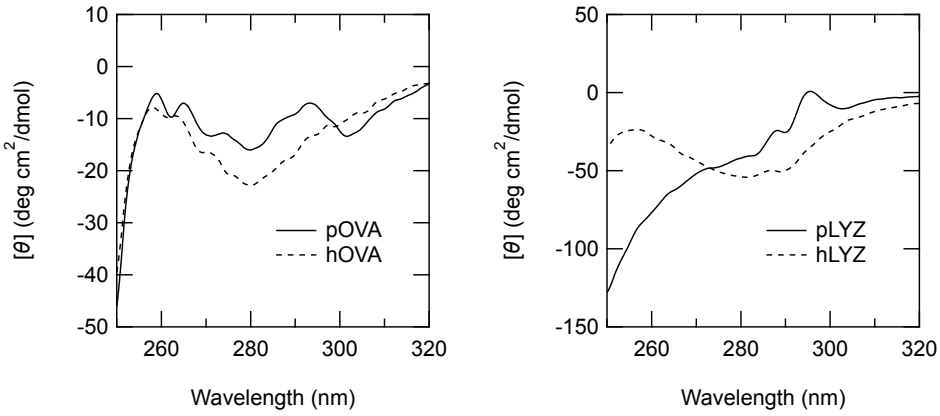

Figure 4.2 The near-UV CD spectra of pOVA, hOVA, pLYZ and hLYZ at pH 8. The samples contain 0.5 mg/mL protein.

Next, the differences of the physicochemical properties of OVA and LYZ before and after heating were evaluated using intrinsic (Fig. 4.1E) and ANS fluorescence spectra (Fig. 4.1F). Upon heat treatment, the peak wavelength of the intrinsic fluorescence of OVA and LYZ shifted toward the long wavelength side. The intensity of ANS fluorescence was significantly increased following heat treatment of both OVA and LYZ, and the peak wavelength shifted toward the short wavelength side. These fluorescence data show that the hydrophobicity of the protein surface was increased by heat treatment.

Figure 4.1G shows the pH dependence of the ζ-potential of pOVA, hOVA, pLYZ, and hLYZ. The absolute values of the ζ-potential of proteins increased at pH values away from the isoelectric point. However, heat treatment did not strongly affect the isoelectric point of the proteins. It is considered that an increase in the density of charged residues on the protein surface is due to thermal unfolding and misfolding during heating and cooling, resulting in the redistribution of counterions on the protein surface [17, 18].

Finally, the colloidal stability of OVA and LYZ before and after heating was investigated by turbidity. Figure 4.1H shows the pH dependence of the turbidity of the protein solutions as monitored by transmittance. The pOVA and pLYZ solutions were also transparent over the pH range of 3–12. hOVA and hLYZ were transparent at neutral pH but cloudy near their respective isoelectric points, as hOVA and hLYZ have hydrophobic patches on their surfaces following heat treatment, resulting in the aggregation-prone state.

Taken together, the protein molecules contained in the hOVA and hLYZ solutions are soluble at neutral pH with increased surface hydrophobicity and electrostatic potential. These results indicate that OVA and LYZ

molecules in the hOVA and hLYZ solutions have different surface properties from these in the pOVA and pLYZ solutions, which probably promoted the spontaneous assembly of complexes by the mixture of OVA and LYZ.

pH sensitivity of spontaneous OVA/LYZ association

Coacervation occurs over the pH range between the isoelectric points of macromolecules [6, 11]. The secondary and tertiary structures of pOVA, hOVA, pLYZ, and hLYZ were maintained over a wide pH range except for pH 12 (Fig. 4.3); Thus, the effect of pH shift on protein structure was neglectable. The turbidity of the pOVA/pLYZ solution increased at pH 6–10 with decreases in the soluble concentrations of OVA and LYZ (Fig. 4.4A). The greatest turbidity was observed at pH 10, and the soluble concentrations of OVA and LYZ reached their nadirs of 45% at pH 9 and 55% at pH 10, respectively. With further increase of the pH above 11, LYZ slightly precipitated due to the decrease in the electrostatic repulsion between LYZ molecules.

The mixture of hOVA/pLYZ displayed increased turbidity at pH 4–11 (Fig. 4.4B). Its turbidity was higher than that of the pOVA/pLYZ solution, indicating that more complexes were formed. At pH 4, the soluble concentration of LYZ remained at 100% despite the increased turbidity, indicating that the unfolded OVA itself precipitates due to its isoelectric point (Fig. 4.1E). The soluble concentration of hOVA in the hOVA/pLYZ sample reached its nadir at pH values between 4 and 10, which was different from the findings for the pOVA/pLYZ sample. By contrast, the pH dependence of the soluble LYZ concentration in the hOVA/pLYZ solution was similar to that for the pOVA/pLYZ solution, although the concentration decreased to 8% at pH 10. These data indicate that both soluble unfolded and aggregated OVA are more prone to form complexes with native LYZ than native OVA.

The turbidity of the pOVA/hLYZ mixture (Fig. 4.4C) was similar to that of hOVA/pLYZ (Fig. 4.4B). However, the soluble concentrations of LYZ in the pOVA/hLYZ mixture displayed a different pattern from that in hOVA/pLYZ mixture. The soluble concentrations of LYZ in the pOVA/hLYZ mixture were nearly zero over the pH range of 3–11 because of undetectability of unfolded LYZ according to SEC.

From these results, two features were found regarding the association between OVA and LYZ. (i) OVA and LYZ spontaneously associated and precipitated at pH values between the isoelectric points of the respective proteins, indicating that electrostatic interactions play an essential role in the spontaneous association. It is well known that protein–protein charge compensation and electroneutrality are general trends of these associations [19]. (ii) Unfolded proteins have greater ability to form complexes with opposite proteins

than native proteins, indicating that hydrophobic interactions also play an important role in the spontaneous association of unfolded proteins with opposite native proteins. Subsequently, these driving forces were analyzed using additives.

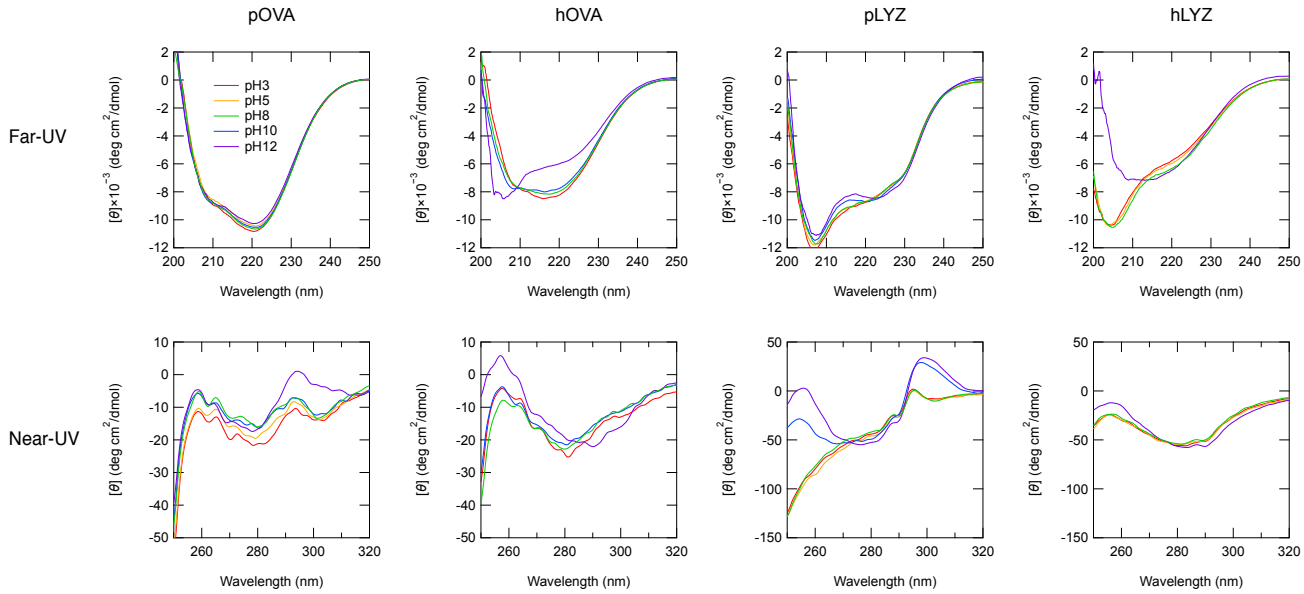

Figure 4.3 The far-UV and near-UV CD spectra of pOVA, hOVA, pLYZ and hLYZ at various pH values. The samples contain 0.5 mg/mL protein and adjusted by small amount of NaOH or HCl at pH 3 (red), pH 5 (orange), pH 8 (green), pH 10 (blue), and pH 12 (purple).

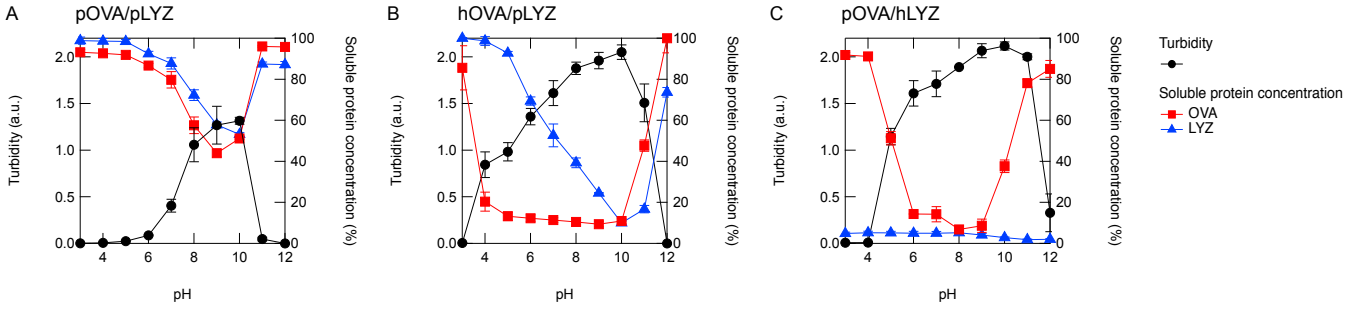

Figure 4.4 pH dependence of the complex. Turbidity (left axis, black circles) and solubility (right axis) of OVA (red squares) and LYZ (blue triangles) as a function of pH value were plotted in the figures. (A) pOVA/pLYZ; (B) hOVA/pLYZ; (C) pOVA/hLYZ.

Electrostatic interactions evaluated using the electrostatic shielding effect of salts

An electrostatic interaction between protein molecules is attenuated by the electrostatic shielding effect of ions. By contrast, the specific binding of ions to a protein is known as the Hofmeister series [20]. The physicochemical properties of the protein surface generally influence the binding of ions with proteins, resulting in the electrostatic shielding effect; i.e., kosmotropes are prone to be excluded on the protein surface, whereas chaotropes are prone to bind to the protein surface [21]. In this experiment, I selected NaCl as the standard ion, NaF as the kosmotrope, and ArgHCl as the chaotrope. It is noted that the addition of salts did not affect the secondary and tertiary structures of proteins (Fig. 4.5).

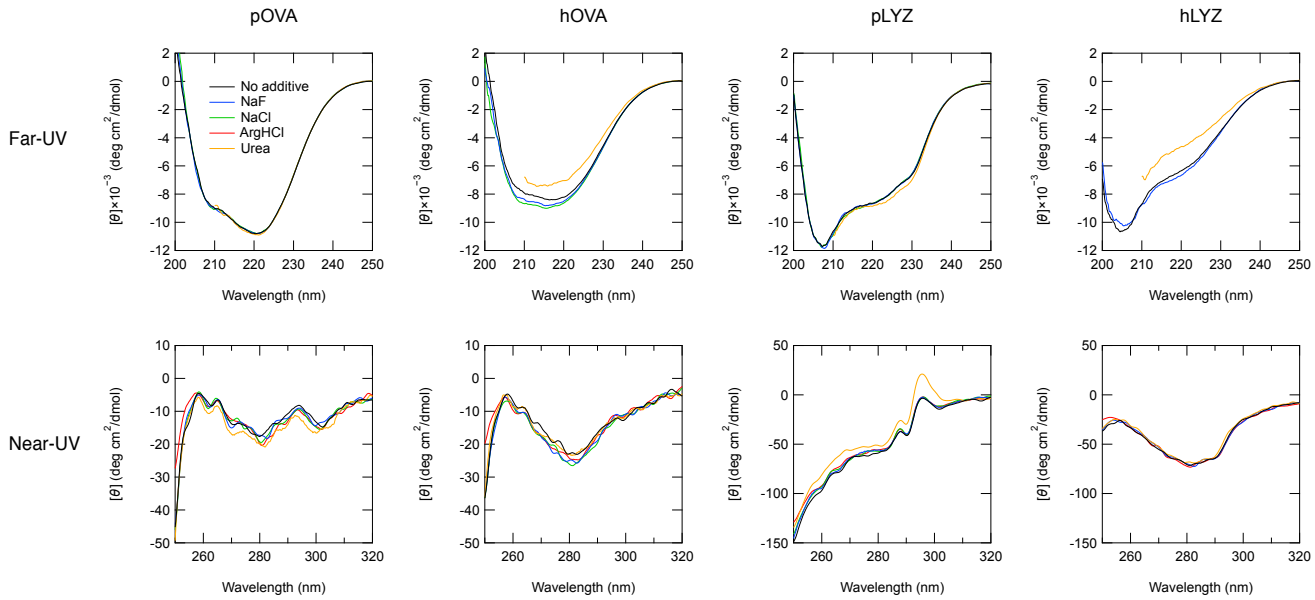

Figure 4.5 The far-UV and near-UV CD spectra of pOVA, hOVA, pLYZ and hLYZ at pH 8 in the presence of additives. The samples contain 0.5 mg/mL protein without (black) or with 200 mM NaF (blue), NaCl (green), ArgHCl (red) or 3 M urea (orange).

The complexes formed in the pOVA/pLYZ solution were composed mainly of monomeric OVA and LYZ as observed by SDS-PAGE (Fig. 4.6A). No complexes were formed in pOVA/pLYZ solution in the presence of NaCl at concentrations of 25 mM or more. The pOVA/pLYZ solutions were apparently transparent even in the presence of 25 mM of any additives (Fig. 4.6B), and the soluble concentration of OVA and LYZ reached 100% (Fig. 4.6C). These results indicate that electrostatic interactions are responsible for the

association of native OVA and native LYZ because all salts at 25 mM prevented complex formation. Furthermore, ArgHCl had a slightly stronger inhibitory effect on complex formation than NaCl and NaF. This is natural because ArgHCl is a chaotrope that suppresses protein aggregation.

The complexes formed in the hOVA/pLYZ solution consisted of various sizes of unfolded OVA and native LYZ (Fig. 4.6D). The whole bands of OVA were faint in the presence of 100 mM NaCl, and the bands of both OVA and LYZ disappeared in the presence of 200 mM NaCl. hOVA/pLYZ solutions containing at least 125 mM NaCl were transparent (Fig. 4.6E). The turbidities of hOVA/pLYZ were in the order of ArgHCl > NaCl > NaF. Corresponding to the turbidity, the soluble protein concentration of the hOVA/pLYZ solution reached 100% at 100 mM ArgHCl and 150 mM NaCl (Fig. 4.6F). The addition of NaF did not sufficiently inhibit the association even at 200 mM despite the absence of turbidity.

The SDS-PAGE pattern of the hOVA/pLYZ solution was clearly different from that of the pOVA/pLYZ solution (Fig. 4.6G). Almost all of the OVA and some of the LYZ were present in the complexes formed in the hOVA/pLYZ solution. The amount of proteins in the complexes decreased with increasing concentrations of NaCl over the range of 0–100 mM (Figs. 4.6G and 4.6H). Further increases of the NaCl concentration resulted in slight increases in the turbidity of the pOVA/hLYZ solution (Fig. 4.6H). Conversely, in the presence of NaF or ArgHCl, the turbidity decreased monotonously with increasing concentrations of the additives (Fig. 4.6H). ArgHCl most effectively decreased the turbidity of the hOVA/pLYZ solution among the additives tested. It has been reported that chaotropic anions at several hundred millimolar concentrations tend to precipitate LYZ [22]. In fact, the turbidity of the hLYZ solution corresponded to that of the pOVA/hLYZ solution in the presence of 200 mM NaCl, indicating that the unfolded LYZ alone was insolubilized by the salts. By contrast, the soluble OVA concentration monotonically increased with increases of the salt concentration (Fig. 4.6I). As the salt concentration increased, the unfolded LYZ tended to form precipitates via the salting-out effect with dissolving native OVA.

As shown in Fig. 4.6, a higher salt concentration was required to inhibit the association containing either unfolded OVA or LYZ than needed for both native OVA and LYZ. This tendency indicates that electrostatic interactions play an important role in the higher stability of complexes of unfolded proteins with opposite native proteins. The enhanced electrostatic interaction resulted from the increase in the surface potential of OVA and LYZ following heat treatment (Fig. 4.1G). Furthermore, considering that a higher salt concentration was required to inhibit complex formation in the hOVA/pLYZ and pOVA/hLYZ solutions than in the

pOVA/pLYZ solution, another strong electrostatic interaction may contribute to the association of unfolded OVA or LYZ with native LYZ or OVA. One of the candidates is the cation–π interaction, a type of electrostatic interaction between conjugated electrons in aromatic moieties and positive charges that is stronger than salt bridge charge–charge interactions [23]. In fact, it has been reported that complexes stabilized via cation–π interactions exhibit resistance to high salt concentrations [24, 25]. Thus, it is believed that the cation–π interaction between aromatic amino acid residues of the unfolded protein molecule and basic amino acid residues on the opposite protein molecule contribute to the formation of complexes consisting of unfolded OVA or LYZ.

The difference in the effect of electrostatic shielding depending on the type of salt can be explained by the binding ability between the ions and the protein surface [26]. NaF less effectively inhibited the association between OVA and LYZ than NaCl in the hOVA/pLYZ and pOVA/hLYZ solutions (Fig. 4.6). By contrast, OVA and LYZ tended to be dissolved in the presence of ArgHCl (Fig. 4.6). These data are expected for the kosmotropic and chaotropic theories because (i) F^- ions as kosmotropes are more strongly excluded from the hydrophobic surface than Cl^- ions [27] and (ii) Arg molecules as chaotropes are more likely to bind to hydrophobic surfaces, especially aromatic moieties, than Na^+ ions, resulting in the suppressive effects on protein aggregation and adsorption [28–32]. More specifically, the proteins in hOVA and hLYZ have higher surface hydrophobicity than those in pOVA and pLYZ, and hence, Cl^- and Arg more effectively bind to heated proteins than F^- and Na^+ to cover the hydrophobic surface. Thus, the salts tend to shield the intermolecular electrostatic interactions between protein molecules in the order of ArgHCl > NaCl > NaF.

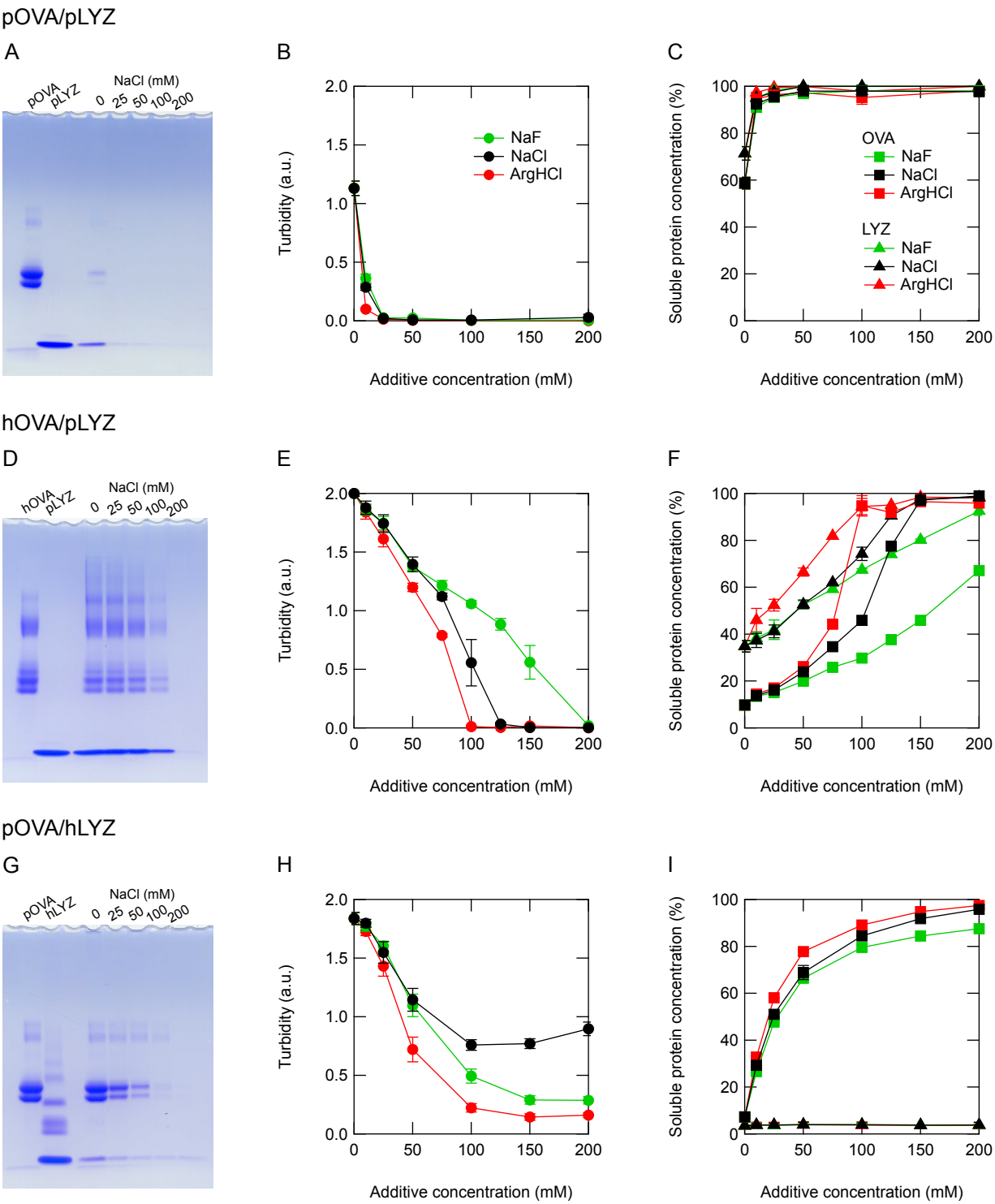

Figure 4.6 Complex of OVA and LYZ in the presence of salts. (A–C) pOVA/pLYZ; (D–F) hOVA/pLYZ; (G–I) pOVA/hLYZ. The precipitates obtained in the OVA/LYZ solution in the presence of 0–200 mM NaCl analyzed by SDS-PAGE with the entire OVA or LYZ solution as controls (A, D, and G), and the turbidity (B, E, and H) and soluble concentrations (C, F, and I) of OVA (squares) and LYZ (triangles) as a function of NaF (green), NaCl (black), and ArgHCl (red) concentration.

Hydrogen bonding and hydrophobic interaction evaluated upon the addition of urea

In addition to electrostatic interactions, hydrogen bonding and hydrophobic interactions have been reported to contribute to the formation of oppositely charged macromolecule complexes [33, 34]. As heat-treated proteins display surface hydrophobicity due to unfolding, hydrophobic interactions are expected to contribute to the formation of complexes composed of unfolded proteins (Figs. 4.1E and 4.1F). Urea is a disruptor of hydrogen bonding at low concentrations and a suppressor of hydrophobic interaction between protein molecules at high concentrations, although whether bonding occurs dominantly via hydrogen bonds or van der Waals interactions remains controversial [35–37]. The formation of OVA/LYZ complexes was also assessed according to turbidity and soluble protein concentration measurements in the presence of urea. Because urea perturbs protein structures at high concentrations, it was added to a concentration of 3 M, which does not affect the structures of OVA and LYZ (Fig. 4.5).

The turbidity of pOVA/pLYZ solution decreased with increasing urea concentrations (Fig. 4.7A). Almost all of the OVA and LYZ were steeply dissolved in 1 M urea, which does not influence the tertiary structures of OVA and LYZ (data not shown). This result suggests that hydrogen bonding contributes to the association of native OVA with native LYZ. Similarly, it was concluded that hydrogen bonding also contributes to the formation of complexes between protein and polyelectrolyte using urea in the hundred millimolar range [38]. A previous report revealed using Fourier transform infrared spectroscopy that hydrogen bonding influenced the formation of complexes consisting of native OVA and LYZ [39].

The addition of urea to a concentration of no more than 3 M slightly decreased the turbidity and increased the soluble protein concentration in the hOVA/pLYZ solution (Fig. 4.7B). The effect of urea on the hOVA/pLYZ solution appeared at high concentrations of 1–3 M, as the behavior was distinct from that in the pOVA/pLYZ solution (Fig. 4.7A). Similarly, the addition of urea to the pOVA/hLYZ solution gradually decreased the turbidity and increased the soluble OVA concentration (Fig. 4.7C). These results indicate that both hydrogen bonding and hydrophobic interactions contribute to intermolecular interactions between native OVA or LYZ and unfolded LYZ or OVA.

Several molars of urea both disrupt hydrogen bonds and suppress hydrophobic interactions [40]. These data indicate that hydrogen bonding and hydrophobic interactions contribute to the stability of complexes consisting of either unfolded OVA or LYZ. This change of dependence on the urea concentration may arise from the exposure of a buried hydrophobic region of proteins. The increase in protein surface hydrophobicity

stabilized the complexes against urea exposure. These results suggest that intermolecular hydrogen bonding and hydrophobic interactions between OVA and LYZ became stronger in the unfolded state than in the native state.

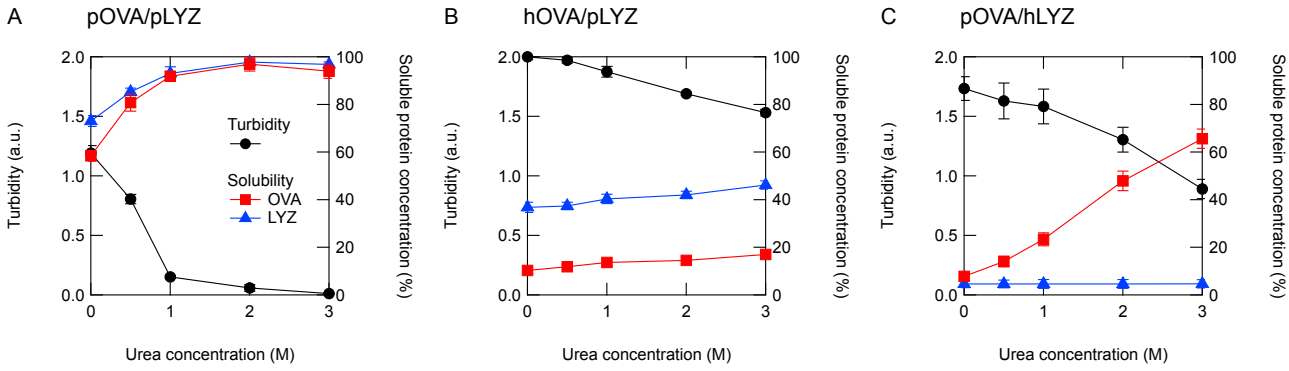

Figure 4.7 Complex of OVA and LYZ in the presence of urea. (A) pOVA/pLYZ; (B) hOVA/pLYZ; (C) pOVA/hLYZ (C). The figure shows the turbidity (left axis, black circles) and soluble concentrations (right axis) of OVA (red squares) and LYZ (blue triangles).

Morphology of complexes consisting OVA and LYZ

The difference of interactions between the aforementioned proteins affects their microscopic morphology. The complexes formed in OVA/LYZ solutions were imaged via phase contrast microscopy, which can be used to observe proteins in situ without drying. The observed structures in the pOVA/pLYZ solution were spherical droplets with a size of several micrometers (Fig. 4.8A), which is an important feature of coacervates [6]. On the contrary, amorphous aggregates with sizes of several tens of micrometers were observed in both the hOVA/pLYZ and pOVA/hLYZ solutions (Figs. 4.8B and 4.8C). They were solid-like coaggregates with irregular shapes that featured a fractal network structure. It was noted that the observed particles are building blocks with a primary microstructure formed in a small amount of solution volume of 1 μL. Therefore, it may be expected that large network structures will be observed in a large-scale experimental system.

Complexes in the solution were observed via microscopy in the distinguishable forms of either coacervate or coaggregate. The distinction between coacervate and coaggregate is shown in Figure 4.9. The formation of liquid-like coacervates obtained in the pOVA/pLYZ solution has been explained to be driven by liquid–liquid phase separation followed by growth via fusion. The complexes consisting of native proteins have fluidity due to highly multivalent and reversible electrostatic interactions and hydrogen bonding.

Conversely, the solid-like coaggregates obtained in the hOVA/pLYZ and pOVA/hLYZ solutions appeared to grow hierarchically via collision and adsorption, suggesting a diffusion-limited reaction. Amorphous aggregates of OVA and LYZ have been observed to be formed instantly during co-heating [41, 42]. The complexes containing unfolded proteins lost their fluidity due to low-reversibility hydrophobic interactions, resulting in an irregular structure. In the same principle, it is thought that the complexes consisting of both unfolded proteins (e.g., hOVA/hLYZ system) insolubilize by the additional intermolecular hydrophobic interactions, resulting in the formation of amorphous coaggregates.

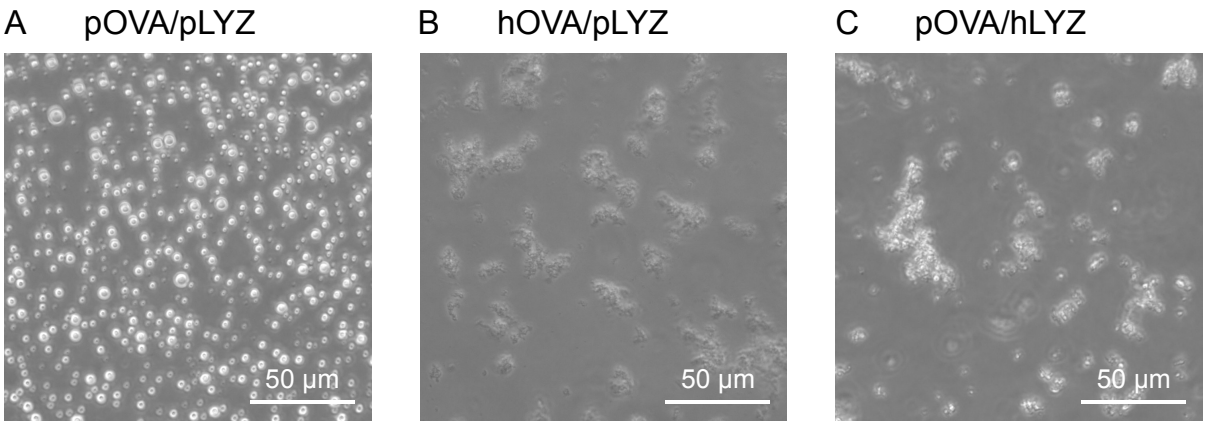

Figure 4.8 Images of OVA/LYZ complexes observed using phase contrast optical micrographs. (A) pOVA/pLYZ; (B) hOVA/pLYZ; (C) pOVA/hLYZ. The scale bars represent 50 μm.

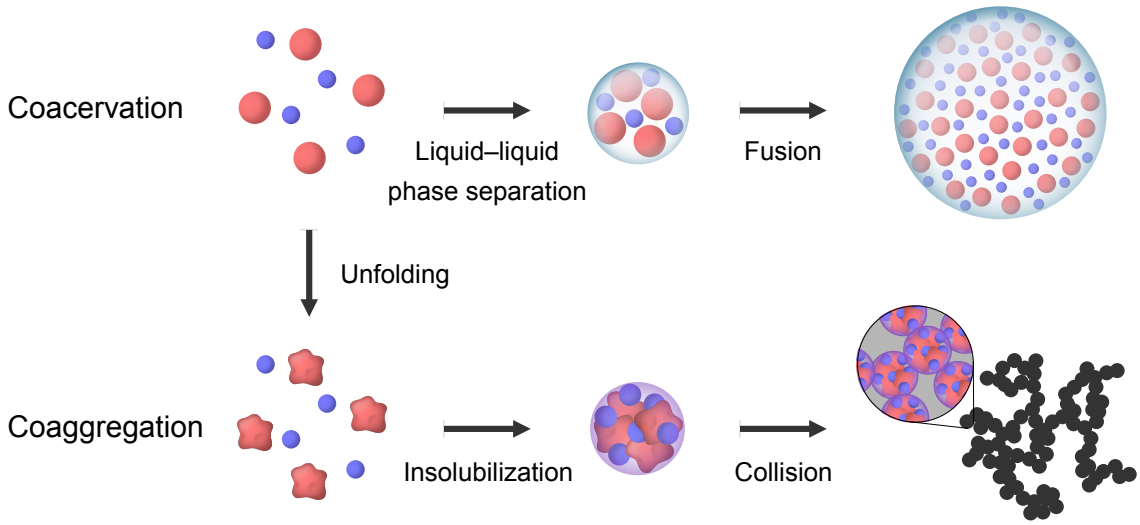

Figure 4.9 The conceptual diagram of the formation of coacervates vs. coaggregates.

Interaction mode between OVA and LYZ

The formation of protein complexes is generally determined by the balance of the enthalpy and entropy of the interactions. The enthalpy is related to Coulomb forces, hydrogen bonding, and van der Waals forces, and the entropy is related to the release of counterions and hydrophobic effects derived from water structure ordering [1]. It has been reported that the coacervate formed by native OVA and native LYZ occurred with enthalpically favorable and entropically unfavorable contributions according to calorimetric analysis [39]. Native OVA and native LYZ formed coacervates via electrostatic interactions including Coulomb forces and counterion release, and hydrogen bonding. In this study, unfolded OVA or LYZ and native LYZ or OVA formed complexes throughout hydrophobic interactions. Moreover, heat treatment increased the ζ-potential of proteins, leading to enhancement of the electrostatic interactions.

Sugimoto *et al*. has reported the binding region between unfolded OVA and native LYZ [43]. In this report, a peptide fragment (229 ILELPFASGT MSMLVLLPDE VSGLEQLESIINFEK 263) of the sequence in the core region inside the OVA molecule bound strongly to the native LYZ. On the contrary, the peptide fragments (112 RNRCKGTDVQAW 123) located on the LYZ surface bind to the native OVA molecule. Considering the sequences of the fragments, it is believed that both electrostatic and hydrophobic interactions occurred between unfolded OVA and native LYZ. In addition, a peptide fragment (54 GILQINSRW 62) of the sequence inside LYZ tended to bind to native OVA. As the peptide has high hydrophobicity, it is supported the assumption that hydrophobic interactions occurred between native OVA and unfolded LYZ.

Fate of liquid-like coacervate and solid-like coaggregate

Similar to the coacervation of native proteins, it is believed that unfolded proteins naturally assemble into liquid-like coacervates and/or solid-like coaggregates. Under the association process, the morphology of complexes as coacervates or coaggregates depends on the strength and mode of the interaction between two macromolecules. Polyelectrolytes usually form coacervates with a liquid-like spherical structure, but densely-charged polyelectrolytes form aggregates with a random structure [44]. Coacervates of poly-Glu and poly-Lys transform into aggregates depending on the degree of hydrophobic modification of poly-Glu [25]. LYZ and apo α-lactalbumin formed amorphous precipitates at low temperature (5°C), whereas they formed coacervates at 45°C, at which the apo α-lactalbumin adopts a molten globule state with a more flexible structure [9, 45, 46]. The uptake of small reactive molecules into complexes favored the formation of amorphous aggregates rather

than coacervates due to the induction of charge reduction and self-aggregation [47, 48]. Consequently, excessively strong electrostatic and hydrophobic interactions lead to the irregular structure of coaggregates that can not undergo subsequent structural rearrangements. Contrarily, the flexibility of macromolecules plays an important role in coacervate structures with liquid-like spherical shapes. However, it is not fully understood about the properties of unfolded proteins that govern the stoichiometry of protein composition and the stability of coaggregates. Furthermore, because the solution containing the complexes of OVA and LYZ becomes cloudy, it is difficult to analyze the protein structure in the complexes by spectroscopic experiments. It is a fundamental challenge to clarify the three-dimensional structure of proteins constituting the complex, compared with that in the dispersed state. These issues should be clarified in the future.

4.4 Conclusion

The spontaneous association of oppositely charged proteins was predominantly driven by electrostatic interactions in low ionic strength solutions, regardless of the degree of unfolding. Hydrogen bonding played a secondary role in the complexes of OVA and LYZ in the native state. Hydrophobic interactions influenced complex formation between OVA and LYZ in the unfolded state. It is noted that coacervation or aggregation by many types of unfolded proteins is generally well suppressed by a chaotropic salt of ArgHCl. The coacervate in the pOVA/pLYZ solution was sensitive to ionic strength, whereas the coaggregates in the hOVA/pLYZ and pOVA/hLYZ solutions had amorphous shapes due to the hydrophobic interactions. The simple system using OVA and LYZ has improved our understanding of the difference between reversible coacervates caused by the liquid–liquid phase separation of proteins and irreversible aggregates caused by insolubilization. In addition, this paper also proposes the value of small molecular additives that can be used to understand the interactions between protein molecules. Adequate control of the state of protein structures is needed to construct the building blocks of protein-based biomaterials for food industrial and pharmacological fields.

References

[1] Moschakis, T. & Biliaderis, C. G. Biopolymer-based coacervates: Structures, functionality and applications in food products. *Curr. Opin. Colloid Interface Sci.* 28, 96–109 (2017).

[2] Chen, L., Remondetto, G. E. & Subirade, M. Food protein-based materials as nutraceutical delivery systems. *Trends Food Sci. Technol.* 17, 272–283 (2006).

[3] Reineccius, G. Use of proteins for the delivery of flavours and other bioactive compounds. *Food Hydrocolloids* 86, 62–69 (2019).

[4] Imai, E., Saito, K., Hatakeyama, M., Hatae, K. & Shimada, A. Effect of physical properties of food particles on the degree of graininess perceived in the mouth. *J. Texture Stud.* 30, 59–88 (1999).

[5] Howell, N. K., Yeboah, N. A. & Lewis, D. F. V. Studies on the electrostatic interactions of lysozyme with α-lactalbumin and β-lactoglobulin. *Int. J. Food Sci. Tech.* 30, 813–824 (2007).

[6] Bouhallab, S. & Croguennec, T. Spontaneous assembly and induced aggregation of food proteins. in *Polyelectrolyte Complexes in the Dispersed and Solid State II Advances in Polymer Science* 67–101 (2013).

[7] Turgeon, S. L., Schmitt, C. & Sanchez, C. Protein–polysaccharide complexes and coacervates. *Curr. Opin. Colloid Interface Sci.* 12, 166–178 (2007).

[8] van der Linden, E. & Venema, P. Self-assembly and aggregation of proteins. *Curr. Opin. Colloid Interface Sci.* 12, 158–165 (2007).

[9] Nigen, M., Croguennec, T., Renard, D. & Bouhallab, S. Temperature affects the supramolecular structures resulting from α-lactalbumin−lysozyme interaction. *Biochemistry* 46, 1248–1255 (2007).

[10] Matsuda, A., Mimura, M., Maruyama, T., Kurinomaru, T., Shiuhei, M. & Shiraki, K. Liquid droplet of protein-polyelectrolyte complex for high-concentration formulations. *J. Pharm. Sci.* 107, 2713–2719 (2018).

[11] Schmitt, C. & Turgeon, S. L. Protein/polysaccharide complexes and coacervates in food systems. *Adv. Colloid Interface Sci.* 167, 63–70 (2011).

[12] Abeyrathne, E. D. N. S., Lee, H. Y. & Ahn, D. U. Egg white proteins and their potential use in food processing or as nutraceutical and pharmaceutical agents—A review. *Poult. Sci.* 92, 3292–3299 (2013).

[13] Takahashi, N., Onda, M., Hayashi, K., Yamasaki, M., Mita, T. & Hirose, M. Thermostability of refolded ovalbumin and S-ovalbumin. *Biosci. Biotechnol. Biochem.* 69, 922–931 (2005).

[14] Huntington, J. A. & Stein, P. E. Structure and properties of ovalbumin. *J. Chromatogr. B Biomed. Sci. Appl.* 756, 189–198 (2001).

[15] Rao, Q., Rocca-Smith, J. R. & Labuza, T. P. Moisture-induced quality changes of hen egg white proteins in a protein/water model system. *J. Agric. Food Chem.* 60, 10625–10633 (2012).

[16] Guez, V., Roux, P., Navon, A. & Goldberg, M. E. Role of individual disulfide bonds in hen lysozyme early folding steps. *Protein Sci.* 11, 1136–1151 (2002).

[17] Nau, F., Pasco, M., Desert, C., Molle, D., Croguennec, T. & Guerin-Dubiard, C. Identification and characterization of ovalbumin gene Y in hen egg white. *J. Agric. Food Chem.* 53, 2158–2163 (2005).

[18] Matsuda, T., Watanabe, K. & Sato, Y. Heat-induced aggregation of egg white proteins as studied by vertical flat-sheet polyacrylamide gel electrophoresis. *J. Food Sci.* 46, 1829–1834 (1981).

[19] Desfougeres, Y., Croguennec, T., Lechevalier, V., Bouhallab, S. & Nau, F. Charge and size drive spontaneous self-assembly of oppositely charged globular proteins into microspheres. *J. Phys. Chem. B* 114, 4138–4144 (2010).

[20] Lo Nostro, P. & Ninham, B. W. Hofmeister phenomena: an update on ion specificity in biology. *Chem. Rev.* 112, 2286–2322 (2012).

[21] Guinn, E. J., Pegram, L. M., Capp, M. W., Pollock, M. N. & Record, M. T., Jr. Quantifying why urea is a protein denaturant, whereas glycine betaine is a protein stabilizer. *Proc. Natl. Acad. Sci. U.S.A.* 108, 16932–16937 (2011).

[22] Zhang, Y. & Cremer, P. S. The inverse and direct hofmeister series for lysozyme. *Proc. Natl. Acad. Sci. U.S.A.* 106, 15249–51523 (2009).

[23] Gallivan, J. P. & Dougherty, D. A. A computational study of cation−π interactions vs salt bridges in aqueous media: Implications for protein engineering. *J. Am. Chem. Soc.* 122, 870–874 (2000).

[24] Kim, S., Yoo, H. Y., Huang, J., Lee, Y., Park, S., Park, Y., Jin, S., Jung, Y. M., Zeng, H., Hwang, D. S. & Jho, Y. Salt triggers the simple coacervation of an underwater adhesive when cations meet aromatic π electrons in seawater. *ACS Nano* 11, 6764–6772 (2017).

[25] Akagi, T., Watanabe, K., Kim, H. & Akashi, M. Stabilization of polyion complex nanoparticles composed of poly(amino acid) using hydrophobic interactions. *Langmuir* 26, 2406–2413 (2010).

[26] Fu, J. & Schlenoff, J. B. Driving forces for oppositely charged polyion association in aqueous solutions: Enthalpic, entropic, but not electrostatic. *J. Am. Chem. Soc.* 138, 980–990 (2016).

[27] López-León, T., Santander-Ortega, M. J., Ortega-Vinuesa, J. L. & Bastos-González, D. Hofmeister effects in colloidal systems: Influence of the surface nature. *J. Phys. Chem. C* 112, 16060–16069 (2008).

[28] Arakawa, T., Ejima, D., Tsumoto, K., Obeyama, N., Tanaka, Y., Kita, Y. & Timasheff, S. N. Suppression of protein interactions by arginine: A proposed mechanism of the arginine effects. *Biophys. Chem.* 127, 1–8 (2007).

[29] Sanchez-Ruiz, J. M., Shikiya, Y., Tomita, S., Arakawa, T. & Shiraki, K. Arginine inhibits adsorption of proteins on polystyrene surface. *PLoS ONE* 8, e70762 (2013).

[30] Hirano, A., Kameda, T., Arakawa, T. & Shiraki, K. Arginine-assisted solubilization system for drug substances: solubility experiment and simulation. *J. Phys. Chem. B* 114, 13455–13462 (2010).

[31] Shiraki, K., Tomita, S. & Inoue, N. Small amine molecules: Solvent design toward facile improvement of protein stability against aggregation and inactivation. *Curr. Pharm. Biotechnol.* 17, 116–125 (2016).

[32] Hong, T., Iwashita, K., Handa, A. & Shiraki, K. Arginine prevents thermal aggregation of hen egg white proteins. *Food Res. Int.* 97, 272–279 (2017).

[33] Croguennec, T., Renault, A., Beaufils, S., Dubois, J. J. & Pezennec, S. Interfacial properties of heat-treated ovalbumin. *J. Colloid Interface Sci.* 315, 627–636 (2007).

[34] Cousin, F., Gummel, J., Ung, D. & Boué, F. Polyelectrolyte−protein complexes: structure and conformation of each specie revealed by SANS. *Langmuir* 21, 9675–9688 (2005).

[35] Hua, L., Zhou, R., Thirumalai, D. & Berne, B. J. Urea denaturation by stronger dispersion interactions with proteins than water implies a 2-stage unfolding. *Proc. Natl. Acad. Sci. U.S.A.* 105, 16928–16933 (2008).

[36] Stumpe, M. C. & Grubmuller, H. Aqueous urea solutions: structure, energetics, and urea aggregation. *J. Phys. Chem. B* 111, 6220–6228 (2007).

[37] Zou, Q., Habermann-Rottinghaus, S. M. & Murphy, K. P. Urea effects on protein stability: Hydrogen bonding and the hydrophobic effect. *Proteins: Struct., Funct., Genet.* 31, 107–115 (1998).

[38] Liu, J., Shim, Y. Y., Wang, Y. & Reaney, M. J. T. Intermolecular interaction and complex coacervation between bovine serum albumin and gum from whole flaxseed (*Linum usitatissimum* L.). *Food Hydrocolloids* 49, 95–103 (2015).

[39] Santos, M. B., Costa, A. R. D. & Garcia-Rojas, E. E. Heteroprotein complex coacervates of ovalbumin and lysozyme: Formation and thermodynamic characterization. *Int. J. Biol. Macromol.* 106, 1323–1329 (2018).

[40] Stumpe, M. C. & Grubmuller, H. Interaction of urea with amino acids: Implications for urea-induced protein denaturation. *J. Am. Chem. Soc.* 129, 16126–16131 (2007).

[41] Oki, S., Iwashita, K., Kimura, M., Kano, H. & Shiraki, K. Mechanism of co-aggregation in a protein mixture with small additives. *Int. J. Biol. Macromol.* 107, 1428–1437 (2018).

[42] Iwashita, K., Handa, A. & Shiraki, K. Co-aggregation of ovalbumin and lysozyme. *Food Hydrocolloids* 67, 206–215 (2017).

[43] Sugimoto, Y., Kamada, Y., Tokunaga, Y., Shinohara, H., Matsumoto, M., Kusakabe, T., Ohkuri, T. & Ueda, T. Aggregates with lysozyme and ovalbumin show features of amyloid-like fibrils. *Biochem. Cell Biol.* 89, 533–544 (2011).

[44] Kayitmazer, A. B., Koksal, A. F. & Kilic Iyilik, E. Complex coacervation of hyaluronic acid and chitosan: Effects of pH, ionic strength, charge density, chain length and the charge ratio. *Soft Matter* 11, 8605–8612 (2015).

[45] Salvatore, D. B., Duraffourg, N., Favier, A., Persson, B. r. A., Lund, M., Delage, M.-M., Silvers, R., Schwalbe, H., Croguennec, T., Bouhallab, S. d. & Forge, V. Investigation at residue level of the early steps during the assembly of two proteins into supramolecular objects. *Biomacromolecules* 12, 2200–2210 (2011).

[46] Salvatore, D., Croguennec, T., Bouhallab, S., Forge, V. & Nicolai, T. Kinetics and structure during self-assembly of oppositely charged proteins in aqueous solution. *Biomacromolecules* 12, 1920–1926 (2011).

[47] Tavares, G. M., Croguennec, T., Hamon, P., Carvalho, A. F. & Bouhallab, S. How the presence of a small molecule affects the complex coacervation between lactoferrin and β-lactoglobulin. *Int. J. Biol. Macromol.* 102, 192–199 (2017).

[48] Chapeau, A.-L., Tavares, G. M., Hamon, P., Croguennec, T., Poncelet, D. & Bouhallab, S. Spontaneous co-assembly of lactoferrin and β-lactoglobulin as a promising biocarrier for vitamin B9. *Food Hydrocolloids* 57, 280–290 (2016).

Chapter 5 General Discussion

As heteroprotein systems, whole egg white proteins (EWPs) and binary systems with oppositely charged proteins were selected. This chapter describes the features of protein aggregation at a high concentration and in a multicomponent protein system compared to the diluted single component ideal protein solution system typically used in conventional protein aggregation studies.

Hen egg whites contain more than 40 kinds of protein with concentrations reaching 100 mg/mL. Although highly concentrated protein mixtures are common in the food industry, the effects of a crowded environment containing salts on protein stability and aggregation have only been investigated using pure protein solutions. In Chapter 2, I investigated the thermal aggregation of EWP at various concentrations in the presence of inorganic salts by solubility measurements and SDS-PAGE. EWP at 1 mg/mL formed aggregates with increasing temperature above 55°C; the aggregation temperatures increased in the presence of inorganic salt with the Hofmeister series. Namely, the chaotrope 0.5 M NaSCN completely suppressed the thermal aggregation of 1 mg/mL EWP. As the protein concentration increased, NaSCN unexpectedly enhanced the protein aggregation; the aggregation temperatures of 10 and 100 mg/mL EWP solutions dramatically decreased at 62°C and 47°C, respectively. This decrease in aggregation temperatures due to the chaotrope was described by the excluded volume effect, based on a comparative experiment using Ficoll 70 as a neutral crowder. By contrast, the kosmotrope Na_2SO_4 did not affect the aggregation temperature at concentrations from 1 to 100 mg/mL EWPs.

Ovotransferrin (OVT) is the main protein component of egg white responsible for initial gelation due to its high thermal susceptibility. Coaggregation of lysozyme (LYZ) is involved in OVT aggregate formation at low temperatures during pasteurization. Undesirable formation of aggregates limits the degree of thermal processing that can be applied to egg white products. However, the characteristics of coaggregates of OVT and LYZ have not been elucidated. In Chapter 3.1, I determined the thermal coaggregation process of OVT and LYZ in terms of protein composition, structure, intermolecular forces, and morphology. The amount of LYZ involved in coaggregates was dependent on the amount of aggregated OVT regardless of the mixing ratio. Native LYZ had the capability to precipitate soluble OVT aggregates by non-covalent association. The coaggregates of OVT and LYZ formed colloidal particles with a large network, which was not observed in systems consisting of either protein individually. The hierarchical coaggregation of OVT and LYZ started with

the aggregation of OVT involving LYZ non-covalently, which suppressed electrostatic repulsion between soluble OVT aggregates, followed by the growth of insoluble aggregates by disulfide bond crosslinkage between the soluble aggregates.

Hen egg white has excellent heat-induced gelation properties. However, the molecular mechanisms underlying the aggregation of EWPs remain unclear due to their complex composition. In Chapter 3.2, I focused on thermal coaggregation of the main EWP component, namely ovalbumin (OVA), with well studied LYZ in terms of protein composition, aggregation rate, intermolecular forces, and morphology. Size exclusion chromatographic analysis of an OVA–LYZ mixture by heat treatment at 70°C indicated that the aggregation rate constant of LYZ increased 64-fold in the presence of equimolar OVA. By contrast, the aggregation rate of OVA was not dependent on the presence of LYZ. Enzyme assay and SDS-PAGE analysis showed that LYZ forms precipitates with unfolded OVA via reversible non-covalent interactions and irreversible disulfide bonds. The unfolding of OVA triggers coaggregation by exposure of the aggregation-prone region, followed by disulfide bond exchange between OVA and LYZ. LYZ links covalently to small OVA aggregates through disulfide bonds, leading to the hierarchical growth of OVA–LYZ aggregates with larger networks.

Coacervates are self-assemblies formed by oppositely charged macromolecules in aqueous solution. Although coacervates usually take a homogeneous spherical shape with flowability, they have the potential to adopt unexpected macroscopic structures. In Chapter 4, I investigated the influence of the interaction mode and morphology on unfolded proteins constituting coacervates and coaggregates using OVA and LYZ as model systems. The unfolded proteins were prepared via heating at 80°C and then incubated at ambient temperature. OVA and LYZ formed complexes at pH values between their respective isoelectric points in both their native and unfolded states. Unfolded proteins were more prone to form complexes than native proteins due to hydrophobic interactions, rather than electrostatic attraction. Interestingly, native OVA and LYZ formed liquid-like coacervates with spherical shapes, whereas unfolded OVA and LYZ formed solid-like coaggregates with amorphous structures. Understanding the difference between coacervates and coaggregates can provide fundamental information on the differences between amorphous aggregation and liquid–liquid phase separation of proteins.

Here, I describe the differences in protein aggregation between single and binary systems. A protein has a positive or negative net charge at a specific pH determined by its intrinsic isoelectric point. Therefore, protein molecules are generally repulsed in solution. By contrast, some proteins attract each other in solution at a pH

between their respective isoelectric points. Thus, aggregation in a single protein system is caused by hydrophobic attraction and electrostatic, whereas coaggregation of two types of proteins occurs via hydrophobic and electrostatic attraction.

Coaggregation of OVA and LYZ was contributed by the effect of electrostatic attraction with hydrophobic interaction. OVA was more unstable than LYZ when treated with heat. The onset of coaggregation of OVA and LYZ occurred via the formation of small aggregates of OVA that associated with native LYZ. Similar coaggregation was shown to occur with OVT and LYZ. It should be emphasized that coaggregate nucleation occurs via electrostatic attraction of oppositely charged proteins, which is quite different from aggregation in a single protein system. It was noted that native OVA and native OVT are not capable of association with native LYZ at ambient temperatures in 50 mM buffer solution at neutral pH. Thus, the unfolding of protein is indispensable for coaggregation. Interestingly, (i) native OVA and native LYZ did not form a complex in more than 25 mM NaCl, (ii) unfolded OVA and native LYZ formed a complex under the same conditions and in buffer solution, and (iii) more than 150 mM NaCl or 100 mM Arg was necessary for dissociation between unfolded OVA and native LYZ, suggesting that both electrostatic attraction and hydrophobic interactions between proteins play indispensable roles in the formation of the OVA–LYZ complex. Thus, it was concluded that nucleation of coaggregation drives both electrostatic and hydrophobic interactions.

As mentioned above, coaggregation of two oppositely charged proteins is markedly different from aggregation of a single protein. Relatively unstable proteins unfold, even if the structures are slightly perturbed, followed by rapid formation of aggregation nuclei via the combination of electrostatic attraction and hydrophobic interaction, even when the opposite protein is in its native state. During this process, electrostatic attraction plays an important role in coaggregation of different proteins in solution. Coaggregate nuclei are composed of oppositely charged proteins associated with other coaggregates. Protein–protein charge compensation and electroneutrality result in colloidal instability of coaggregates, leading to rapid growth of the coarse fractal structure network via additional disulfide crosslinkage.

Chapter 6 Concluding Remarks

This thesis describes thermal coaggregation processes and their driving forces in a heterogeneous protein system. Chapter 2 showed that the rate-limiting step of thermal aggregation is changed from the association of unfolded protein molecules at a low protein concentration to the unfolding of the protein molecules to a high protein concentration. This protein concentration dependent behavior was similar in heterogeneous and single protein systems. The unexpected finding that a chaotrope enhanced protein aggregation at a high concentration provides new insight into the aggregation phenomenon with the Hofmeister effect, as well as the crude state of highly concentrated proteins. Chapter 3 described the thermal coaggregation processes of the OVT–LYZ and OVA–LYZ systems. Thermal unfolding of OVT and OVA, which are more thermolabile than LYZ, triggered the coaggregation. The unfolded OVT and OVA had a capability for native LYZ; this reaction is the distinguishing step of coaggregation not observed in a single protein system. Chapter 4 clarified the driving forces of association of unfolded OVA with native LYZ. Coaggregation was facilitated by electrostatic attractions between OVA and LYZ surface net charge and hydrophobic interactions via surfaces exposed from inside the OVA molecule.

One advantage of using EWPs as the model system in these researches was that the results are relevant to efficient pasteurization and thermal processing of hen egg whites in food engineering. In recent years, EWP has attracted growing attention for its nutritional content as well as an ingredient with desirable textural characteristics and health-promoting effects. The coaggregation mechanisms of OVA, OVT, and LYZ can be applied to support processing methods of EWPs based on protein science.

Coaggregation reported in this thesis is an important process across interdisciplinary fields; for example, therapy of neurodegenerative diseases caused by protein aggregation in pharmaceutics, the formation of aggresomes and granules for protein quality control in cell biology, rigorous purification in biotechnology, and optimization of processing in food engineering. This work reviewed interactions driving coaggregation with nonspecific protein components in heterogeneous systems that have been previously overlooked. In these researches, binary systems composed of globular proteins were adopted. However, intrinsically disordered proteins, DNA, and RNA are also representative biomacromolecules. Further elucidation of the interaction between nonspecific heterogeneous biomacromolecules will shed light on the mechanisms of coaggregation observed in various scenes from fundamental phenomena to industrial problems.

List of Publications

Related publications

1 **Kazuki Iwashita**, Akihiro Handa, Kentaro Shiraki. Co-aggregation of ovotransferrin and lysozyme. *Food Hydrocolloids* 89, 416–424 (2019).

2 **Kazuki Iwashita**, Akihiro Handa, Kentaro Shiraki. Coacervates and coaggregates: Liquid–liquid and liquid–solid phase transitions by native and unfolded protein complexes. *Int. J. Biol. Macromol.* 120, 10–18 (2018).

3 **Kazuki Iwashita**, Akihiro Handa, Kentaro Shiraki. Co-aggregation of ovalbumin and lysozyme. *Food Hydrocolloids* 67, 206–215 (2017).

4 **Kazuki Iwashita**, Naoto Inoue, Akihiro Handa, Kentaro Shiraki. Thermal aggregation of hen egg white proteins in the presence of salts. *Protein J.* 34, 212–219 (2015).

Other publications

1 **Kazuki Iwashita**, Masahiro Mimura, Kentaro Shiraki. Control of aggregation, coaggregation, and liquid droplet of proteins using small additives. *Curr. Pharm. Biotechnol.* 19, 953–962 (2018).

2 Taehun Hong, **Kazuki Iwashita**, Kentaro Shiraki. Viscosity control of protein solution by small solutes: A review. *Curr. Protein Pept. Sci.* 19, 746–758 (2018).

3 Atsushi Hirano, **Kazuki Iwashita**, Shun Sakuraba, Kentaro Shiraki, Tsutomu Arakawa, Tomoshi Kameda. Salt-dependent elution of uncharged aromatic solutes in ion-exchange chromatography. *J. Chromatogr. A* 1546, 46–55 (2018).

4 Shogo Oki, **Kazuki Iwashita**, Kentaro Shiraki. Mechanism of co-aggregation in a protein mixture with small additives. *Int. J. Biol. Macromol.* 107, 1428–1437 (2018).

5 Taehun Hong, **Kazuki Iwashita**, Akihiro Handa, Kentaro Shiraki. Arginine prevents thermal aggregation of hen egg white proteins. *Food Res. Int*. 97, 272–279 (2017).

6 **Kazuki Iwashita**, Motoki Sumida, Kazuya Shirota, Kentaro Shiraki. Recovery method of surimi wash-water protein by pH shift and heat treatment. *Food Sci. Technol. Res.* 22, 743–749 (2016).

7 **Kazuki Iwashita**, Kentaro Shiraki, Rieko Ishii, Takeshi Tanaka, Atsushi Hirano. Arginine suppresses the adsorption of lysozyme onto single-wall carbon nanotubes. *Chem. Lett.* 45, 952–954 (2016).

8 **Kazuki Iwashita**, Kentaro Shiraki, Rieko Ishii, Takeshi Tanaka, Atsushi Hirano. Liquid chromatographic analysis of the interaction between amino acids and aromatic surfaces using single-wall carbon nanotubes. *Langmuir* 31, 8923–8929 (2015).

Acknowledgements

This work has involved a team of collaborators. I do not think any of the achievements which I have mentioned would have been possible without the help of my colleagues at Tsukuba University and the valuable assistance which I received from those outside.

First, I would like to express my sincere gratitude to Prof. Kentaro Shiraki for his kind guidance, fruitful discussions, and warm encouragement throughout this work. He has given me a very precious opportunity and environment to conduct my research and his invaluable supervision.

Second, I am profoundly grateful to Dr. Akihiro Handa for providing the support and inspiration to pursue this work. This work could not have been completed without him.

Third, I am grateful to Dr. Atsushi Hirano, Dr. Shunsuke Tomita, Dr. Eisuke Takai, Dr. Takaaki Kurinomaru, and Dr. Shunsuke Yoshizawa for discussion to pursue this work. I have learned many important things for science research, including spirit, attitude, knowledge, and technique, from them.

Fourth, I would like to thank my published articles' readers who gave me valuable suggestions and a lot of encouragement.

Fifth, my sincere thanks go to the Lab's members: Mr. Takahiro Nonaka, Mr. Naoto Inoue, Mr. Gai Ohashi, Mr. Takuya Maruyama, Mr. Kengo Kuwada, Mr. Tomohito Nakayama, Ms. Ayumi Matsuda, Mr. Takumi Miyatake, Mr. Akihiro Endo, Mr. Shogo Oki, Mr. Taehun Hong, Ms. Chika Shibata, Mr. Masahiro Mimura, Mr. Keisuke Tsumura, Mr. Suguru Nishinami, Mr. Tomoto Ura, Mr. Yoshiki Kihara, Mr. Yoshitaka Nakauchi, and Ms. Yasuho Takashima.

This work was supported by Japan Society for the Promotion of Science (JSPS) KAKENHI Grant Number JP17J03290.

Finally, I am also deeply grateful to my family for plenty of physical, mental, and economic support.

Allow me to express my most sincere and everlasting gratitude to everyone involved.

Kazuki Iwashita

February 2019